Development of novel cross-linked polymer inclusion membranes (PIMs) for the separation of metallic and non-metallic species

Bosirul Hoque

Submitted in total fulfilment of the requirement of the degree of Doctor of Philosophy

November 2019

School of Chemistry

University of Melbourne

To my father

Abstract

Separation based on polymer inclusion membranes (PIMs) has gained significant interest in recent years as an environmentally friendly separation technique. PIMs are generally classified as a type of liquid membrane in which the membrane organic phase (containing the extractant and in some cases a plasticizer or modifier) is immobilised within the entangled chains of a polymer. The majority of the extractants used in PIMs are liquids, although solid extractants such as trioctylphosphine oxide (TOPO) can also be used when liquified because of the presence of impurities (e.g., solvents). Different base polymers, such as poly(vinyl chloride) (PVC), cellulose triacetate (CTA), and poly(vinylidene fluoride-co-hexafluoropropylene) (PVDF-HFP), have been used as the polymeric support of PIMs. Although the extractants are the active PIM components, the nature of the polymeric support also plays a vital role in the performance of these membranes. In the research described in this thesis the structure of the PIM polymeric support has been altered using different cross-linking agents (i.e., polymer of monomers) and their effect on PIM extraction and separation performance has been studied.

Cross-linked PIMs containing di-2-ethylhexyl phosphoric acid (D2EHPA) as the extractant, poly(ethylene glycol) dimethylacrylate (PEGDMA) as the cross-linking agent and 2,2-dimethoxy-2-phenyl acetophenone (DMPA) as the initiator were developed for the extraction, transport and separation of Zn(II). Three different base polymers were tested, namely PVC, CTA, and PVDF-HFP, but only cross-linked PIMs containing CTA or PVDF-HFP were found to be homogenous with oil free surfaces. When comparing the performance of these two successful cross-linked PIMs with their non-cross-linked counterparts, only the CTA-based cross-linked PIM showed superior performance in terms of the amount of Zn(II) extracted and the rate of extraction. Therefore, the composition of the CTA-based cross-linked PIM was optimised in terms of the ratio between the base polymer and the cross-linking agent and the membrane liquid phase composition. The CTA-based cross-linked PIM with optimum composition and its non-cross-linked counterpart were then assessed with respect to their stability over 5 consecutive extraction and back-extraction experiments (i.e., 5 cycles). Results showed that the cross-linked PIM was stable over the course of the experiment, while the performance of the non-cross-linked PIM deteriorated significantly after the second cycle. Morphology analysis of the cross-linked and non-crosslinked PIMs revealed that the higher surface area of the cross-linked PIMs was one of the factors behind the enhancement of the membrane performance.

Cross-linking agents of different types have been screened to prepare homogeneous cross-linked PIMs comprised of PVC, CTA or PVDF-HFP as the base polymer and D2EHPA or Aliquat 336 as the extractant. These two extractants were selected as they are among the most extensively used and studied PIM extractants and in addition they have been well characterised. PEGDMA, poly(ethylene glycol) divinylether (PEGDVE) and N-ethylmaleimide (NEM) were tested as cross-linking agents. The efficacy of initiating the cross-linking among the units of the cross-linking agent was also examined in a PVC-based membrane without extractant using the three photo-initiators DMPA, triarylsulfonium hexafluorophosphate (TASHFP) and triphenylphosphine oxide (TPO). Among the three photo-initiators, DMPA was effective for both PEGDMA and NEM while TASHFP was effective for PEGDMA and PEGDVE. The photo-initiator TPO was not effective for any of the tested cross-linking agents under the present conditions. The cross-linking conditions were then optimised in terms of the amount of photo-initiator and the UV-irradiation time separately for the three base polymers studied. The extractants D2EHPA or Aliquat 336 were then added to the membrane composition to form cross-linked PIMs using the optimum cross-linking conditions established earlier, and successful and homogenous cross-linked PIMs were applied for the extraction of either Zn(II) or thiocyanate (SCN^-), respectively. Assessment of the extraction results indicated that 12 out of 13 cross-linked PIMs were superior compared to the corresponding non-cross-linked PIMs in terms of the amount extracted and extraction rate of Zn(II) or SCN^-.

The ionic liquid Cyphos® IL104 was used as extractant to fabricate cross-linked PIMs for the recovery of Au(III) from electronic waste digests using aqua regia . The compatibility of Cyphos® IL104 with the cross-linking agents and initiators mentioned above was assessed under the optimal cross-linking conditions established earlier. The three base polymers, mentioned above, were tested. Cross-linked PIMs containing PVC did not produce homogeneous membranes, although those containing PVDF-HFP and CTA produced 4 successful cross-linked PIMs in total, which were all assessed for their ability to extract Au(III). Only the PVDF-HFP-based cross-linked PIMs showed superior extraction performance compared to their non-cross-linked counterparts as well as the CTA-based PIMs. PVDF-HFP-based cross-linked PIMs were then used for Au(III) transport from 2.5 mol L^{-1} HCl feed solutions into Na_2SO_3 receiving solutions, and Au(III) could be completely transported two times faster in comparison with the respective non-cross-linked PIM system. No deterioration in PIM performance was observed in 3 consecutive transport experiments. In highly acidic medium (e.g., digested aqua regia) only the cross-linked PIM produced from PVDF-HFP,

PEGDMA, TASHFP, and Cyphos® IL104 was able to effectively transport Au(III), and hence it was used successfully for the complete recovery of Au(III) from an aqua regia digest of electronic waste containing other metal ions at much higher concentrations than that of Au(III) in less than 24 h.

Declaration

This is to certify that:

- the thesis comprises only my original work towards the PhD.
- due acknowledgement has been made in the text to all other materials used.
- the thesis is fewer than 100 000 words in length, exclusive of tables, maps, bibliographies and appendices.

Bosirul Hoque, November 2019

Preface

All the research work presented in this thesis was conducted by the author of this thesis. However, the author benefited from his supervisors through group meeting sessions in which they provided technical comments and guidance.

The thesis has not been submitted for any other qualifications. All the work towards the thesis was carried out after the enrolment in the degree.

Bosirul Hoque

Acknowledgements

Being at the last stage of my four-year PhD journey, I am already getting mixed feelings. Although I am happy about completing my PhD and stepping on a new stage of my life, lots of memories, in campus and off campus, are appearing in the canvas of my mind. I will always cherish the memories of meeting with the people of beautiful mind and soul, beautiful and natural campus and this lovely city of Melbourne. There were ups and downs during these four years of my PhD studies, but I have been lucky that helping hands were always around. Each day of these four years has been a great opportunity for learning and improving myself, thanks to my advisors, colleagues, friends, and family.

Firstly, I would like to express my sincere gratitude to my principal supervisor Prof. Spas D. Kolev for his guidance, motivation, support, suggestions, patience, and encouragement to complete the journey of this PhD. He is an excellent supervisor with all quality of humanity.

The more I say, about Dr. Inês Almeida, will be less. I would always admire and embrace the support, advice and help I have received from her from the very beginning till the end.

Emeritus Prof. Robert W. Cattrall has provided much appreciated advice during our meetings and in my reports, which helped me to conduct quality research with deep understanding about the subjects. It has been a rewarding experience to work with him, which I would cherish forever.

Dr. T.G. Gopakumar, collaborator from IIT Kanpur, was very supportive and kind all the time I have visited there. His technical advice and suggestions helped me in great extent to conduct the collaborative research smoothly and effectively.

Many thanks to the Advisory Committee, Assoc. Prof Brendan Abrahams and Prof. Muthupandian Ashokkumar for their advice, support and suggestions.

I would like to thank Melbourne India Postgraduate Program (MIPP) for the scholarship and support.

To all the members of the Kolev (Analytical and Environmental Chemistry) and Gopakumar (Molecular Functional Materials) research groups, thank you for your friendship and support. I would like to make special mention of Charles Croft, a fellow PhD student in Kolev group,

for his generous support from the very beginning even before joining the lab, and Fidelis Nitti, another fellow PhD student in Kolev group, for his extensive support and friendship.

My thanks go to the members of the Technical Workshop of the Faculty of Science at the University of Melbourne for their hard work in making and repairing equipment used in my research and the members of the Advance Imaging Centre at IIT Kanpur for helping me with my measurements during my visits there.

My heartfelt thanks and gratitude also go out to each and every member of my extended family for their love, care, support, and encouragement. Mom, Lucy and Zonash, your sacrifices are the pillars of this journey and I am deeply indebted to you for your love, motivation and patience. I would like to specially mention my father who always encouraged me to pursue higher studies and I dedicate this thesis to you.

Table of Contents

Chapter 2. Effect of cross-linking on the performance of polymer inclusion membranes (PIMs) for the extraction, transport and separation of Zn(II)

Chapter 3. Improving the performance of polymer inclusion membranes by cross-linking their polymeric backbone

Chapter 4. Enhancing polymer inclusion membrane efficiency in gold recovery from electronic waste by membrane cross-linking

List of tables

Chapter 1

Chapter 2

Chapter 3

Chapter 4

List of figures

Chapter 1

Chapter 2

Figure 4. Effect of the ratio between CTA and PEG-DMA on the transient concentration of Zn(II) extracted into the corresponding PIM (expressed as mg Zn per g of PIM): (●) 5:5; (■) 6:4; (♦) 7:3; (▲) 8:2, and (○) 9:1. PIM composition, 35 wt% D2EHPA, 20 wt% NPOE, 0.6% initiator; feed solution, 100 mL of 30 mg L^{-1} Zn(II) at pH 3; PIMs thicknesses varied between 50 and 55 µm (Table S1, Supplementary Material). Errors bars, ± SD (n=3).

Figure 5. Transient Zn(II) concentrations in a cross-linked (a) and a non-cross-linked (b) CTA-based PIM (mg Zn(II) per g PIM) for five consecutive extraction experiments. D2EHPA concentration, 40 wt%; NPOE concentration, 10 wt%; polymers ratio, 6:4; initiator concentration, 0.6 wt%; feed solution, 100 mL of 30 mg L^{-1} Zn(II) at pH 3; receiving solution, 1.0 M HCl. Error bars, ± SD (n=3).

Figure 6. Mass spectra of the feed solution after the first (a) and second (b) extraction experiments involving the same cross-linked membrane (PIM 5, Table 2.1).

Figure 7. Percentage mass loss of a cross-linked CTA-based PIM (PIM 5) during the stability study (i.e., five consecutive extraction and back-extraction cycles). Error bars, ± SD (n=3).

Figure 8. Constant force AFM topographs of a cross-linked (a) and non-cross-linked (b) membrane (cross-linked PIM composition: 40 wt% D2EHPA, 10 wt% NPOE, polymers ratio 6:4, 0.6 wt% initiator; non-cross-linked PIM composition: 40 wt% D2EHPA, 10 wt% NPOE, 50 wt% CTA).

Figure 9. Contrast saturated AFM topographs of a cross-linked (a) and non-cross-linked (b) membrane. The voids present in cross-linked and non-cross-linked membranes are clearly visible (cross-linked PIM composition: 40 wt% D2EHPA, 10 wt% NPOE, polymers ratio 6:4, 0.6 wt% initiator; non-cross-linked PIM composition: 40 wt% D2EHPA, 10 wt% NPOE, 50 wt% CTA).

Figure 10. Constant force AFM topographs of cross-linked membranes containing different NPOE concentrations: (a) 5 wt%, (b) 10 wt% and (c) 20 wt%, and the corresponding initial flux values (d). D2EHPA concentration, 40 wt% D2EHPA; polymers ratio (CTA:PEG-DMA), 6:4; initiator (DMPA) concentration, 0.6 wt%.

Figure 11. Transient concentrations of (●) Zn(II), (■) Cd(II), (▲) Co(II), (♦) Cu(II), and (○) Ni(II) in the feed solutions at pH 3 in which the potential interfering metal ions have the same concentration as Zn(II) (a) or have a concentration five times higher than that of Zn(II) (b). Cross-linked PIM composition, 40 wt% D2EHPA, 10 wt% NPOE, CTA:PEG-DMA 6:4, 0.6

wt% initiator; feed solution, 100 mL of 30 mg L^{-1} of each metal ion (a) and 30 mg L^{-1} Zn(II) and 150 mg L^{-1} for each interferent (b).

Figure 12. Transient concentrations of Zn(II) (□) and Fe(III) (◆) in a feed solution containing 30 mg L^{-1} of each ion, and of Zn(II) (●) in a feed solution of the same Fe(III) and Zn(II) composition in the presence of Na2HPO4. Cross-linked PIM composition, 40 wt% D2EHPA, 10 wt% NPOE, CTA : PEG-DMA 6:4, 0.6 wt% initiator. Error bars, ± SD (n=3).

Figure 13. Transient Zn(II) concentrations in the feed solutions (100 mL) containing initially 65 (■), 46 (●) and 27 (◆) mg L^{-1} of Zn(II) at pH 3 and in the respective receiving solutions (100 mL) during transport experiments using the cross-linked CTA-based PIM with D2EHPA concentration of 40 wt%, NPOE concentration of 10 wt%, polymers ratio of 6:4, and initiator concentration of 0.6 wt%. The receiving solution contained 1.0 M HCl. Transport experiments were performed in duplicate.

Figure S1. Concentration of Zn(II) in the feed solution during the extraction experiment involving a membrane containing no carrier (i.e., D2EHPA).

Figure S2. Concentration of Zn(II) in the receiving solution during a back-extraction experiment. PIM composition, 40 wt% D2EHPA, 10 wt% NPOE, 0.6% initiator; receiving solution, 1.0 M HCl. Error bars, ± SD (n=3).

Figure S3. Percentage of Zn(II) back-extracted into the receiving solution during five consecutive extraction/back-extraction experiments. PIM composition, 6:4 polymer ratio, 40 wt% D2EHPA, 10 wt% NPOE, 0.6% initiator; receiving solution, 1.0 M HCl. Error bars, ± SD (n=3).

Figure S4. Photographic image of a non-cross-linked PIM (40 wt% D2EHPA, 10 wt% NPOE and 50 wt% CTA) after the second extraction/back-extraction cycle.

Chapter 3

Figure 1. ATR-FTIR spectra of the PEGDVE membranes containing PVC as the base polymer (6:4 PVC:PEGDVE mass ratio) and 2 wt% of one of the following photo-initiators: (◆) DMPA, (●) TASHFP, (■) TPO. Membrane (▲) did not contain a photo-initiator and was not UV irradiated. UV-irradiation time was 15 min.

Figure 2. Cross-linking of PEGDVE.

Figure 3. ATR-FTIR spectra of the PEGDMA membranes containing PVC as the base polymer (6:4 PVC:PEGDMA mass ratio) and 2 wt% of one of the following photo-initiators: (◆) DMPA, (●) TASHFP, (■) TPO. Membrane (▲) did not contain a photo-initiator and was not UV irradiated. UV-irradiation time was 15 min.

Figure 4. Cross-linking of PEGDMA (R. refers to a radical).

Figure 5. ATR-FTIR spectra of the NEM membranes, containing PVC as the base polymer (6:4 PVC:NEM weight ratio) and 2 wt% of one of the following photo-initiators: (◆) DMPA, (●) TASHFP, (■) TPO. Membrane (▲) did not contain a photo-initiator and was not UV irradiated. UV-irradiation time was 15 min.

Figure 6. Cross-linking of NEM (R. refers to a radical).

Figure 7. Flowchart representing the optimum cross-linking conditions for PVC-based membranes. (a) base polymer; (b) cross-linking agent (i.e., PEGDMA and PEGDVE polymers and NEM monomer); (c) photo-initiator; (d) optimum concentration of photo-initiator; (e) optimum UV-treatment time. Mass ratio of base polymer to cross-linking agent, 6:4.

Figure 8. Flowchart representing the optimum cross-linking conditions for PVDF-HFP-based membranes. (a) base polymer; (b) cross-linking agent (i.e., PEGDMA and PEGDVE polymers and NEM monomer); (c) photo-initiator; (d) optimum concentration of photo-initiator; (e) optimum UV-treatment time. Mass ratio of base polymer to cross-linking agent, 6:4.

Figure 9. Flowchart representing the optimum cross-linking conditions for CTA-based membranes. (a) base polymer; (b) cross-linking agent (i.e., PEGDMA and PEGDVE polymers and NEM monomer); (c) photo-initiator; (d) optimum concentration of photo-initiator; (e) optimum UV-treatment time. Mass ratio of base polymer to cross-linking agent, 6:4.

Figure 10. Mass spectrum in the positive mode of an acetonitrile solution of the white precipitate formed in the reaction between Aliquat 336 and TASHFP.

Figure 11. Transient concentrations of SCN^- (a, b, c) and Zn^{2+} (d, e) during extraction experiments involving PIMs 1-3 (a); 4-6 (b); 7-10 (c), 11-15 (d); and 16-18 (e). PIM compositions and experimental conditions as in Table 2. Error bars = ±standard deviation (n=3).

Figure S1. Coloration of PVC based membrane upon longer UV-irradiation.

Figure S2. Coloration of PVDF-HFP based membrane upon longer UV-irradiation.

Chapter 4

Figure 1. Transient percentage of Au(III) extracted into the successful Cyphos® IL 104-based cross-linked PIMs (Table 1) and their respective non-cross-linked counterparts. (■) PIM 1, (◆) PIM 2, (▲) PIM 3, (●) PVDF-HFP non-cross-linked PIM, (×) PIM 4, and (◆) CTA non-cross-linked PIM. Feed solution, 100 mg L^{-1} Au(III) and 2.5 M HCl. Detailed compositions of the PIMs are presented in Table 1.

Figure 2. Constant force AFM topographic images of the CTA and PVDF-HFP cross-linked membranes and their respective non-cross-linked PIMs. (a) PIM 4 (Table 1), (b) CTA non-cross-linked PIM, (c) PIM 1, (d) PIM 2, (e) PIM 3 (Table 1), (f) PVDF-HFP non-cross-linked PIM.

Figure 3. Contrast saturated AFM topographic images of the PVDF-HFP cross-linked membranes: (a) PIM 1, (b) PIM 2, (c) PIM 3 (Table 1), and (d) respective non-cross-linked PIM, highlighting the indentations present in the membranes (represented by the white and yellow colour).

Figure 4. Transient Au(III) concentrations in the feed (dashed lines) and receiving (solid lines) solutions using the PVDF-HFP cross-linked membranes: (●) PIM 1, (▲) PIM 2, (◆) PIM 3 and their respective (■) non-cross-linked PIM. Initial feed solution composition, 100 mg L^{-1} Au(III) and 2.5 M HCl; receiving solution composition, 0.5 M Na_2SO_3. The data points are the average of duplicate experiments. PIMs thickness: PIM 1, 20.1 ± 1.0 µm; PIM 2, 20.1 ± 4.0 µm; PIM 3, 21.5 ± 1.2 µm; non-cross-linked PIM, 18.5 ± 1.8 µm.

Figure 5. Five consecutive transport experiments using (a) PIM 1 and (b) PIM 2 (Table 1): 1st (×), 2nd (●), 3rd (▲), 4th (■) and 5th (◆) experiment. The transient Au(III) concentration in the feed and receiving solutions is represented by the dashed and solid line, respectively. Initial feed solution composition, 100 mg L^{-1} Au(III) and 2.5 M HCl; receiving solution composition, 0.5 M Na_2SO_3. The data points are the average of duplicate experiments.

Figure 6. Transient Au(III) concentrations in the feed (dashed line) and receiving (solid line) solutions in transport experiments using (a) PIM 1 and (b) PIM 2 (Table 1). Initial feed

solution,110 mg L^{-1} Au(III) in digested aqua regia solution; receiving solution composition, 0.5 M Na_2SO_3. The error bars = ±standard deviation (n=3).

Figure 7. Transient normalized concentration of Au(III) (●) in the feed (dashed line) and receiving solutions (solid line), respectively, and of the major metal ions (i.e., Ni(II), Al(III), Co(II), Cu(II), Zn(II) and Cr(III)) present in the feed solution. The transient percentage of Au(III) recovered is also presented. Feed solution, electronic waste digest; receiving solution, 0.5 M Na_2SO_3. Cross-linked PIM composition, 30 wt% Cyphos® IL 104, PVDF-HFP, PEGDMA (PVDF-HFP to PEGDMA ratio 6:4) and 2 wt% TASHFP. PIMs thickness: 20.1 ± 4.0 µm.

Figure 8. Transient normalized concentration of Au(III) in the feed (dashed line) and receiving solutions (solid line) for cross-linked PIM (■) and non-cross-linked PIM (◆) , respectively, and of the major metal ions (i.e., Ni(II), Al(III), Co(II), Cu(II), Zn(II) and Cr(III)) present in the feed solution. The transient percentage of Au(III) recovered is also presented. Feed solution, electronic waste digest; receiving solution, 0.5 M Na_2SO_3. Cross-linked PIM composition, 30 wt% Cyphos® IL 104, PVDF-HFP, PEGDMA (PVDF-HFP to PEGDMA ratio 6:4) and 2 wt% TASHFP and non-cross-linked PIM containing 30 wt% Cyphos® IL 104, PVDF-HFP.

Table S1. Concentration of Au(III) (mg L^{-1}) transported in five consecutive transport experiments across PIM 1 and PIM 2 (Table 1). Initial feed solution composition, 100 mg L^{-1} Au(III) and 2.5 M HCl; receiving solution composition, 0.5 M Na_2SO_3.

List of publications

- Bosirul Hoque, M. Inês G.S. Almeida, Robert W. Cattrall, Thiruvancheril G. Gopakumar, Spas D. Kolev, Effect of cross-linking on the performance of polymer inclusion membranes (PIMs) for the extraction, transport and separation of Zn(II), Journal of Membrane Science 589 (2019) 117256.
- Bosirul Hoque, M. Inês G.S. Almeida, Robert W. Cattrall, Thiruvancheril G. Gopakumar, Spas D. Kolev, Improving the performance of polymer inclusion membranes by cross-linking their polymeric backbone, Submitted to Separation and Purification Technology.

List of conferences

- Development of a new type of polymer inclusion membrane with faster extraction and greater stability, 25th Annual RACI R&D Topics Conference, December 2017, University of Tasmania, Australia.
- Development of a new cross-linked polymer inclusion membrane (PIM) with high stability and selectivity for the extraction and separation of Zn(II), Emerging Trends in Separation Science and Technology (SESTEC-2018), May 2018, BITS Pilani Goa, India.
- Cross-linked polymer inclusion membrane (PIM): Faster extraction and longer stability, Euromembrane-2018, July 2018, Universitat Politècnica de València, Spain.
- Modifying polymer inclusion membranes (PIMs) with cross-linking polymers for improving membrane extraction and stability, Membrane Society Australasia Early Carrier Researcher Symposium 2019, January 2019, University of Melbourne, Australia.
- Compatibility of cross-linking polymers in polymer inclusion membranes (PIMs) and their effect on membrane performance, stability and morphology, 14th International Conference Membrane Science and Technology Conference (MST2019), June 2019, Nanyang Technological University, Singapore.
- Application of cross-linking polymer in enhancing the efficiency of polymer inclusion membrane (PIM)-based extraction of Au(III) using Cyphos® IL 104 as the extractant, The 12th International conference of the Aseanian Membrane Society (AMS12), July 2019, Jeju, Korea.

Chapter 1

Introduction: evolution of polymer inclusion membranes (PIMs) as a powerful separation tool

1. General introduction

Since ancient times, people have needed to separate different materials and have used different separation techniques in their daily lives. The history of separation is long, from the separation of grains from their stalks to metals from their ores. In the modern era, every single step of our daily life relies directly or indirectly on the application of different separation techniques. From our daily food to the production of valuable materials, there is a need for contamination to be minimized and we rely on different separation techniques to achieve this.

Different separation techniques have been discovered according to their necessity at the time [1, 2]. According to the requirements, people have developed separation techniques like evaporation, distillation, filtration, centrifugation, adsorption, decantation, extraction, and chromatographic separation [3-14]. All these techniques especially solvent extraction and chromatography are among the most essential separation techniques used in research laboratories as well as in industry. Separation techniques are used not only for producing pure quality products but also to treat waste before its disposal as industrial and domestic waste contains different pollutants which may cause severe adverse effects on living organisms if not treated before discharge [15-17]. In order to make the separation process more environmentally friendly, membrane-based separation processes were introduced a few decades ago [18, 19]. There are three basic pathways, namely passive transport, facilitated transport and active transport, through which membrane separation processes take place. Basically, the membrane acts as a semipermeable barrier allowing specific chemical species to pass through depending on the experimental conditions. Membrane based filtration processes, such as ultrafiltration, nanofiltration and reverse osmosis, are very popular and have been industrialised worldwide. These filtration techniques work on the principle of size exclusion. Membrane based water desalination is a very effective process in tackling the present potable water crisis [20-22]. Membranes have also been tested for removing the greenhouse gas carbon dioxide from industrial fuel gases [22-24]. Other types of membranes that have also been under extensive

development are those which employ the facilitated transport mechanism. These types of membranes are called liquid membranes and they mimic the process of solvent extraction [25, 26]. The following sections describe the basic principles of separation using liquid membranes with a particular emphasis on polymer inclusion membranes (PIMs), which are the focus of the research described in this thesis. Solvent extraction is also briefly discussed since it is the separation technique that liquid membrane-based separation mimics.

2. Solvent extraction

Solvent extraction is a very important and essential part of analytical and industrial chemistry. This separation technique is well recognised due to its ease of operation, simplicity and broad scope [27-29]. Solvent extraction commonly involves the mixing of two immiscible phases, one aqueous feed phase containing the target species and one organic phase accommodating the extractant. This technique is often used by analytical chemists for the extraction, separation and preconcentration of species of interest since it utilizes equipment as simple as a separatory funnel and requires just a few minutes to be performed. It is also very applicable to analytes at both trace and macro levels. In the late 1940s, solvent extraction received more attention due to its superiority over precipitation methods [30, 31]. In precipitation methods, contamination due to co-precipitation is very common while solvent extraction is a much cleaner process in this regard. In atomic energy research separating and purifying elements became easier and more effective with the aid of solvent extraction [30]. This technique has become even more useful in recent years with the introduction of different selective chelating extractants [32]. Proper choice of the chelating extractant can ensure the selective separation of trace elements with high efficiencies. The three main purposes that solvent extraction serves are: a) preconcentration of trace elements, b) elimination of matrix interferences, and c) separation of chemical species [13, 33, 34]. Although solvent extraction has great advantages as a separation technique, the use of large volumes of volatile and often flammable organic diluents makes this technique not environmentally friendly. Also, the use of volatile organic diluents raises occupational health and safety concerns. Therefore, newer technologies have been developed to mimic the solvent extraction separation process while avoiding the use of high volumes of volatile organic solvents.

3. Liquid membranes

Liquid membranes were introduced to avoid the use of a large inventory of organic diluents while maintaining the advantages of solvent extraction. Moreover, they allow for the target species to be transferred from a feed aqueous phase to a receiving aqueous phase in one single step, unlike in solvent extraction where extraction and back-extraction have to be performed in two separate steps. There are different types of liquid membranes, and the most frequently used among them are bulk liquid membranes (BLMs), emulsion liquid membranes (ELMs), supported liquid membranes (SLMs), and polymer inclusion membranes (PIMs) [25].

3.1. Bulk liquid membranes

BLMs are a type of liquid membranes where two miscible aqueous liquid phases (feed and receiving phases) are separated by an organic phase which is the liquid membrane that holds the extractant (often referred to as carrier). A schematic representation of a BLM is displayed in Figure 1. Continuous stirring of the feed solution facilitates transfer of the target species to the membrane liquid phase which contains an extractant. The target species then diffuses through the liquid membrane and is stripped into the receiving phase which is also being stirred continuously. Metal ion transport through liquid membranes can be described with the aid of two different models. The first and more frequently used approach, was developed by Reusch and Cussler in 1973 [35]. This approach basically deals with the concentration diffusion layers and treats the interfaces between the organic and aqueous phases as the areas wherein the complexation and decomplexation involving the target species and the extractant occur [36]. In the second approach [37], it is assumed that the carrier moves slightly out of the organic phase into the aqueous feed phase and the reaction occurs in the portion of this aqueous phase known as “Big Carrousel”. However, there are a few major drawbacks in using BLMs for large scale applications, namely low interfacial surface area and flow rate, which reduces the overall mass transfer efficiency.

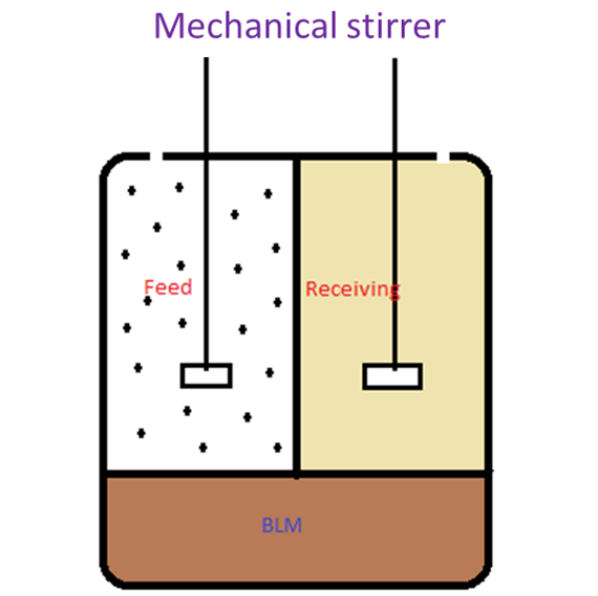

Figure 1. Schematic diagram of a bulk liquid membrane (BLM) system [38].

3.2. Emulsion liquid membranes

The simplest approach that can be adopted to improve the diffusion rate of a target species through a liquid membrane consists of increasing the contact area between the phases and lowering the diffusion path length. Based on these two factors, Cahn and Li introduced a new type of membranes called emulsion liquid membranes (ELMs) [39]. Since then many researchers have made considerable effort to demonstrate the feasibility of performing separation using ELMs with specific formulations [40, 41]. ELMs are basically double emulsions produced by emulsifying two immiscible phases. There are two configurations possible, such as i) oil-in-water-in-oil (O/W/O) and ii) water-in-oil-in-water (W/O/W) (Figure 2). Mass transfer takes places from an external feed phase to an internal receiving phase through the ELM. After the extraction process the membrane must be demulsified with the aid of heating, applying an electric field or centrifugation.

Coalescence of droplets inhibits the dispersion of one liquid phase in the other causing instability of the ELM. Marr et al. created an approach for producing stable emulsions which is based on manipulating factors such as the volume ratio of the different phases (internal, external and membrane), the organic phase viscosity and the surfactant hydrophilic-lipophilic balance (HLB) value [42]. Overall, these membranes are not all that stable to withstand the

shear force generated from the mixing process during extraction and demulsification after extraction. This instability detracts ELMs from widespread industrial applications [41, 43-46].

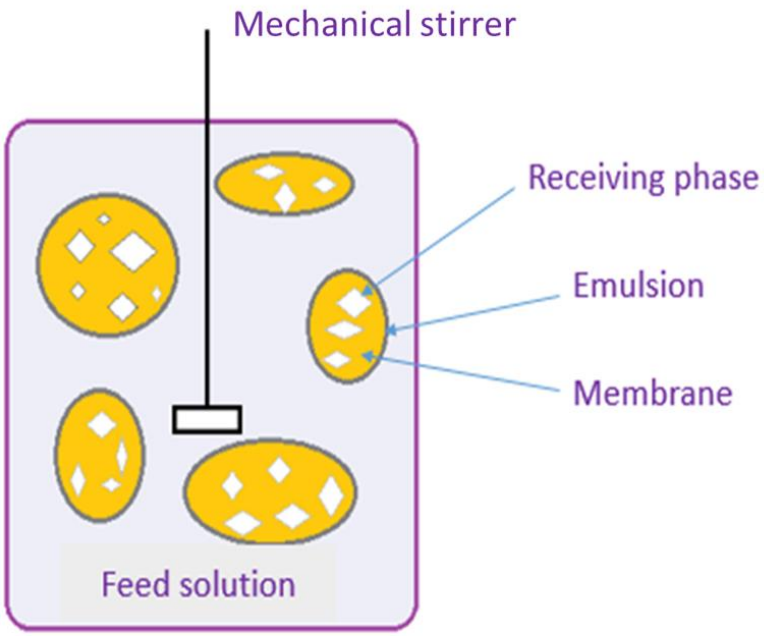

Figure 2. Schematic diagram of an emulsion liquid membrane (ELM) system [47].

3.3. Supported liquid membranes

This type of liquid membranes is formed by a thin layer of organic phase, immobilised into a suitable microporous support, sandwiched between two aqueous phases of different compositions (Figure 3) [48-52]. The porous polymeric support does not play an active role in the separation but acts as a supportive layer to hold the organic phase loaded with an extractant [53]. The extractant, in contact with the feed solution, extracts the target chemical species and releases it to the receiving solution. This advantage of simultaneous extraction and back-extraction along with the high selectivity and comparatively better stability than BLMs and ELMs, leads to the application of SLMs in recovering valuable metals from different sources. However, there are still problems in the use of SLMs for large-scale applications. The main drawback is the poor stability of SLMs due to the slow leaching of the membrane liquid phase into the adjacent aqueous solutions, as a result of the week capillary forces involved in holding the organic phase within the support [43]. Therefore, a new type of liquid membranes was introduced where the organic extractant is incorporated within a matrix of entangled polymer

chains. In this case the intermolecular forces between the organic phase (containing the extractant) and the base polymer are stronger, thus minimising the leaching of extractant into the adjacent aqueous phases. These liquid membranes are known as polymer inclusion membranes (PIMs). This type of liquid membranes is the focus of the research presented in this thesis and, therefore, the following sections contain a more detailed discussion related to PIMs.

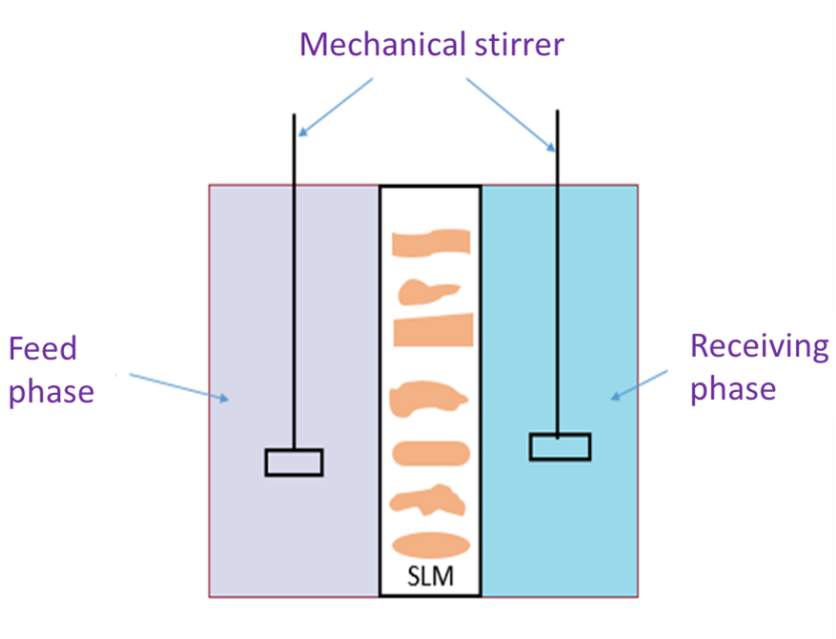

Figure 3. Schematic diagram of a supported liquid membrane (SLM) system [54].

3.4. Polymer inclusion membranes

Due to the inherent problems associated with the above mentioned three types of liquid membranes and the existing demand for membrane-based separation techniques, extensive research has been focused on eliminating the drawbacks of existing liquid membranes and the development of PIMs [55-59]. PIMs are generally comprised of a base polymer and a liquid phase, containing an extractant (carrier) and sometimes also a plasticizer/modifier. The role of the base polymer is to provide mechanical strength to the membrane and to act as a backbone of the membrane. The carrier molecule is a complexing agent or an ion exchanger which can transport the target chemical species from the feed to the receiving side of the PIM. Sometimes other components such as plasticizers and/or modifiers are added to produce flexible membranes by lowering the glass transition temperature (T_g) and/or to improve the solubility

of the adduct of the extracted target species and the carrier within the membrane liquid phase [60, 61]. The following sections will provide more information on each PIM component.

3.4.1. Base polymers

Polymers that are used in PIMs are thermoplastic. The two factors which provide the mechanical strength to a thermoplastic membrane are intermolecular forces and the process of entanglement. Intermolecular forces determine the flexibility and high intermolecular forces lead to a rigid membrane. Poly(vinyl chloride) (PVC) and cellulose triacetate (CTA) are two of the more commonly used base polymers, as they are compatible with different extractants and can be dissolved in volatile solvents and the corresponding solutions can be used for casting PIMs.

CTA is a polar and highly crystalline polymer with a large number of hydroxyl and acetyl groups [62]. The presence of these polar functional groups favours the formation of hydrogen bonds [43]. CTA has a wide range of compatibility with different types of extractants [63, 64] as demonstrated later in this Chapter. In some cases, if the extractant does not act as a plasticizer, a separate plasticizer should be introduced to allow the casting of a flexible and homogeneous membrane. CTA-based PIMs have been studied for extracting different inorganic and organic ions and other organic compounds. However, CTA-based membranes have limited applicability when highly acidic aqueous solutions are used, as under such conditions CTA is readily hydrolysed [65, 66].

The presence of the C-Cl functional groups in PVC makes it polar. Non-specific dispersion forces dominate the intermolecular interactions and make the polymer amorphous with a small degree of crystallinity. Like CTA, PVC is also a very extensively used polymer for preparing PIMs due to its compatibility with different extractants and ability to produce mechanically stable membranes. PVC-based PIMs have been used for different applications which are discussed later in this Chapter. Under some extreme conditions, such as highly basic feed or receiving solutions, PVC undergoes dehydrochlorination that alters its chemical structure [67].

In order to broaden the applicability of PIMs so that they can be used under highly acidic or basic conditions, different polymers such as poly(vinylidene fluoride) (PVDF) and poly(vinylidene fluoride-co-hexafluoropropylene) (PVDF-HFP) have been tested recently as base polymers. PVDF is a semi-crystalline polymer which has been selected as a base polymer

in PIMs because of its high hydrophobicity and low surface energy. With the incorporation of the hexafluoropropylene unit in PVDF, the degree of crystallinity of the polymer is reduced. This change in the crystallinity makes PVDF-HFP-based membranes more flexible than their PVDF counterparts. Both base polymers have been tested with different extractants. Guo et al. have reported PIMs composed of PVDF and ionic liquids with long reusability and higher fluxes compared to other PIMs and SLMs when Cr(VI) was the target species [68]. Turgut et al. have reported another PVDF-HFP-based PIM for the Cr(VI) removal using ionic liquids with different alkyl-chains, and have discussed the alkyl-chain length effect on the membrane performance and morphology [69]. PVDF-HFP-based PIMs containing Aliquat 336 as the extractant have also been evaluated by O'Bryan et al. for their applicability in extracting inorganic ions such as thiocyanate [70]. These researchers have demonstrated the higher stability of PVDF-HFP-based PIMs and their ability to extract and back-extract thiocyanate at a much higher rate than PVC-based PIMs.

3.4.2. Extractants (carriers)

In a PIM, the base polymer does not play an active role in the extraction process, but it provides mechanical support for the membrane liquid phase which consists of the extractant and in some cases may include a plasticizer or a modifier. The extractant is often an ion-exchanger or a complexing agent and is responsible for the extraction and/or transport of the target species [58]. The resulting ion-pair or complex solubilised in the membrane liquid phase is transported across the membrane driven by its concentration gradient. Most of the extractants used in PIMs are those used in solvent extraction and there is a recent trend of synthesising new highly selective extractants for various target chemical species [71, 72]. There are many extractants which have been used in PIMs and they are categorised as acidic, basic, neutral, and chelating. In general, basic extractants are salts with an amine functional group such as quaternary alkylammonium salts and protonated tertiary alkylamines. Aliquat 336, a commercial solvent extraction reagent, is often classified as a basic extractant. Several authors have reported the use of Aliquat 336 for extracting and separating different metal ions such as Co(II), Cd(II), Fe(III), Cu(II), Cr(VI), Pt(IV), and Au(III) under different experimental conditions [73-76]. Since Aliquat 336 also has plasticizing properties it can be used with different base polymers without the addition of a separate plasticizer. Other basic carriers that have been used are tri-n-octyl amine (TOA) and tri-n-hexyl amine (THA) [77, 78]. An example of a neutral extractant

is tri-n-butylphosphate [79]. Extractants which are categorised as acidic and chelating carriers belong to a different class of organic compounds such as organophosphoric acids (e.g., di-(2-ethylhexyl) phosphoric acid (D2EHPA), Cyanex 272, Cyanex 301), sulfonic acids (e.g., DNNS), carboxylic acids (e.g., Lasalocid A, N-6-(t-dodecylamido)-2-pyridinecarboxylic acid (t-DAPA)), quinolines (e.g., Kelex 100), and hydroxyoximes (e.g., LIX reagents) [80-87]. Acidic carrier mediated extraction and transport of a metal cation is governed by the exchange of the metal ion for protons of the carrier [43]. Because of this, the pH of the source solution is an important parameter to control the effectiveness of the separation process. In addition, careful pH control of the source solution can result in good PIM extraction selectivity which will be similar to that of the corresponding solvent extraction system. Another group of extractants includes macromolecular compounds such as crown ethers, calixarenes, and cyclodextrins. These extractants are usually expensive and therefore not particularly suitable for large scale solvent extraction processes, however, they can possibly be used in preparing PIMs where only relatively small amounts of extractants are required. The hydrophobic nature of these macromolecular extractants makes them much less soluble in aqueous solutions than other extractants which improves the PIM reusability. A considerable number of research papers have reported on PIMs with macromolecular carriers for alkali and alkaline earth metal ion extraction and separation [88-90]. Recently they have been applied to separate radioactive metal ions as well [90, 91]. The fact that the structures of these carriers can be tailored to a particular metal ion has attracted considerable interest, although the majority of these extractants are not commercially available.

3.4.3. Plasticizers and modifiers

As already mentioned above, sometimes a plasticizer is also incorporated in the membrane composition if the extractant cannot plasticize the PIM adequately. A plasticizer decreases the glass transition temperature of the polymeric membrane and thus improves its flexibility [58]. Plasticizers improve the compatibility between membrane components by shielding the polar groups present in the base polymers and increasing the inter-chain distances [43]. Two physiochemical properties of the plasticizer, namely its viscosity and polarity, largely contribute to its effect on the membrane structure and properties. It has been suggested that the initial flux value should increase with the polarity and decrease with the viscosity of the plasticizer. O-nitrophenyl octyl ether (NPOE) and o-nitrophenyl pentyl ether (NPPE) are

among the most commonly used plasticizers. Other frequently used plasticizers are dibutyl phthalate (DBP), dioctyl phthalate (DOP) and bis(2-ethylhexyl) adipate (DEHA) [78, 92-94]. Another component which is added occasionally to the membrane composition is a modifier, which improves the solubility of the target species - extractant adduct in the membrane liquid phase. Long alkyl chain alcohols such as 1-dodecanol and 1-tetradecanol are commonly used as modifiers [60]. Cho et al. have used 1-tetradecanol as a modifier in preparing a PIM containing PVC as the base polymer and Aliquat 336 as the extractant [95].

4. Techniques used for characterization of PIMs

Several techniques can be employed to study and characterize PIMs in terms of extraction/transport efficiency, morphology and thermal properties. This section describes the basics of the most commonly used techniques to optimize and characterize PIMs.

4.1. Extraction and transport

PIMs are designed to conduct a similar separation process as achieved by solvent extraction. The capability of extracting different chemical species is a basic feature of a PIM and is an attractive alternative to solvent extraction. One of the major advantages of the PIM-based separation process is the simultaneous extraction and back-extraction of a target chemical species that is achieved in a transport configuration. However, separate extraction and back-extraction is also often applied in PIM studies. The evaluation of a PIM's performance in terms of efficiency of extraction and/or transport of a particular chemical species is performed by monitoring the transient concentrations of the target chemical species in the feed and receiving solutions.

Extraction experiments are conducted by immersing the PIM of appropriate size, thickness and mass inside a suitable container (e.g., beaker, glass jar) containing an aqueous feed solution of the chemical species of interest. To ensure proper mixing of the feed solution throughout the extraction process, the PIM and feed solution need to be agitated vigorously. This is usually done in two common ways: a) using an orbital shaker or b) by placing a magnetic stirrer bar inside the jar positioned on a magnetic stirrer. A small volume of the feed solution is removed at pre-selected time intervals to monitor the extraction process. After completion of the extraction experiment, the membrane loaded with the target chemical species is removed and

placed in a jar containing a receiving solution, if recovery of the extracted chemical species is required. A schematic of a batch extraction system is shown in Figure 4.

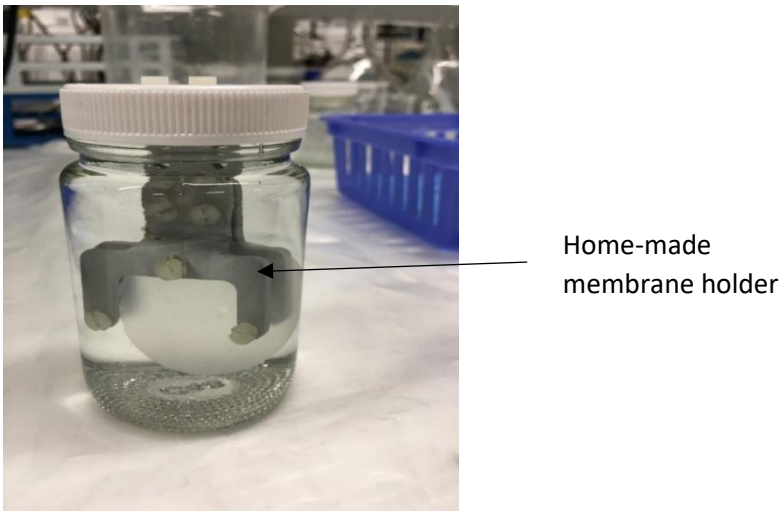

Figure 4. Photographic image of a batch extraction experimental setup where the PIM is immersed in a jar containing the feed solution and is supported there by a home-made membrane holder.

In a transport experiment, the PIM is sandwiched between two gaskets and is placed in a two-compartment transport cell with one compartment containing the feed solution and the other the receiving solution as shown in Figure 5, along with a schematic of generic facilitated transport mechanism. Both the feed and receiving solutions are stirred throughout the transport experiment using mechanical stirrers. In the general case, the temperature of both solutions can be controlled by using a jacketed transport cell connected to a water bath, nevertheless experiments were performed in an airconditioned laboratory at a constant temperature of 21^{o}C and therefore the cells used for the transport experiments described in this thesis were non-jacketed.

(a) **(b)**

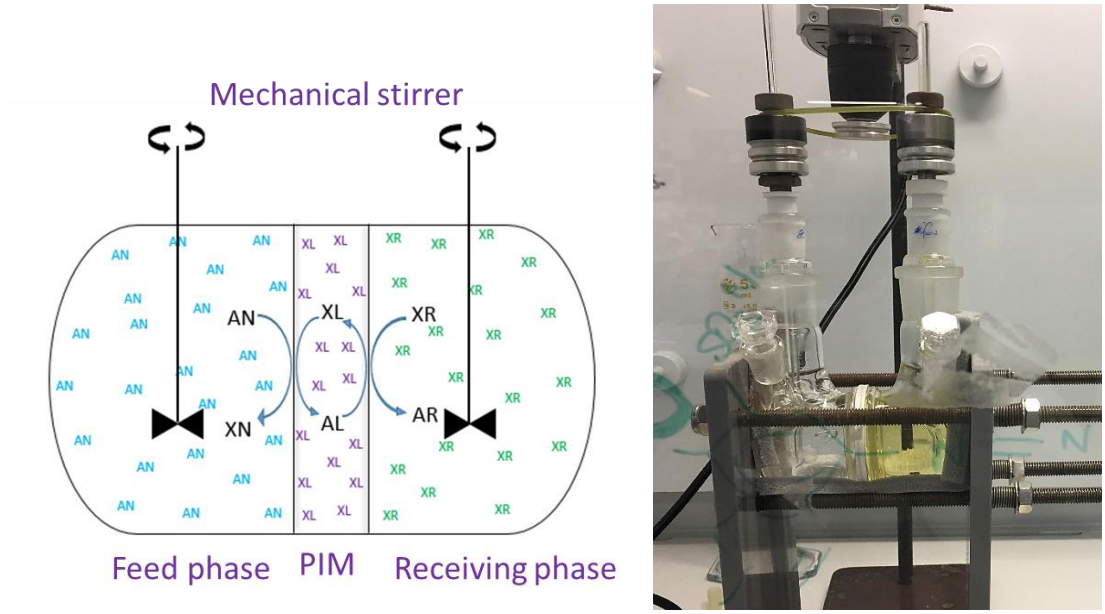

Figure 5. (a) Schematic presentation of a transport cell and a generic PIM facilitated ion-exchange transport mechanism in the case of a monovalent target cation (A^+). N^-, counter anion; X^+L^-, ion-exchange extractant (carrier); X^+R^-, stripping reagent. (b) Photographic image of the transport cell set up in the laboratory.

4.2. Analytical measurements

The efficiency of the extraction and transport processes is monitored by measuring the target chemical species concentration at preselected time intervals, and different techniques or instruments can be used for this purpose. Metal ions are generally analysed by atomic absorption spectrometry (AAS) or inductively coupled plasma optical emission spectrometry (ICP-OES). In some cases, spectrophotometry is used where metal ions form coloured complexes in the presence of colorimetric reagents [96]. Also, colorimetric reactions can be performed in an automatic fashion by using flow injection systems to determine inorganic ions such as SCN^- or NH_4^+ [97, 98]. Organic chemical species are often measured by techniques

such as gas chromatography (GC) or high performance liquid chromatography (HPLC) with flame-ionization, conductivity or UV-Vis diode array detection [64, 99, 100].

As this thesis is mainly focused on metal ion separation, AAS and ICP-OES will be discussed in more detail in the following sections.

Fourier transformed infrared spectrometry is very widely used analytical technique which can provide information related to the different types of chemical bonds present in a molecule. This technique has been used extensively in the research, reported in this thesis, to elucidate the structural details of chemical species present in the PIMs studied.

4.2.1. AAS and ICP-OES

The phenomenon of light absorption of atoms in a flame or atomic cloud is the basis of AAS [101]. AAS as an analytical technique was first developed by Alan Walsh in 1955 [102] with the use of flame to atomise the sample and in 1960 flame AAS was used for the determination of the calcium content in blood serum [103, 104].

An atomic absorption spectrometer consists of four essential parts: a hollow cathode lamp as the light source, a pre-mix burner for flame AAS or graphite furnace for electrothermal AAS, a grating monochromator, and a photomultiplier as the light detector. The hollow cathode lamp for a particular metal emits radiation characteristic of this element because its cathode is made of this metal. In the flame of the pre-mix burner or graphite furnace (in case of flame AAS or electrothermal AAS, respectively) the sample is atomised, and the unexcited atoms absorb the radiation emitted from the hollow cathode lamp. The monochromator is tuned to allow light with the analytical wavelength to pass through it and reach the light detector where its intensity is measured and used for calculating the absorbance which according to Beer's law is directly proportional to the concentration of the analyte metal ion in the sample [104, 105].

In ICP-OES the emitted radiation from excited atoms of different elements in the plasma torch of the spectrometer is measured and related to their concentrations in the sample thus allowing simultaneous multielement determinations at the nanogram/millilitre level [106]. The plasma temperature ranges from 7000 to 10000 K and the emitted radiation can also be used to identify the elements in the sample [107, 108].

These two techniques were used to monitor the concentration of the target species in the feed and/or receiving solutions during extraction, back-extraction and transport experiments.

4.2.2. FT-IR

Infrared spectroscopy is a very popular analytical technique for material characterization [109, 110]. IR spectra of molecules are like their fingerprints. Therefore, this technique can assist in identifying chemical species. Most interferometers in FT-IR instruments employ a beam-splitter which splits the incoming infrared beam into two optical beams. One of the beams is reflected from a fixed flat mirror and the other beam is reflected from a movable (typically a few millimetres) flat mirror. The two reflected beams are recombined once they meet again at the beam-splitter. As the two beams travel different pathlengths, interference of these two beams produces a signal in the interferometer. The resulting signal is called an interferogram which has the unique property that every data point (a function of the moving mirror position), which makes up the signal, contains information about every infrared frequency emitted from the source. This signal is processed using a mathematical technique called Fourier transformation and a frequency spectrum is generated.

FT-IR has been used very extensively to study polymerisation processes [111, 112]. In the present study FT-IR has been used to monitor the presence of particular chemical bonds related to the presence of specific chemical species of interest.

4.3. PIM morphology

The word morphology in Greek means the study of shapes. Studying the morphology of a material using modern techniques can reveal its micro- to nano-level structural details. This information provides a better insight into the material properties and can lead to discovering new applications. Different techniques such as atomic force microscopy (AFM), scanning electron microscopy (SEM), scanning tunnelling microscopy (STM), and transmission electron microscopy (TEM) have been extensively used in morphological analysis of materials [113, 114].

AFM is a very popular surface analysis technique for versatile range of surface characterisations [115-117]. The advantage of this technique over other surface analysis

techniques is the elimination of the usual sample preparation step. The sample surface does not need to be conductive to be imaged (e.g., SEM) and thus sample coating with a conductive material is not required [118, 119]. This technique works on the basis of the interaction force between the tip of the cantilever and the sample surface. The cantilever scans over the sample surface and its tip is subject to a force which depends on the tip to surface distance. Therefore, during the scan, the cantilever deflects inward or upward. The deflection of the cantilever changes the position of the reflected beam on the photodetector. The signal received by the photodetector is then processed by the computer to reveal the surface morphology (Figure 6). In most AFM studies, three types of morphological data are generally obtained and these are topography, phase image and height.

Morphology of the PIMs are examined to understand the structural changes that have occurred within the membrane due to the in-situ cross-linking of the different monomers/oligomers tested. Topography images of the PIMs are assessed for roughness and surface area evaluation.

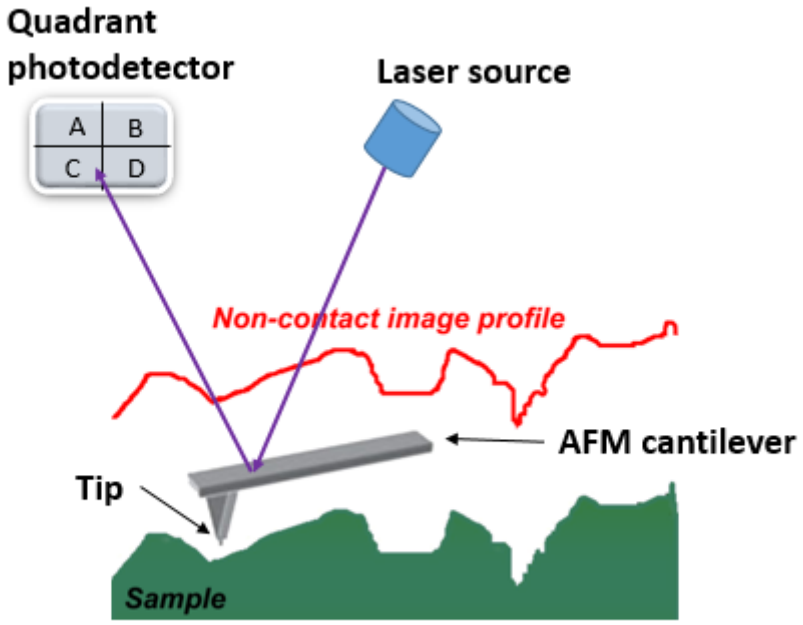

Figure 6. Schematic presentation of the working principles of atomic force microscopy (AFM)[120].

4.4. Thermal analysis

Thermal analysis comprises a family of measuring techniques which measure the response of a material being cooled or heated. This information allows the establishment of relationships

between temperature and specific physical properties of the material. The most popular thermal analysis techniques are thermogravimetric analysis (TGA), differential scanning calorimetry (DSC), thermomechanical analysis (TMA), and dynamic mechanical analysis (DMA) [121].

Differential scanning calorimetry (DSC) is commonly referred to as the "workhorse" of thermal analysis. In DSC the heat flow rate difference between the material studied and a reference is measured as a function of the temperature, while subjected to a controlled temperature program. This technique is commonly used in the polymer and pharmaceutical industries [122]. The simple and fast determination of the glass transition temperature, the heat of fusion, the heat of reaction, the heat capacity, melting and crystallisation temperatures, are just a few applications of DSC. In thermal analysis, the temperature and the mass of the sample material are the only measured properties. All other details are calculated from the temperature change using different thermodynamic equations. The enthalpy change is calculated from the temperature difference between the sample material and the reference. The enthalpy of the system increases during an endothermic process (melting, absorption) while it decreases during an exothermic process (condensation, crystallisation).

In DSC the sample and reference material (inert aluminium oxide) are heated at a linear heating rate. The heating and cooling rate are very important and can affect the quality of the results. Faster heating can save considerable amount of time, but it influences the DSC curves' shape and the subsequent results calculated from them [123, 124].

In TGA, the mass of a sample is measured while heating it at a constant rate [121]. The heating range varies from ambient temperature to about 1000 ^{o}C and the measurements are conducted in an inert atmosphere created by flowing purge gas containing nitrogen, argon or helium. It is also worthy to mention that heating in air is also conducted in certain cases. Mass loss of the samples during heating proceeds in different steps as volatile components are lost. In case of a polymer, general degradation proceeds by a free radical path initiated by bond dissociation at the temperature of pyrolysis. Obviously, this path is different for different polymers and is related to their structure. In order to precisely describe the mass loss and determine the degradation mechanism, TGA is often used in a combination with evolved gas analysis measurements. The most frequently used methods of determining the evolved gases are mass spectroscopy and Fourier transformed infrared spectroscopy (FT-IR) [125-127].

Simultaneous TGA/DSC analysis has several advantages over separate TGA and DSC measurements [128]. The main advantages include the removal of potential ambiguities in the

interpretation of the results that might arise from differences in the samples, atmospheric conditions, temperature, and other variables [129, 130].

5. Applications of PIMs

From the very beginning of their development PIMs have been widely used to extract metal ions, inorganic anions and small organic molecules from aqueous media [131]. They have been used to treat synthetic nuclear waste arising from nuclear reactors [90]. They have also been used in chemical sensing for more than 40 years as the polymeric membranes in ion-selective electrodes (ISEs) [132].

5.1. PIMs in chemical sensing

Liquid membranes were used initially as ion-selective membranes in ISEs [133]. Early commercial ISEs employed SLMs where the liquid phases were composed of a liquid ion-exchangers such as the calcium salt of bis(di-n-decyl) phosphoric acid dissolved in di-n-octylphenylphosphonate for sensing the Ca^{2+} ion and long chain alkylammonium salts in NPOE for sensing common anions [134]. Later the organic liquid phase was immobilised in PVC [135]. These polymeric membranes, which by definition are essentially PIMs (except that for ISEs a lower amount of extractant is required), have also been applied in optical chemical sensors (optodes) [136, 137]. In recent research on membrane-based sensors the focus has been on further decreasing the limit of detection. The use of carbon nanotubes (CNTs) in the construction of ISEs has made them capable of detecting nanomole to femtomole concentrations which is comparable to the ICP-OES techniques [138]. Plasticizer free membrane preparation techniques have also been developed using methacrylate co-polymers [139, 140]. A PIM based electrochemical sensor has been developed by Apostu et al. for the quantitative determination of ranitidine, famotidine and nizatidine [141]. Silva et al. have described the use of PIMs for in-situ gold nanoparticle synthesis and applied these PIMs for the detection of salmonella typhimurium [142]. Ohshima et al. have reported the application of PIMs as a sorbent in a flow injection analysis system [143]. The PIM used in this study was composed of PVC, Aliquat 336 and 1-tetradecanol and was used to coat the internal walls and packing of a preconcentration column to enhance the sensitivity of the corresponding flow analysis system to measure thiocyanate as an impurity in ammonium sulfate fertilizer. The

PIM-based electromembrane extraction (EME) process was also adopted by Cristina et al. to extract non-steroidal anti-inflammatory drugs (NSAIDs) and highly polar acidic drugs [144]. The optimized PIM containing 29 wt% CTA and 71 wt% Aliquat 336 was capable of extracting NSAIDs (salicylic acid, ketoprofen, naproxen, and ibuprofen) and four highly polar acidic drugs (anthranilic acid, nicotinic acid, amoxicillin, and hippuric acid) simultaneously with a recovery percentages ranging between 81% and 34%. Pantuckova et al. have demonstrated, for the first time microextraction across a PIM as a separation method for clinical analysis [99]. The microextraction device with the PIM was coupled to a commercial capillary zone electrophoresis (CZE) instrument which ensured complete automation of the entire analytical procedure consisting of formate extraction, injection, CZE separation, and quantification.

5.2. PIMs for sample pre-treatment

Sample pre-treatment is an important step in chemical analysis. It is often hard to measure a particular analyte in a mixture containing interferants or at a low concentration. Sample pre-treatment plays an important role in minimising interferences and improving sensitivity. This is particularly true for the analysis of pharmaceutical, clinical and environmental samples. Modern instruments can achieve very low detection limits; however, these can still be too high to satisfy particular requirements, and pre-concentration of the analyte is a necessity. In addition, the sample volume available is sometimes limited, and samples often have complex matrices and need to undergo pre-treatment for the removal of interferences. Traditional sample pre-treatment techniques such as liquid-liquid extraction (LLE) and solid-phase extraction (SPE) are time consuming and often use harmful volatile organic solvents [145]. Liquid membranes such as PIMs have proven their efficiency in sample pre-treatment for analytical purposes [146]. An encapsulated carrier molecule in a PIM can simultaneously allow extraction and back-extraction of the analyte of interest which will assist in eliminating an interfering species as well as in pre-concentrating the analyte prior to measurement. PIMs can be used in two different modes, namely, off-line and on-line. In the off-line mode, samples are collected manually from the receiving phase and subsequently analysed by an appropriate instrument, whereas in the on-line mode no such manual involvement is necessary. Flow injection analysis is such an on-line technique where it is possible to separate, pre-concentrate and measure the analyte automatically [147, 148]. Nagul et al. have reported a PIM-based system to determine orthophosphate under flow injection and continuous flow conditions [149]. The membrane was

composed of PVC and Aliquat 336 and the continuous flow system was able to measure phosphate in the μg L^{-1} range using the multipoint standard addition method. Mamat and See have designed a PIM system for EME to replace the existing SLM in a device for the pre-treatment step of matrix removal prior to the quantification of different drugs [150]. The authors selected the three basic drugs amphetamine, methamphetamine, and 3,4-methylenedioxy-N-methylamphetamine and studied the extraction of these drugs from human plasma using a PIM comprised of CTA, tris(2-ethylhexyl) phosphate (TEHP) and D2EHPA. The same authors have also applied this PIM to extract cationic and anionic herbicides present in river water samples using the same EME system but integrating it with bubbleless electrodes [151].

5.3. PIMs for pollution monitoring

PIMs can be used as the semi-permeable barrier of passive sampling devices [133, 152]. These devices allow the measurement of the time-weighted average concentration of an analyte in an aqueous medium such as a lake, river or drain. Unlike spot sampling, where the collection and analysis of numerous discrete spot samples require significant time and labour, passive sampling involves continuous accumulation of the analyte of interest over a certain sampling period of time and the accumulated amount can be used for calculating the time-weighted average concentration of the analyte of interest over the sampling period [153]. A PIM-based passive sampling device has some advantages over other passive samplers such as Chemcatcher®, semipermeable membrane devices (SPMDs) or polar organic chemical integrative samplers (POCISs) [153-156]. In a PIM-based passive sampler, the analyte of interest is automatically back-extracted into the stripping solution which opens the possibility of on-site analysis of the receiving solution (e.g., by using paper-based analytical devices [157]). Moreover, if the extractant used and the receiving solution are acidic, this protects the PIM from biofouling, which is one of the disadvantages of other passive samplers. Garcia-Rodríguez et al. have also reported a PIM-based passive sampling device for monitoring sulphamethoxazole, one of the most frequently detected antibiotics in wastewater treatment plant effluents and environmental waters [158].

5.4. PIMs for extraction and separation of metallic and non-metallic species

PIMs have been widely applied in the extraction and separation of different metallic and non-metallic species with the potential to replace industrial solvent extraction applications. This is reflected by the increasing number of publications in the last two decades. Nghiem et al. and Almeida et al. have comprehensively reviewed and summarised the research focusing on PIMs' applications for metal and non-metal separation until 2012 [43, 58]. Examples of more recent PIM applications are listed in Table 1.

Table 1. Examples of recently developed PIMs for the extraction and separation of metallic and non-metallic species. PIM composition (i.e., base polymer, extractant and plasticizer/modifier) and aqueous phases composition are also provided.

Base polymer	Extractant	Plasticizer/ Modifier	Feed solution (F)	Receiving solution (R)	Applications	References
CTA	D2EHAG and D2EHAF	-	Sulfuric acid / ammonium sulfate buffer solutions	0.5 mol L^{-1} H_2SO_4	Sc(III) separation in the presence of Y(III), La(III), Nd(III), and Dy(III)	[159]
CTA or PBAT	Aliquat 336	-	10 mg L^{-1} of Cr(VI) in 0.1 mol L^{-1} HCl	0.1 mol L^{-1} NaOH	Transport of Cr(VI)	[160]
CTA or PVC	Cyphos IL 101, 104 or 167	NPOE	1.5 mmol L^{-1} Zn(II) in 0.58 mol L^{-1} HCl, 5 mol L^{-1} Cl^-	1 mol L^{-1} H_2SO_4	Transport of Zn(II)	[161, 162]
CTA	p-Tert-butyl calix[4]arene	NPPE	5 mol L^{-1} metal ions	Deionised water	Selective transport of Pb^{2+}	[163]
CTA	DABA, TABA, PABA or SABA	DOP	Mixture of metals at pH 4.1	3.0 mol L^{-1} HCl	Selective transport of Cr(III). Selectivity order: Cr(III) > Co(II) > Ba(II) > Sr(II)	[164]

Base polymer	Extractant	Plasticizer/ Modifier	Feed solution (F)	Receiving solution (R)	Applications	References
CTA	TOMATS and TOMAS	NPOE	1 mg L^{-1} Hg	1 m mol L^{-1} cysteine	Hg preconcentration	[165]
CTA	D2EHPA and TBP	NPOE	0.01 mol L^{-1} $La(NO_3)_3$ and $Ce(NO_3)_3$	2 mol L^{-1} H_2SO_4	Recovery of lanthanum(III)	[166]
CTA	Aliquat 336 or Cyphos IL 101	-	HCl (F)	HCl (R) (concentration ratio F:R = 5)	Waste acid recovery	[167]
CTA		NPOE	River water containing pesticides (chlorpyrifos, diazinon and cyprodinil)	1 mL acetonitrile	Recovery of pesticides prior to GC-MS detection	[100]
PVC	β-Cyclodextrin	DBP	Ibuprofen (20 mg L^{-1}) in deionized water or progestron (20 mg L^{-1}) in deionized water/ethanol (60/40 v/v)	-	Pharmaceutical pollutant removal from wastewater	[168]

Base polymer	Extractant	Plasticizer/ Modifier	Feed solution	Receiving solution	Applications	References
PVC	Cyphos® IL 104	1-Dodecanol	100 mg L^{-1} in 2.5 mol L^{-1} HCl	0.10 mol L^{-1} Na_2SO_3	Extraction and back-extraction of Au(III)	[169]
PVC	DNNS	1-Tetradecanol	Metal ions in 0.001 or 0.1 mol L^{-1} HCl	-	Extraction of different metal ions	[170]
PVC	2-hydroxy-5-nonyl-benzaldoxime (M5640)	NPOE	Mix metal at pH 4.5	0.5 mol L^{-1} H_2SO_4	Recovery of Cu(II) from Ni(II), Co(II), and Zn(II)	[171]
PVDF-HFP	LIX84I	NPOE	1 mmol L^{-1} copper sulfate and 75 mmol L^{-1} ammonium sulfate at a pH of 8.5	1 mol L^{-1} H_2SO_4	Extraction and transport of Cu(II)	[172]
PVDF-HFP	Cyphos® IL101	NPOE	50 mg L^{-1} V(V)	6 mol L^{-1} H_2SO_4	Selective extraction of vanadium(V)	[173]
PVDF and CTA	D2EHPA	Tris(2-ethylhexyl) phosphate	50 mg L^{-1} solution of Zn, Pb and Ni	Distilled water	Selective transport of Ni(II), Zn(II) and Pb(II)	[174]

Base polymer	Extractant	Plasticizer/ Modifier	Feed solution (F)	Receiving solution (R)	Applications	References
PVDF	Aliquat 336	-	100 mg L^{-1} of As(V)	-	Removal of As(V)	[175]
PVC	D2EHPA	Bis(2-ethylhexyl) adipate	5 mmol L^{-1} Zn(II) and 4 mmol L^{-1} $NaNO_3$ at pH 1.61	0.1 mol L^{-1} HNO_3	Separation of Zn(II)	[176]
PVC	D2EHPA	-	120 µmol L^{-1} Ln(III) (pH - 0.5 to 2.25)	0.3 – 7 mol L^{-1} H_2SO_4	Separation of Yb(III), Gd(III) and La(III)	[177]

D2EHAG: N-[N, N-di (2-ethylhexyl) aminocarbonylmethyl] glycine, D2EHAF: N-[N, N-di (2-ethylhexyl) aminocarbonylmethyl] phenylalanine, DABA: 2-dodecanamidobenzoic acid, LIX841: 2-hydroxy-5-nonylacetophenone oxime, PABA: 2-palmitamidobenzoic acid, PBAT: poly (butylene adipate-co-terephthalate), PMA: phosphomolybdic acid, SABA: 2-stearamidobenzoic acid, TABA: 2-tetradecanamidobenzoic acid, TBP: tributyl phosphate, TOMA: methyltrioctylammonium chloride, TOMAS: trioctylmethylammonium salicylate, TOMATS: trioctylmethylammonium thiosalicylate.

Wang et al. have reported the effective Cu(II) transport using PIMs composed of PVC as the base polymer and LIX 84-I as the carrier [178]. They reported a significant enhancement in the extraction and back-extraction PIM efficiencies for Cu(II) when 30 wt% of the plasticizer NPOE was included in the membrane composition. Wang et al. have also compared the role of different base polymers such as PVC, CTA and PVDF-HFP in separating Cu(II) from its ammonium sulfate/ammonia solutions at pH 8.5 [179]. It has been reported that only the PVDF-HFP-based PIM was suitable in separating Cu(II) under the conditions mentioned above without affecting the membrane integrity. Yildiz et al. have tested the applicability of Alamine 336 as an extractant to produce a homogeneous PIM with CTA as the base polymer [180]. The resulting membrane was examined for the separation of Cu(II), Cd(II), Co(II), and Ni(II). Co(II) separation was studied by Manzak et al. using a CTA-based PIM containing Aliquat 336 as the extractant. From the acidic feed medium (100 mg L^{-1} Co(II) + 100 mg L^{-1} Ni(II)), 95.7% Co(II) was separated into the receiving solution. Another extractant, named N,N,N′,N′-tetra-n-octyl diglycolamide, TODGA, was introduced by Mahanty et al. in preparing a PIM containing CTA as the base polymer and NPOE as a plasticizer [71]. The PIM's performance was studied for the separation of actinide ions such as Am^{3+}, Pu^{4+}, UO_2^{2+}, and Th^{4+} from acidic feed solutions. The amount transported across the PIM followed the order $Am^{3+} > Pu^{4+} > Th^{4+} > UO_2^{2+}$ when the feed solution contained nitric acid (1-3 M) and the receiving solution contained alpha-hydroxy-iso-butyric acid (AHIBA). Kubota et al. and Bonggotgetsakul et al. have reported two different PIM systems for recovering gold from electronic waste using the synthesized extractant N-[N,N-di(2-ethylhexyl)aminocarbonyl-methyl]glycine (D2EHAG) and the commercially available extractant Cyphos® IL 104, respectively [72, 181]. Both PIMs showed promising results in the selective and quantitative separation of Au(III) from digested electronic waste.

PIMs are not only limited to metal ion separation since they can also be used to separate different inorganic anions and organic and bio-organic compounds. Schmidt-Marzinkowski et al. have investigated the extraction process of different inorganic anions using CTA-based PIMs [182]. Aliquat 336 was incorporated in the membrane to extract ions with low lipophilicity such as phosphate whereas no such carrier was required to extract highly lipophilic ions such as perchlorate in an electric field driven process. A PVDF-HFP-based PIM containing Aliquat 336 has been reported by O'Bryan et al. to extract thiocyanate from aqueous feed solutions [183]. The same authors also compared the performance of previously developed PIMs with a newly developed cross-linked PIM for the transport of thiocyanate [184]. PIMs

have also been reported by Almeida et al. to be capable of extracting ammonia [97]. In this study, the authors have screened different membrane compositions and best results were achieved with PIMs containing either 70 wt% CTA and 30 wt% commercial dinonylnaphthalene sulfonic acid (DNNS) or 80 wt% PVC, 10 wt% DNNS and 10 wt% 1-tetradecanol. Przewoźna et al. have studied the use of PIMs for the separation of different organic acids such as lactic, tartaric oxalic and succinic acids [108]. They used a PIM composed of CTA as the base polymer and 1-alkiloimidazole as the carrier to study the effect of the PIM composition on the transport rate of the selected organic acids to produce a cost effective and environmentally benign process for succinic acid separation. Pratiwi et al. produced a PIM made of PVC and Aliquat 336 which was able to separate succinic acid from a feed solution of pH 4 using Na_2CO_3 as the stripping reagent [109]. The extensive use of phenol in industrial processes has caused a major environmental concern and the removal of phenol from wastewater is of utmost priority. PIMs have been developed to remove phenol from aqueous solutions and polluted water. Perez-Silva et al. have developed a PIM containing CTA as the base polymer, Cyanex 923 as the carrier and NPOE as a plasticizer [110]. The resulting PIMs were employed to remove phenol from feed solutions of different pH using NaOH as a stripping reagent. Kiswandono et al. have also reported the use of copoly(eugenol-divinylbenzene) (DVB) as the carrier to transport phenol through a membrane using a $NaNO_3$ striping solution [185]. PIMs have also been used for gas permeation and for fuel cells by Farrukh et al. and Hernández-Fernández et al., respectively [186, 187]. Antibiotics are very widely used drugs which are now considered as emerging organic contaminants as the presence of antibiotics in natural waters is of great concern [64]. Benavente et al. have developed a PIM composed of CTA, Aliquat 336 and NPOE to transport six frequently used antibiotics (four sulfonamides and two tetracyclines) [188].

The development of PIMs continues to grow exponentially. However, there are still a few challenges to overcome, namely further improving PIMs permeability and stability. One strategy proposed to achieve this consists of cross-linking the polymeric structure of PIMs [189].

6. Cross-linking process

In polymer chemistry, cross-link is the formation of a bond that links two neighbouring units [190-192]. A schematic presentation of a generic cross-linking process is shown in Figure 7. The newly formed cross-linking bond can be of different nature such as O-O, O-Si, Si-Si, O-C, or C-C depending on the types of cross-linking agents present in the system [193-197].

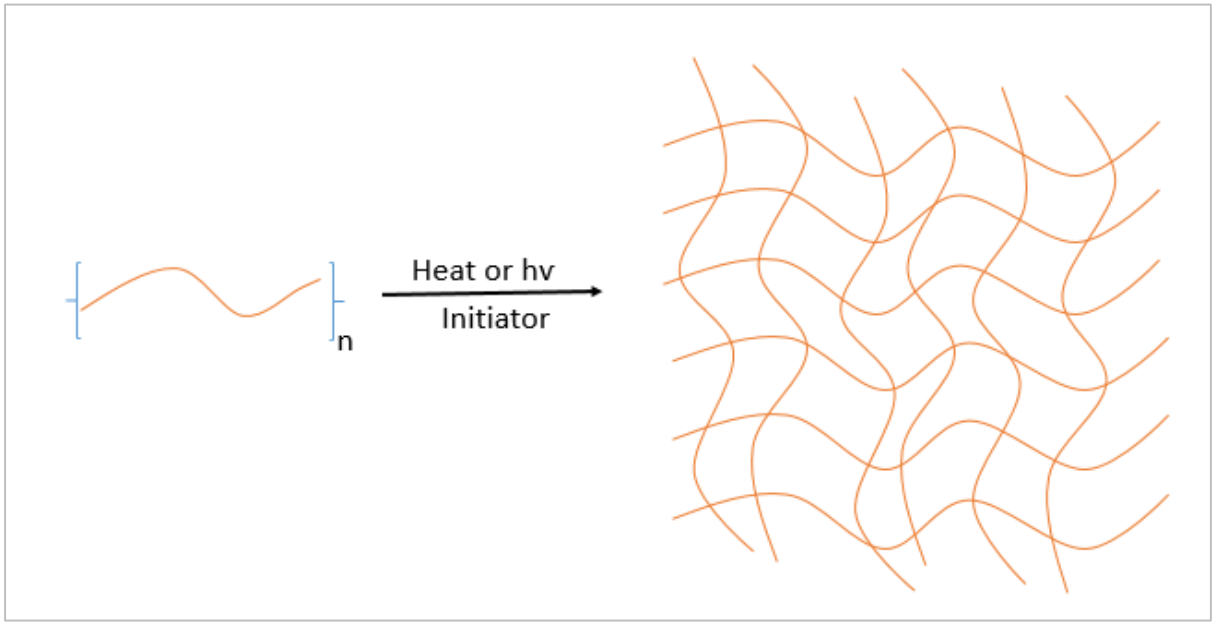

Figure 7. Schematic presentation of a cross-linking process.

Cross-linking among different neighbouring monomer/oligomer proceeds with the aid of external stimuli, such as heat or light, and a chemical initiator. Photoinduced cross-linking is more versatile and effective compared to thermal cross-linking which exhibits disadvantages such as low conversion rate, coloration and brittleness [184, 198]. In a photoinduced cross-linking system the photo-initiator absorbs incident light of appropriate wavelength which promotes it to an electronically excited state. The excited initiator subsequently decomposes to generate reactive free radicals or ions which initiate the polymerisation process [199, 200]. The rate of initiation (r_i) depends on parameters such as intensity of incident light (I_o), sample thickness (l), quantum yield of initiation (Φ_i), molar absorptivity (ε), and concentration of the photo-initiator [PI]. The rate of initiation can be described by the following equation:

$$r_i = \Phi_i . I_o \, [1-\exp(-\varepsilon . l . [PI])] \quad (1)$$

After the initiation of polymerisation, the propagation step proceeds very fast by attaching neighbouring multifunctional monomers/oligomers in all directions and yields a three-dimensional cross-linked polymer network. There are two major paths of polymerisation processes which are photo-initiated radical polymerisation and photo-initiated cationic polymerisation. Different types of acrylate-based monomers/oligomers polymerise in the radical polymerisation path [193]. It has also been reported that maleimide based monomers/oligomers also follow the radical polymerisation path without the presence of an initiator [201-203]. Maleimide molecules get excited by absorbing radiation and produce radicals which abstract labile hydrogen from the neighbouring donor molecules (e.g., glucose, isopropanol or 1,1-diethoxyethane). Epoxide and vinyl ether types of molecules, which are inactive to radicals, polymerise in the presence of cations produced from initiators. Cationic polymerisation has a few advantages over radical polymerisation such as this process is not affected by the presence of oxygen and can proceed long after the irradiation has ceased [197, 204, 205].

Cross-linking polymers are modern engineering materials which have high potential in enhancing material quality in diverse coating applications ranging from industry to medicine. The advantage of using cross-linking polymers in coating systems is that they can heal themselves after mechanical damage which is a great advantage in case of long-term applications. There are a lot of membranes based on polyimide (PI) which has outstanding heat resistance and good mechanical strength, as well as chemical resistance to many solvents once crosslinked (imide to amide conversion) [206, 207]. Cross-linked PI backbone structure makes it heat and chemical resistant. Cross-linking polymer based hydrogels are very popular in medicinal chemical applications [111, 208]. Dental curing is one of the major sectors where the crosslinking approach is used for sealing purposes [209]. Applications of hydrogel in drug delivery and tissue engineering are hot topics of research [111, 210]. Hydrogels are also used in load bearing applications due to its high tensile strength and toughness [211, 212]. The use of different types of cross-linking agents (i.e., polymers or monomers) such as polysiloxane, epoxide, maleimide, vinyl ether, and acrylate is often reported in the literature [194, 213, 214]. Different cross-linking agents have their own advantages which is beneficial for some applications. For example, polysiloxane has been reported to have good ionic conductivity at room temperature and can be used for the production of polymer electrolyte membranes [178]. Acrylate and maleimide based cross-linking agents which possess hydrogel formation capabilities are suitable for drug delivery applications [179-181]. Cross-linked resins have

many other applications such as dental filler, fast-drying coating, adhesive, and microlithography [182, 183].

Cross-linking has been widely used to improve the properties of materials, although there is currently only one report on its effect on PIMs [189]. The promising results obtained in this study justify further research.

7. Research aims and thesis structure

As mentioned above, separation based on PIMs is a promising green alternative to traditional solvent extraction by eliminating the use of a large inventory of volatile, toxic and flammable organic diluents. PIMs are more stable than SLMs, the most frequently used liquid membranes at present, and provide similar rates of separation. However, this stability and rates of separation are often still not adequate for industrial applications. The research reported in this thesis is focused on overcoming these deficiencies of PIMs by exploring the potential of cross-linking their polymer backbone.

The thesis consists of 5 chapters presented in a 'thesis by publication' style. The experimental chapters 2, 3 and 4 are written in a style accepted by journals for publication.

Chapter 1 provides an introduction into PIMs and describes their composition, properties and techniques and instrumentation used in their optimization and characterization, followed by a description of the most recent PIM applications. This chapter also provides an insight in the cross-linking process.

Chapter 2 describes the fabrication of cross-linked PIMs, composed of CTA, PVC or PVDF-HFP as the base polymer, D2EHPA as the extractant and PEG-DMA as a cross-linking agent, and their superior extraction properties for Zn(II) compared to non-cross-linked PIMs. This chapter has been published in *Journal of Membrane Science.*

Chapter 3 reports on the development of cross-linked PIMs of the three base polymers mentioned above which incorporate one of three most commonly used cross-linking agents, one of three commonly used photo-initiators and one of the two most commonly used extractants (i.e., D2EHPA or Aliquat 336). The performance of the successful cross-linked PIMs in the extraction of Zn(II) or SCN^- is compared with that of their non-cross-linked

counterparts to illustrate the potential of the cross-linking approach. This chapter has been submitted for publication in *Separation and Purification Technology*.

Chapter 4 reports on the fabrication of cross-linked PIMs incorporating Cyphos® IL104 as the extractant and their application for Au(III) recovery from aqua regia digest of electronic waste. The chapter has been prepared as a manuscript that will be submitted for publication in the journal *Desalination*.

Chapter 5 summarises the main outcomes of the research described in this thesis and proposes directions for future research.

References:

[1] C. Testa, D. Desideri, F. Guerra, M. Meli, C. Roselli, G. Jia, The importance of separation chemistry for the determination of radionuclides in environmental samples, J. Radioanal. Nucl. Chem., 229 (1998) 23-32.

[2] W. Kujawski, A. Warszawski, W. Ratajczak, T. Porebski, W. Capała, I. Ostrowska, Removal of phenol from wastewater by different separation techniques, Desalination, 163 (2004) 287-296.

[3] S. Ahuja, Chromatography and separation science, Elsevier, 2003.

[4] I.L. de Mattos, M.L. de Castro, M. Valcárcel, Pervaporation: An integrated evaporation/gas-diffusion approach to analytical continuous separation techniques, Talanta, 42 (1995) 755-763.

[5] D. Sheorey, A. Dorle, Preparation and in vitro evaluation of rosin microcapsules: solvent evaporation technique, J. Microencapsul, 7 (1990) 261-264.

[6] L.L. Durr, B.J. Clay, L.J. Durr, Dry cleaning solvent filtration and steam distillation recovery system, in, Google Patents, 1991.

[7] S. Srisurichan, R. Jiraratananon, A. Fane, Mass transfer mechanisms and transport resistances in direct contact membrane distillation process, J. Mem. Sci., 277 (2006) 186-194.

[8] B. Van der Bruggen, C. Vandecasteele, Distillation vs. membrane filtration: overview of process evolutions in seawater desalination, Desalination, 143 (2002) 207-218.

[9] R.J. Perper, T.W. Zee, M.M. Mickelson, Purification of lymphocytes and platelets by gradient centrifugation, J Lab Clin Med., 72 (1968) 842-848.

[10] R.T. Yang, Gas separation by adsorption processes, Butterworth-Heinemann, 2013.

[11] A. Ghoshal, S. Manjare, Selection of appropriate adsorption technique for recovery of VOCs: an analysis, J LOSS PREVENT PROC, 15 (2002) 413-421.

[12] C.C. Tzschucke, C. Markert, W. Bannwarth, S. Roller, A. Hebel, R. Haag, Modern separation techniques for the efficient workup in organic synthesis, Angew. Chem. Int. Ed., 41 (2002) 3964-4000.

[13] J. Rydberg, Solvent extraction principles and practice, revised and expanded, CRC press, 2004.

[14] N.E. Belkhouche, M. Amine Didi, D. Villemin, Separation of nickel and copper by solvent extraction using di-2 ethylhexylphosphoric acid-based synergistic mixture, Solvent Extr. Ion Exch., 23 (2005) 677-693.

[15] N.L. Nemerow, A. Dasgupta, Industrial and hazardous waste treatment, (1991).

[16] S. El Haggar, Sustainable industrial design and waste management: cradle-to-cradle for sustainable development, Academic Press, 2010.

[17] I. Costa, G. Massard, A. Agarwal, Waste management policies for industrial symbiosis development: case studies in European countries, J. Clean. Prod., 18 (2010) 815-822.

[18] R.W. Baker, Membrane technology and applications, John Wiley & Sons, 2012.

[19] N.N. Li, A.G. Fane, W.W. Ho, T. Matsuura, Advanced membrane technology and applications, John Wiley & Sons, 2011.

[20] G. Amy, N. Ghaffour, Z. Li, L. Francis, R.V. Linares, T. Missimer, S. Lattemann, Membrane-based seawater desalination: Present and future prospects, Desalination, 401 (2017) 16-21.

[21] B. Li, K.K. Sirkar, Novel membrane and device for vacuum membrane distillation-based desalination process, J. Mem. Sci., 257 (2005) 60-75.

[22] J.R. McCutcheon, R.L. McGinnis, M. Elimelech, A novel ammonia—carbon dioxide forward (direct) osmosis desalination process, Desalination, 174 (2005) 1-11.

[23] N. Du, H.B. Park, G.P. Robertson, M.M. Dal-Cin, T. Visser, L. Scoles, M.D. Guiver, Polymer nanosieve membranes for CO 2-capture applications, Nat. Mater., 10 (2011) 372.

[24] W. Yave, A. Car, K.-V. Peinemann, Nanostructured membrane material designed for carbon dioxide separation, J. Mem. Sci., 350 (2010) 124-129.

[25] V.S. Kislik, Liquid membranes: principles and applications in chemical separations and wastewater treatment, Elsevier, 2009.

[26] H. Tsukube, Liquid Membranes: Chemical Applications, by T. Araki and H. Tsukube, CRC Press, Boca Raton, (1990) 51-75.

[27] G.H. Morrison, Role in Extraction in Analytical Chemistry, Anal. Chem., 22 (1950) 1388-1393.

[28] H. Irving, Solvent extraction and its applications to inorganic analysis, Quarterly Reviews, Chemical Society, 5 (1951) 200-226.

[29] V. Kuznetsov, Chemical theoretical foundations of the extractive recovery of elements, Usp. Khim, 23 (1954) 654.

[30] P.D. Wilson, The nuclear fuel cycle: from ore to wastes, Oxford University Press Oxford, 1996.

[31] N. Cavlina, D. Pevec, T. Bajs, Book of Abstracts of 6th International Conference: Nuclear Option in Countries with Small and Medium Electricity Grids, (2006).

[32] H. Specker, Y. Marcus und AS Kertes: Ion Exchange and Solvent Extraction of Metal Complexes. Interscience Publishers, John Wiley & Sons, New York, London, Sydney 1969. 1037 Seiten. Preis: 315 s, Berichte der Bunsengesellschaft für physikalische Chemie, 73 (1969) 933-933.

[33] D. Peppard, Liquid-liquid extraction of metal ions, in: Adv. Inorg. Chem. Radiochem., Elsevier, 1966, pp. 1-80.

[34] D. Morris, M.A. Khan, Application of solvent extraction to the refining of precious metals—III: Purification of gold, Talanta, 15 (1968) 1301-1305.

[35] C. Reusch, E. Cussler, Selective membrane transport, AIChE Journal, 19 (1973) 736-741.

[36] H.C. Visser, D.N. Reinhoudt, F. de Jong, Carrier-mediated transport through liquid membranes, Chem. Soc. Rev., 23 (1994) 75-81.

[37] A. Mogutov, N. Kocheriginsky, Macrokinetics of facilitated transport across liquid membranes:"Big carrousel", J. Mem. Sci., 79 (1993) 273-283.

[38] A.A. Mohammed, M.A. Hussein, Transport of Pb (II) through bulk liquid membrane containing tri-n-butyl phosphate as a carrier, Asso. Arab Uni. J. Eng. Sci., 25 (2018) 65-79.

[39] N.N. Li, Separating hydrocarbons with liquid membranes, in, Google Patents, 1968.

[40] R.P. Cahn, N.N. Li, Separations of organic compounds by liquid membrane processes, J. Mem. Sci., 1 (1976) 129-142.

[41] W. Kamiński, W. Kwapiński, Applicability of liquid membranes in environmental protection, Pol. J. Environ. Stud., 9 (2000) 37-43.

[42] R. Marr, A. Kopp, Liquid membrane technology—a survey of phenomena, mechanisms, and models, Int. Chem. Eng., 22 (1982) 44-60.

[43] L. Nghiem, P. Mornane, I. Potter, J. Perera, R.W. Cattrall, S.D. Kolev, Extraction and transport of metal ions and small organic compounds using polymer inclusion membranes (PIMs), J. Membr. Sci., 281 (2006) 7-41.

[44] A. Sastre, A. Kumar, J. Shukla, R. Singh, Improved techniques in liquid membrane separations: an overview, Separation and Purification Methods, 27 (1998) 213-298.

[45] A.K. Guha, S. Majumdar, K.K. Sirkar, A larger-scale study of gas separation by hollow-fiber-contained liquid membrane permeator, J. Mem. Sci., 62 (1991) 293-307.

[46] A.K. Ghoshal, P. Saha, Liquid–Membrane Filters, in: Progress in Filtration and Separation, Elsevier, 2015, pp. 155-205.

[47] A.B. Lende, M.K. Dinker, V.K. Bhosale, S.P. Kamble, P.D. Meshram, P.S. Kulkarni, Emulsion ionic liquid membranes (EILMs) for removal of Pb (II) from aqueous solutions, Rsc Adv, 4 (2014) 52316-52323.

[48] W. ZHANG, C. Chunhua, H. Zisu, Transport study of Cu (II) through hollow fiber supported liquid membrane, Chinese Journal of Chemical Engineering, 18 (2010) 48-54.

[49] P. Kittisupakorn, W. Weerachaipichaskul, P. Thitiyasook, Modeling and simulation of copper-ion extraction with hollow fiber supported liquid membrane, J Ind Eng Chem, 13 (2007) 903-910.

[50] B. Swain, K. Sarangi, R. Prasad Das, Separation of cadmium and zinc by supported liquid membrane using TOPS-99 as mobile carrier, Sep. Sci. Technol., 39 (2005) 2171-2188.

[51] P.V. Vernekar, Y.D. Jagdale, A.W. Patwardhan, A.V. Patwardhan, S.A. Ansari, P.K. Mohapatra, V.K. Manchanda, Transport of cobalt (II) through a hollow fiber supported liquid membrane containing di-(2-ethylhexyl) phosphoric acid (D2EHPA) as the carrier, Chem. Eng. Res. Des., 91 (2013) 141-157.

[52] A. Surucu, V. Eyupoglu, O. Tutkun, Selective separation of cobalt and nickel by flat sheet supported liquid membrane using Alamine 300 as carrier, J Ind Eng Chem, 18 (2012) 629-634.

[53] B.K. Dutta, Principles of mass transfer and separation processes, Can. J. Chem. Eng, 87 (2009) 818-819.

[54] P. Parhi, Supported liquid membrane principle and its practices: A short review, Journal of Chemistry, 2013 (2012).

[55] A.J. Schow, R.T. Peterson, J.D. Lamb, Polymer inclusion membranes containing macrocyclic carriers for use in cation separations, J. Mem. Sci., 111 (1996) 291-295.

[56] C.A. Kozlowski, W. Walkowiak, Removal of chromium (VI) from aqueous solutions by polymer inclusion membranes, Water Res., 36 (2002) 4870-4876.

[57] A.Y. Nazarenko, J.D. Lamb, Selective transport of lead (II) and strontium (II) through a crown ether-based polymer inclusion membrane containing dialkylnaphthalenesulfonic acid, J. Inclusion Phenom. Mol. Recognition Chem., 29 (1997) 247-258.

[58] M.I.G.S. Almeida, R.W. Cattrall, S.D. Kolev, Recent trends in extraction and transport of metal ions using polymer inclusion membranes (PIMs), J. Membr. Sci., 415-416 (2012) 9-23.

[59] C. Fontàs, R. Tayeb, M. Dhahbi, E. Gaudichet, F. Thominette, P. Roy, K. Steenkeste, M.-P. Fontaine-Aupart, S. Tingry, E. Tronel-Peyroz, Polymer inclusion membranes: The concept of fixed sites membrane revised, J. Mem. Sci., 290 (2007) 62-72.

[60] Y.Y.N. Bonggotgetsakul, M. Ashokkumar, R.W. Cattrall, S.D. Kolev, The use of sonication to increase extraction rate in polymer inclusion membranes. An application to the extraction of gold (III), J. Mem. Sci., 365 (2010) 242-247.

[61] M. O'Rourke, R.W. Cattrall, S.D. Kolev, I.D. Potter, The extraction and transport of organic molecules using polymer inclusion membranes, Solvent Extr. Res. Dev., 16 (2009) 1-12.

[62] P. Sikorski, M. Wada, L. Heux, H. Shintani, B.T. Stokke, Crystal structure of cellulose triacetate I, Macromolecules, 37 (2004) 4547-4553.

[63] O. Kebiche-Senhadji, L. Mansouri, S. Tingry, P. Seta, M. Benamor, Facilitated Cd (II) transport across CTA polymer inclusion membrane using anion (Aliquat 336) and cation (D2EHPA) metal carriers, J. Mem. Sci., 310 (2008) 438-445.

[64] A. Garcia-Rodríguez, V. Matamoros, S.D. Kolev, C. Fontàs, Development of a polymer inclusion membrane (PIM) for the preconcentration of antibiotics in environmental water samples, J. Mem. Sci., 492 (2015) 32-39.

[65] J.S. Gardner, J.O. Walker, J.D. Lamb, Permeability and durability effects of cellulose polymer variation in polymer inclusion membranes, J. Mem. Sci., 229 (2004) 87-93.

[66] T.G. Levitskaia, J.D. Lamb, K.L. Fox, B.A. Moyer, Selective carrier-mediated cesium transport through polymer inclusion membranes by calix [4] arene-crown-6 carriers from complex aqueous mixtures, Radiochim. Acta, 90 (2002) 43-52.

[67] H. Kise, Dehydrochlorination of poly (vinyl chloride) by aqueous sodium hydroxide solution under two-phase conditions, J Polym Sci Pol Chem, 20 (1982) 3189-3197.

[68] L. Guo, Y. Liu, C. Zhang, J. Chen, Preparation of PVDF-based polymer inclusion membrane using ionic liquid plasticizer and Cyphos IL 104 carrier for Cr (VI) transport, J. Mem. Sci., 372 (2011) 314-321.

[69] H.I. Turgut, V. Eyupoglu, R.A. Kumbasar, I. Sisman, Alkyl chain length dependent Cr (VI) transport by polymer inclusion membrane using room temperature ionic liquids as carrier and PVDF-co-HFP as polymer matrix, Sep. Purifi. Technol., 175 (2017) 406-417.

[70] Y. O'Bryan, R.W. Cattrall, Y.B. Truong, I.L. Kyratzis, S.D. Kolev, The use of poly (vinylidenefluoride-co-hexafluoropropylene) for the preparation of polymer inclusion membranes. Application to the extraction of thiocyanate, J Membrane Sci, 510 (2016) 481-488.

[71] B. Mahanty, D. Raut, P. Mohapatra, D. Das, P. Behere, M. Afzal, Comparative evaluation of actinide ion uptake by polymer inclusion membranes containing TODGA as the carrier extractant, J. Hazard. Mater., 275 (2014) 146-153.

[72] F. Kubota, R. Kono, W. Yoshida, M. Sharaf, S.D. Kolev, M. Goto, Recovery of gold ions from discarded mobile phone leachate by solvent extraction and polymer inclusion membrane (PIM) based separation using an amic acid extractant, Sep. Purifi. Technol.
, 214 (2019) 156-161.

[73] A.H. Blitz-Raith, R. Paimin, R.W. Cattrall, S.D. Kolev, Separation of cobalt (II) from nickel (II) by solid-phase extraction into Aliquat 336 chloride immobilized in poly (vinyl chloride), Talanta, 71 (2007) 419-423.

[74] S. Kagaya, R.W. Cattrall, S.D. Kolev, Solid-phase extraction of cobalt (II) from lithium chloride solutions using a poly (vinyl chloride)-based polymer inclusion membrane with Aliquat 336 as the carrier, Anal. Sci., 27 (2011) 653-653.

[75] L. Wang, W. Shen, Chemical and morphological stability of Aliquat 336/PVC membranes in membrane extraction: A preliminary study, Sep. Purifi. Technol.
, 46 (2005) 51-62.

[76] A. Upitis, J. Peterson, C. Lukey, L.D. Nghiem, Metallic ion extraction using polymer inclusion membranes (PIMs): Optimising physical strength and extraction rate, Desalination and Water Treat., 6 (2009) 41-47.

[77] B. Pośpiech, W. Walkowiak, Separation of copper (II), cobalt (II) and nickel (II) from chloride solutions by polymer inclusion membranes, Sep. Purifi. Technol.
, 57 (2007) 461-465.

[78] C.A. Kozlowski, W. Walkowiak, Applicability of liquid membranes in chromium (VI) transport with amines as ion carriers, J. Mem. Sci., 266 (2005) 143-150.

[79] M.I.G.S. Almeida, R.W. Cattrall, S.D. Kolev, Recent trends in extraction and transport of metal ions using polymer inclusion membranes (PIMs), J. Mem. Sci., 415 (2012) 9-23.

[80] A.M. St John, R.W. Cattrall, S.D. Kolev, Extraction of uranium (VI) from sulfate solutions using a polymer inclusion membrane containing di-(2-ethylhexyl) phosphoric acid, J. Mem. Sci., 364 (2010) 354-361.

[81] C.A. Kozlowski, Facilitated transport of metal ions through composite and polymer inclusion membranes, Desalination, 198 (2006) 132-140.

[82] J. Kozlowska, C.A. Kozłowski, J.J. Koziol, Transport of Zn (II), Cd (II), and Pb (II) across CTA plasticized membranes containing organophosphorous acids as an ion carriers, Sep. Purifi. Technol.
, 57 (2007) 430-434.

[83] C.A. Kozlowski, W. Walkowiak, Competetive transport of cobalt-60, strontium-90, and cesium-137 radioisotopes across polymer inclusion membranes with DNNS, J. Mem. Sci., 297 (2007) 181-189.

[84] R. Tayeb, C. Fontas, M. Dhahbi, S. Tingry, P. Seta, Cd (II) transport across supported liquid membranes (SLM) and polymeric plasticized membranes (PPM) mediated by Lasalocid A, Sep. Purifi. Technol.

, 42 (2005) 189-193.

[85] T. Tasaki, T. Oshima, Y. Baba, Selective extraction and transport of copper (II) with new alkylated pyridinecarboxylic acid derivatives, Talanta, 73 (2007) 387-393.

[86] J. de Gyves, A.M. Hernández-Andaluz, E.R. de San Miguel, LIX®-loaded polymer inclusion membrane for copper (II) transport: 2. Optimization of the efficiency factors (permeability, selectivity, and stability) for LIX® 84-I, J. Mem. Sci., 268 (2006) 142-149.

[87] E. Rodríguez de San Miguel, A.V. Garduño-García, J.C. Aguilar, J. de Gyves, Gold (III) transport through polymer inclusion membranes: Efficiency factors and pertraction mechanism using Kelex 100 as carrier, Ind. Eng. Chem. Res., 46 (2007) 2861-2869.

[88] D. Raut, P. Kandwal, G. Rebello, P. Mohapatra, Evaluation of polymer inclusion membranes containing calix [4]-bis-2, 3-naptho-crown-6 for Cs recovery from acidic feeds: Transport behavior, morphology and modeling studies, J. Mem. Sci., 407 (2012) 17-26.

[89] S. Chaudhury, A. Bhattacharyya, A. Goswami, Electrodriven selective transport of Cs+ using chlorinated cobalt dicarbollide in polymer inclusion membrane: a novel approach for cesium removal from simulated nuclear waste solution, Environ. Sci. Technol., 48 (2014) 12994-13000.

[90] P. Mohapatra, D. Lakshmi, A. Bhattacharyya, V. Manchanda, Evaluation of polymer inclusion membranes containing crown ethers for selective cesium separation from nuclear waste solution, J. Hazard. Mater., 169 (2009) 472-479.

[91] A. Gabor, C.M. Davidescu, A. Popa, A. Negrea, M. Ciopec, M. Motoc, L. Lupa, A.R. Buzatu, P. Negrea, Equilibrium Studies for Crown Ether Impregnated Solid Support Used in the Removal Process of Nd (III), La (III), Sr (II), Tl (I), Eu (III), Revista de Chimie 67 (2016) 580-583.

[92] O. Kebiche-Senhadji, S. Tingry, P. Seta, M. Benamor, Selective extraction of Cr (VI) over metallic species by polymer inclusion membrane (PIM) using anion (Aliquat 336) as carrier, Desalination, 258 (2010) 59-65.

[93] R. Kumar, A.K. Pandey, M.K. Sharma, L. Panicker, S. Sodaye, G. Suresh, S.V. Ramagiri, J.R. Bellare, A. Goswami, Diffusional transport of ions in plasticized anion-exchange membranes, J. Phys. Chem. B, 115 (2011) 5856-5867.

[94] M. Ulewicz, U. Lesinska, M. Bochenska, W. Walkowiak, Facilitated transport of Zn (II), Cd (II) and Pb (II) ions through polymer inclusion membranes with calix [4]-crown-6 derivatives, Sep. Purifi. Technol.

, 54 (2007) 299-305.

[95] Y. Cho, C. Xu, R.W. Cattrall, S.D. Kolev, A polymer inclusion membrane for extracting thiocyanate from weakly alkaline solutions, J Membrane Sci, 367 (2011) 85-90.

[96] C.F. Croft, M.I.G.S. Almeida, R.W. Cattrall, S.D. Kolev, Separation of lanthanum(III), gadolinium(III) and ytterbium(III) from sulfuric acid solutions by using a polymer inclusion membrane, J Membrane Sci, 545 (2018) 259-265.

[97] M.I.G.S. Almeida, A.M. Silva, R.W. Cattrall, S.D. Kolev, A study of the ammonium ion extraction properties of polymer inclusion membranes containing commercial dinonylnaphthalene sulfonic acid, J. Mem. Sci., 478 (2015) 155-162.

[98] Y. O'Bryan, Y.B. Truong, R.W. Cattrall, I.L. Kyratzis, S.D. Kolev, Electrospun polystyrene/Aliquat 336 for preconcentration and determination of thiocyanate in flow analysis, Electrospinning, 1 (2017) 100-110.

[99] P. Pantůčková, P. Kubáň, P. Boček, In-line coupling of microextractions across polymer inclusion membranes to capillary zone electrophoresis for rapid determination of formate in blood samples, Anal. Chim. Acta., 887 (2015) 111-117.

[100] R. Vera, S. Insa, C. Fontàs, E. Anticó, A new extraction phase based on a polymer inclusion membrane for the detection of chlorpyrifos, diazinon and cyprodinil in natural water samples, Talanta, 185 (2018) 291-298.

[101] J.A. Van Loon, Analytical atomic absorption spectroscopy: selected methods, Elsevier, 2012.

[102] A. Walsh, The application of atomic absorption spectra to chemical analysis, Spectrochim. Acta, 7 (1955) 108-117.

[103] J. Willis, The determination of metals in blood serum by atomic absorption spectroscopy—I: calcium, Spectrochimica Acta, 16 (1960) 259-E255.

[104] Z. Fang, Flow injection atomic absorption spectrometry, Wiley Chichester, 1995.

[105] M. Amos, J. Willis, Use of high-temperature pre-mixed flames in atomic absorption spectroscopy, Spectrochimica Acta, 22 (1966) 1325-1343.

[106] V.A. Fassel, R.N. Kniseley, Inductively coupled plasma. Optical emission spectroscopy, Anal. Chem., 46 (1974) 1110A-1120a.

[107] D.J. Kalnicky, R.N. Kniseley, V.A. Fassel, Inductively coupled plasma-optical emission spectroscopy: Excitation temperatures experienced by analyte species, SPECTROCHIM ACTA B, 30 (1975) 511-525.

[108] B. Charles, K.J. Fredeen, Concepts, instrumentation and techniques in inductively coupled plasma optical emission spectrometry, Perkin Elmer Corporation, (1997).

[109] P.R. Griffiths, J.A. De Haseth, Fourier transform infrared spectrometry, John Wiley & Sons, 2007.

[110] R.J. Markovich, C. Pidgeon, Introduction to Fourier transform infrared spectroscopy and applications in the pharmaceutical sciences, Pharm. Res., 8 (1991) 663-675.

[111] S. Bäckström, J. Benavente, R.W. Berg, K. Stibius, M.S. Larsen, H. Bohr, C. Hélix-Nielsen, Tailoring properties of biocompatible PEG-DMA hydrogels with UV light, Mat. Sci. Appl., 3 (2012) 425.

[112] J.A. Killion, L.M. Geever, D.M. Devine, J.E. Kennedy, C.L. Higginbotham, Mechanical properties and thermal behaviour of PEGDMA hydrogels for potential bone regeneration application, J Mech Behav Biomed Mater, 4 (2011) 1219-1227.

[113] Y. Leprince-Wang, K. Yu-Zhang, Study of the growth morphology of TiO2 thin films by AFM and TEM, Surf. Coat. Technol., 140 (2001) 155-160.

[114] M. Lackinger, T. Müller, T. Gopakumar, F. Müller, M. Hietschold, G.W. Flynn, Tunneling voltage polarity dependent submolecular contrast of naphthalocyanine on graphite. A STM study of close-packed monolayers under ultrahigh-vacuum conditions, J. Phys. Chem. B, 108 (2004) 2279-2284.

[115] P. Saha, K. Yadav, S. Chacko, A.T. Philip, R. Ramapanicker, T.G. Gopakumar, Controlling growth to one dimension in nanoislands of ferrocene-sugar derivatives, J. Phys. Chem. C, 120 (2016) 9223-9228.

[116] A. Bhattacharyya, P. Mohapatra, P. Hassan, V. Manchanda, Studies on the selective Am3+ transport, irradiation stability and surface morphology of polymer inclusion membranes containing Cyanex-301 as carrier extractant, J. hazard. mater., 192 (2011) 116-123.

[117] A.F. Guedes, F.A. Carvalho, I. Malho, N. Lousada, L. Sargento, N.C. Santos, Atomic force microscopy as a tool to evaluate the risk of cardiovascular diseases in patients, Nat. Nanotechnol., 11 (2016) 687.

[118] G. Binnig, C.F. Quate, C. Gerber, Atomic force microscope, Phys. Rev. Lett., 56 (1986) 930.

[119] S. Morita, F.J. Giessibl, E. Meyer, R. Wiesendanger, Noncontact atomic force microscopy, Springer, 2015.

[120] U. Maver, T. Maver, Z. Peršin, M. Mozetič, A. Vesel, M. Gaberšček, K. Stana-Kleinschek, Polymer characterization with the atomic force microscope, Polymer Science, 4 (2013).

[121] J.D. Menczel, R.B. Prime, Thermal analysis of polymers, Wiley Online Library, 2009.

[122] M.P. Sepe, Thermal analysis of polymers, iSmithers Rapra Publishing, 1997.

[123] S. Strella, Differential thermal analysis of polymers. I. The glass transition, J. Appl. Polym. Sci., 7 (1963) 569-579.

[124] E. Turi, Thermal characterization of polymeric materials, Elsevier, 2012.

[125] S. Singh, C. Wu, P.T. Williams, Pyrolysis of waste materials using TGA-MS and TGA-FTIR as complementary characterisation techniques, J Anal Appl Pyrolysis, 94 (2012) 99-107.

[126] J. Feng, J. Hao, J. Du, R. Yang, Using TGA/FTIR TGA/MS and cone calorimetry to understand thermal degradation and flame retardancy mechanism of polycarbonate filled with solid bisphenol A bis (diphenyl phosphate) and montmorillonite, Polym. Degrad. Stab., 97 (2012) 605-614.

[127] M.V. Kök, M.A. Varfolomeev, D.K. Nurgaliev, Crude oil characterization using tga-dta, tga-ftir and tga-ms techniques, Journal of Petroleum Science and Engineering, 154 (2017) 537-542.

[128] J. Golebiewski, A. Galeski, Thermal stability of nanoclay polypropylene composites by simultaneous DSC and TGA, Compos. Sci. Technol., 67 (2007) 3442-3447.

[129] S. Vossoughi, G.W. Bartlett, G.P. Willhite, Development of a kinetic model for in-situ combustion and prediction of the process variables using TGA/DSC techniques, in: SPE annual technical conference and exhibition, Society of Petroleum Engineers, 1982.

[130] B. Li, G. Chen, H. Zhang, C. Sheng, Development of non-isothermal TGA–DSC for kinetics analysis of low temperature coal oxidation prior to ignition, Fuel, 118 (2014) 385-391.

[131] L.D. Nghiem, P. Mornane, I.D. Potter, J.M. Perera, R.W. Cattrall, S.D. Kolev, Extraction and transport of metal ions and small organic compounds using polymer inclusion membranes (PIMs), J. Mem. Sci., 281 (2006) 7-41.

[132] M.I.G.S. Almeida, R.W. Cattrall, S.D. Kolev, Polymer inclusion membranes (PIMs) in chemical analysis: A review, Anal. Chim. Acta., 987 (2017) 1-14.

[133] M.I.G.S. Almeida, R.W. Cattrall, S.D. Kolev, Polymer inclusion membranes (PIMs) in chemical analysis - A review, Anal. Chim. Acta, 987 (2017) 1-14.

[134] G. Eisenman, J. Sandblom, J. Walker, Membrane structure and ion permeation, Science, 155 (1967) 965-974.

[135] G. Moody, R.B. Oke, J. Thomas, A calcium-sensitive electrode based on a liquid ion exchanger in a poly (vinyl chloride) matrix, Analyst, 95 (1970) 910-918.

[136] E. Bakker, P. Bühlmann, E. Pretsch, Carrier-based ion-selective electrodes and bulk optodes. 1. General characteristics, Chem. Rev., 97 (1997) 3083-3132.

[137] P. Bühlmann, E. Pretsch, E. Bakker, Carrier-based ion-selective electrodes and bulk optodes. 2. Ionophores for potentiometric and optical sensors, Chem. Rev., 98 (1998) 1593-1688.

[138] A.T. Lawal, Synthesis and utilization of carbon nanotubes for fabrication of electrochemical biosensors, Mat. Res. Bulletin, 73 (2016) 308-350.

[139] Y. Liu, Y. Gao, R. Yan, H. Huang, P. Wang, Disposable Multi-Walled Carbon Nanotubes-Based Plasticizer-Free Solid-Contact Pb2+-Selective Electrodes with a Sub-PPB Detection Limit, Sensors-Basel, 19 (2019) 2550.

[140] L.Y. Heng, E.A. Hall, Taking the Plasticizer out of Methacrylic-Acrylic Membranes for K+-Selective Electrodes, Electroanalysis: An International Journal Devoted to Fundamental and Practical Aspects of Electroanalysis, 12 (2000) 187-193.

[141] M. Apostu, M. HĂNCIANU, G. ȚANTARU, M. Vieriu, N. Bibire, A.D. Panainte, Electrochemical sensors with pharmaceutical applications based on polymer inclusion membranes containing phosphomolybdic acid complexes, Farmacia, 66 (2018) 587-591.

[142] N.F. Silva, J.M. Magalhães, M.F. Barroso, T. Oliva-Teles, C. Freire, C. Delerue-Matos, In situ formation of gold nanoparticles in polymer inclusion membrane: Application as platform in a label-free potentiometric immunosensor for Salmonella typhimurium detection, Talanta, 194 (2019) 134-142.

[143] T. Ohshima, S. Kagaya, M. Gemmei-Ide, R.W. Cattrall, S.D. Kolev, The use of a polymer inclusion membrane as a sorbent for online preconcentration in the flow injection determination of thiocyanate impurity in ammonium sulfate fertilizer, Talanta, 129 (2014) 560-564.

[144] R.-H. Cristina, M.-V.M. Jesús, F.-T. Rut, B.-L.M. Ángel, Use of polymer inclusion membranes (PIMs) as support for electromembrane extraction of non-steroidal anti-inflammatory drugs and highly polar acidic drugs, Talanta, 179 (2018) 601-607.

[145] C.F. Poole, New trends in solid-phase extraction, TrAC-TREND ANAL CHEM, 22 (2003) 362-373.

[146] J.A. López-López, C. Mendiguchía, J.J. Pinto, C. Moreno, Liquid membranes for quantification and speciation of trace metals in natural waters, Trends Analyt Chem, 29 (2010) 645-653.

[147] Y. Zhang, M. Miró, S.D. Kolev, An automatic flow assembly for on-line dynamic fractionation of trace level concentrations of mercury in environmental solids with high organic load, Anal. Chim. Acta., 975 (2017) 1-10.

[148] Y. Zhang, M. Miró, S.D. Kolev, Hybrid flow system for automatic dynamic fractionation and speciation of inorganic arsenic in environmental solids, Environ. Sci. Technol., 49 (2015) 2733-2740.

[149] E.A. Nagul, C. Fontàs, I.D. McKelvie, R.W. Cattrall, S.D. Kolev, The use of a polymer inclusion membrane for separation and preconcentration of orthophosphate in flow analysis, Anal. Chim. Acta., 803 (2013) 82-90.

[150] N.A. Mamat, H.H. See, Development and evaluation of electromembrane extraction across a hollow polymer inclusion membrane, J. Chromatogr. A, 1406 (2015) 34-39.

[151] N.A. Mamat, H.H. See, Simultaneous electromembrane extraction of cationic and anionic herbicides across hollow polymer inclusion membranes with a bubbleless electrode, J. Chromatogr. A, 1504 (2017) 9-16.

[152] L.O.C. Šraj, M.I.G.S. Almeida, C. Bassett, I.D. McKelvie, S.D. Kolev, Gas-diffusion-based passive sampler for ammonia monitoring in marine waters, Talanta, 181 (2018) 52-56.

[153] F. Nitti, M.I.G.S. Almeida, R. Morrison, R.W. Cattrall, V.J. Pettigrove, R.A. Coleman, S.D. Kolev, Development of a portable 3D-printed flow-through passive sampling device free of flow pattern effects, Microchemical Journal, 143 (2018) 359-366.

[154] J.K. Kingston, R. Greenwood, G.A. Mills, G.M. Morrison, L.B. Persson, Development of a novel passive sampling system for the time-averaged measurement of a range of organic pollutants in aquatic environments, Journal of Environmental Monitoring, 2 (2000) 487-495.

[155] F.A. Esteve-Turrillas, V. Yusà, A. Pastor, M. de la Guardia, New perspectives in the use of semipermeable membrane devices as passive samplers, Talanta, 74 (2008) 443-457.

[156] C. Harman, I.J. Allan, E.L. Vermeirssen, Calibration and use of the polar organic chemical integrative sampler—a critical review, Environ. Toxicol. Chem., 31 (2012) 2724-2738.

[157] J.J. Peters, M.I.G.S. Almeida, L.O.C. Šraj, I.D. McKelvie, S.D. Kolev, Development of a micro-distillation microfluidic paper-based analytical device as a screening tool for total ammonia monitoring in freshwaters, Anal. Chim. Acta., (2019).

[158] A. Garcia-Rodríguez, C. Fontàs, V. Matamoros, M.I.G.S. Almeida, R.W. Cattrall, S.D. Kolev, Development of a polymer inclusion membrane-based passive sampler for monitoring of sulfamethoxazole in natural waters. Minimizing the effect of the flow pattern of the aquatic system, Microchemical Journal, 124 (2016) 175-180.

[159] W. Yoshida, Y. Baba, F. Kubota, S.D. Kolev, M. Goto, Selective transport of scandium (III) across polymer inclusion membranes with improved stability which contain an amic acid carrier, J. Mem. Sci., 572 (2019) 291-299.

[160] F. Sellami, O. Kebiche-Senhadji, S. Marais, N. Couvrat, K. Fatyeyeva, Polymer inclusion membranes based on CTA/PBAT blend containing Aliquat 336 as extractant for removal of Cr (VI): Efficiency, stability and selectivity, React Funct Polym, 139 (2019) 120-132.

[161] M. Baczyńska, M. Waszak, M. Nowicki, D. Prządka, S. Borysiak, M. Regel-Rosocka, Characterization of polymer inclusion membranes (PIMs) containing phosphonium ionic liquids as Zn (II) carriers, Ind. Eng. Chem. Res., 57 (2018) 5070-5082.

[162] M. Baczyńska, M. Regel-Rosocka, M. Nowicki, M. Wiśniewski, Effect of the structure of polymer inclusion membranes on Zn (II) transport from chloride aqueous solutions, J. Appl. Polym. Sci., 132 (2015).

[163] M. Soner Engin, S. Sayin, S. Cay, E. Kir, T. Sardohan-Koseoglu, Preparation and characterisation of thiol functionalised p-tert-butylcalix [4] arene-embedded polymer inclusion membranes: performance and selectivity, Int J Environ an Ch, (2019) 1-9.

[164] D.A. Fadel, L.A. Shouman, R.M. Afify, Selective transport of chromium (III), cobalt (II), barium (II) and strontium (II) ions through polymer inclusion membranes, Desalination Water Treat., 103 (2018) 163-174.

[165] G. Elias, S. Díez, C. Fontàs, System for mercury preconcentration in natural waters based on a polymer inclusion membrane incorporating an ionic liquid, J. Hazard. Mater., 371 (2019) 316-322.

[166] A. Makowka, B. Pospiech, Synthesis of Polymer Inclusion Membranes Based on Cellulose Triacetate for Recovery of Lanthanum (III) from Aqueous Solutions, Autex Research Journal, 1 (2019).

[167] N. Zhang, Y. Liu, R. Liu, Z. She, M. Tan, D. Mao, R. Fu, Y. Zhang, Polymer inclusion membrane (PIM) containing ionic liquid as a proton blocker to improve waste acid recovery efficiency in electrodialysis process, J. Mem. Sci., 581 (2019) 18-27.

[168] L. Moulahcene, M. Skiba, F. Bounoure, M. Benanamor, N. Milon, F. Hallouard, M. Lahiani-Skiba, New Polymer Inclusion Membrane Containing β-Cyclodextrin Polymer: Application for Pharmaceutical Pollutant Removal from Waste Water, Int. J. Environ. Res. Public Health, 16 (2019) 414.

[169] Y. Bonggotgetsakul, R. Cattrall, S. Kolev, Extraction of gold (III) from hydrochloric acid solutions with a PVC-based polymer inclusion membrane (PIM) containing Cyphos® IL 104, Membranes, 5 (2015) 903-914.

[170] M. Ershad, M.I.G.S. Almeida, T.G. Spassov, R.W. Cattrall, S.D. Kolev, Polymer inclusion membranes (PIMs) containing purified dinonylnaphthalene sulfonic acid (DNNS): performance and selectivity, Sep. Purifi. Technol.

, 195 (2018) 446-452.

[171] X. Qiu, H. Hu, F. Hu, J. Tang, C. Yang, Y. Zhou, X. Lin, J. Hu, Simultaneous recovery of copper (II) from two different feed solutions based on a three-compartment module with selective polymer inclusion membranes, Hydrometallurgy, (2019).

[172] D. Wang, R.W. Cattrall, J. Li, M.I.G. Almeida, G.W. Stevens, S.D. Kolev, A comparison of the use of commercial and diluent free LIX84I in poly (vinylidene fluoride-co-hexafluoropropylene)(PVDF-HFP)-based polymer inclusion membranes for the extraction and transport of Cu (II), Sep Purif Technol, 202 (2018) 59-66.

[173] M.R. Yaftian, M.I.G.S. Almeida, R.W. Cattrall, S.D. Kolev, Selective extraction of vanadium (V) from sulfate solutions into a polymer inclusion membrane composed of poly (vinylidenefluoride-co-hexafluoropropylene) and Cyphos® IL 101, J. Mem. Sci., 545 (2018) 57-65.

[174] D. Zioui, O. Arous, N. Mameri, H. Kerdjoudj, M. San Sebastian, J. Vilas, J. Nunes-Pereira, S. Lanceros-Méndez, Membranes based on polymer miscibility for selective transport and separation of metallic ions, J. Hazard. Mater., 336 (2017) 188-194.

[175] S. Bey, A. Criscuoli, A. Figoli, A. Leopold, S. Simone, M. Benamor, E. Drioli, Removal of As (V) by PVDF hollow fibers membrane contactors using Aliquat-336 as extractant, Desalination, 264 (2010) 193-200.

[176] K. Witt, E. Radzyminska-Lenarcik, A. Kosciuszko, M. Gierszewska, K. Ziuziakowski, The influence of the morphology and mechanical properties of polymer inclusion

membranes (PIMs) on zinc ion separation from aqueous solutions, Polymers-Basel, 10 (2018) 134.

[177] C.F. Croft, M.I.G. Almeida, R.W. Cattrall, S.D. Kolev, Separation of lanthanum (III), gadolinium (III) and ytterbium (III) from sulfuric acid solutions by using a polymer inclusion membrane, J Membrane Sci, 545 (2018) 259-265.

[178] D. Wang, J. Hu, Y. Li, M. Fu, D. Liu, Q. Chen, Evidence on the 2-nitrophenyl octyl ether (NPOE) facilitating Copper (II) transport through polymer inclusion membranes, J. Mem. Sci., 501 (2016) 228-235.

[179] D. Wang, R.W. Cattrall, J. Li, M.I.G.S. Almeida, G.W. Stevens, S.D. Kolev, A poly (vinylidene fluoride-co-hexafluoropropylene)(PVDF-HFP)-based polymer inclusion membrane (PIM) containing LIX84I for the extraction and transport of Cu (II) from its ammonium sulfate/ammonia solutions, J. Mem. Sci., 542 (2017) 272-279.

[180] O. Tutkun, Y. Yıldız, B. Aydın, A. Manzak, Preparation and application of polymer inclusion membranes (PIMs) including Alamine 336 for extraction of metals from an aqueous solution (2014).

[181] Y.Y.N. Bonggotgetsakul, R.W. Cattrall, S.D. Kolev, Recovery of gold from aqua regia digested electronic scrap using a poly (vinylidene fluoride-co-hexafluoropropene)(PVDF-HFP) based polymer inclusion membrane (PIM) containing Cyphos® IL 104, J. Mem. Sci., 514 (2016) 274-281.

[182] J. Schmidt-Marzinkowski, H.H. See, P.C. Hauser, Electric field driven extraction of inorganic anions across a polymer inclusion membrane, Electroanalysis, 25 (2013) 1879-1886.

[183] Y. O'Bryan, R.W. Cattrall, Y.B. Truong, I.L. Kyratzis, S.D. Kolev, The use of poly(vinylidenefluoride-co-hexafluoropropylene) for the preparation of polymer inclusion membranes. Application to the extraction of thiocyanate, J Membrane Sci, 510 (2016) 481-488.

[184] Y. O'Bryan, Y.B. Truong, R.W. Cattrall, I.L. Kyratzis, S.D. Kolev, A new generation of highly stable and permeable polymer inclusion membranes (PIMs) with their carrier immobilized in a crosslinked semi-interpenetrating polymer network. Application to the transport of thiocyanate, J. Membr. Sci., 529 (2017) 55-62.

[185] A.A. Kiswandono, D. Siswanta, N.H. Aprilita, S.J. Santosa, T. Hayashita, Extending the life time of polymer inclusion membrane containing copoly (Eugenol-DVB) as carrier for phenol transport, Indonesian Journal of Chemistry, 13 (2013) 254-261.

[186] S. Farrukh, F.T. Minhas, A. Hussain, S. Memon, M. Bhanger, M. Mujahid, Preparation, characterization, and applicability of novel calix [4] arene-based cellulose acetate membranes in gas permeation, J. Appl. Polym. Sci., 131 (2014).

[187] F. Hernández-Fernández, A.P. de los Ríos, F. Mateo-Ramírez, M. Juarez, L. Lozano-Blanco, C. Godínez, New application of polymer inclusion membrane based on ionic liquids as proton exchange membrane in microbial fuel cell, Sep. Purifi. Technol.
, 160 (2016) 51-58.

[188] J. Benavente, V. Romero, M. Vázquez, E. Anticó, C. Fontàs, Electrochemical Characterization of a Polymer Inclusion Membrane Made of Cellulose Triacetate and Aliquat 336 and Its Application to Sulfonamides Separation, Separations, 5 (2018) 5.

[189] Y. O'Bryan, Y.B. Truong, R.W. Cattrall, I.L. Kyratzis, S.D. Kolev, A new generation of highly stable and permeable polymer inclusion membranes (PIMs) with their carrier immobilized in a crosslinked semi-interpenetrating polymer network. Application to the transport of thiocyanate, J. Mem. Sci., 529 (2017) 55-62.

[190] K.A. Walker, L.J. Markoski, G.A. Deeter, G.E. Spilman, D.C. Martin, J.S. Moore, CROSS-LINKING CHEMISTRY FOR HIGH-PERFORMANCE POLYMER NETWORKS, Polymer, 35 (1994) 5012-5017.

[191] C. Decker, Recent developments in photoinitiated radical polymerization, Macromolecular Symposia, 143 (1999) 45-63.

[192] C. Decker, Photoinitiated crosslinking polymerisation, Progress in polymer science, 21 (1996) 593-650.

[193] J. Pavlinec, N. Moszner, Photocrosslinking polymerization of methacrylate modified triethoxysilanes polycondensates and multifunctional methacrylates, Macromol. Mater. Eng., 288 (2003) 789-797.

[194] B. Falk, M. Zonca Jr, J. Crivello, Modification of photoinitiated cationic epoxide polymerizations by sulfides, J Polym. Sci. Pol. Chem., 43 (2005) 2504-2519.

[195] C. Decker, T. Nguyen Thi Viet, H. Pham Thi, Photoinitiated cationic polymerization of epoxides, Polym. Int., 50 (2001) 986-997.

[196] C. Decker, C. Bianchi, D. Decker, F. Morel, Photoinitiated polymerization of vinyl ether-based systems, Prog. Org. Coat., 42 (2001) 253-266.

[197] M. Abadie, N. Chia, F. Boey, Cure kinetics for the ultraviolet cationic polymerization of cycloliphatic and diglycidyl ether of bisphenol-A (DGEBA) epoxy systems with sulfonium salt using an auto catalytic model, J. Appl. Polym. Sci., 86 (2002) 1587-1591.

[198] P. Nising, T. Meyer, R. Carloff, M. Wicker, Thermal initiation of MMA in high temperature radical polymerizations, Macromolecular Materials and Engineering, 290 (2005) 311-318.

[199] C. Decker, The use of UV irradiation in polymerization, Polym. Int., 45 (1998) 133-141.

[200] C. Decker, Light-induced crosslinking polymerization, Polym Int, 51 (2002) 1141-1150.

[201] C. Decker, F. Morel, S. Jonsson, S. Clark, C. Hoyle, Light-induced polymerisation of photoinitiator-free vinyl ether maleimide systems, Macromolecular Chemistry and Physics, 200 (1999) 1005-1013.

[202] C. Decker, C. Bianchi, S. Jönsson, Light-induced crosslinking polymerization of a novel N-substituted bis-maleimide monomer, Polymer, 45 (2004) 5803-5811.

[203] L.T. Ng, S. Jönsson, S. Swami, K. Lindgren, Synthesis of hydrogel for drug delivery studies utilizing photoinitiator-free photopolymerization based on the donor/acceptor pair, N-vinylpyrrolidinone and hydroxypentyl maleimide, Polym. Int., 51 (2002) 1398-1403.

[204] J. Crivello, New photoinitiators for cationic polymerization, in: J Polym Sci Symp, 1976, pp. 383-395.

[205] J. Ortyl, R. Popielarz, New photoinitiators for cationic polymerization, Polimery, 57 (2012) 510-517.

[206] Y. Liu, R. Wang, T.-S. Chung, Chemical cross-linking modification of polyimide membranes for gas separation, J Membrane Sci, 189 (2001) 231-239.

[207] K. Vanherck, G. Koeckelberghs, I.F. Vankelecom, Crosslinking polyimides for membrane applications: a review, Prog. Polym. Sci., 38 (2013) 874-896.

[208] T. Fourniols, L.D. Randolph, A. Staub, K. Vanvarenberg, J.G. Leprince, V. Préat, A. des Rieux, F. Danhier, Temozolomide-loaded photopolymerizable PEG-DMA-based hydrogel for the treatment of glioblastoma, J. Control Release, 210 (2015) 95-104.

[209] J.G. Leprince, W.M. Palin, M.A. Hadis, J. Devaux, G. Leloup, Progress in dimethacrylate-based dental composite technology and curing efficiency, Dent. Mater., 29 (2013) 139-156.

[210] G.D. Nicodemus, S.J. Bryant, Cell encapsulation in biodegradable hydrogels for tissue engineering applications, Tissue Eng. Part B Rev., 14 (2008) 149-165.

[211] E.M. Ahmed, Hydrogel: Preparation, characterization, and applications: A review, J. Adv. Res., 6 (2015) 105-121.

[212] T. Huang, H. Xu, K. Jiao, L. Zhu, H.R. Brown, H. Wang, A novel hydrogel with high mechanical strength: a macromolecular microsphere composite hydrogel, Adv. Mater., 19 (2007) 1622-1626.

[213] K.A. Walker, L.J. Markoski, G.A. Deeter, G.E. Spilman, D.C. Martin, J.S. Moore, Crosslinking chemistry for high-performance polymer networks, Polymer, 35 (1994) 5012-5017.

[214] O. Mukbaniani, J. Aneli, T. Tatrishvili, E. Markarashvili, M. Chigvinadze, M.J.M. Abadie, Synthesis of cross-linked comb-type polysiloxane for polymer electrolyte membranes, e-Polymers, 12 (2012).

Chapter 2

Effect of cross-linking on the performance of polymer inclusion membranes (PIMs) for the extraction, transport and separation of Zn(II)

1. Introduction

Emerging as a potential alternative to traditional solvent extraction, separation based on polymer inclusion membranes (PIMs), consisting of a base-polymer, carrier (extractant) and plasticizer or modifier in some cases, has been attracting increased attention in recent years [1]. The main reason behind this trend is based on the better stability of PIMs than supported liquid membranes (SLMs) which are the most frequently used liquid membranes at present [1-10]. Despite the better stability of PIMs [1, 11], their robustness is still considered insufficient for applications on an industrial scale. Hence, recent research on PIMs has also been focused on further improving their stability together with other performance characteristics such as rate of extraction and extractive capacity.

The limited stability of PIMs in terms of their reusability is mainly caused by the loss of membrane liquid phase, composed of the PIM carrier and plasticizer or modifier (if used), to the aqueous phase(s) (i.e., feed and receiving solutions) in contact with the membrane [12-14]. The factors, responsible to a great extent for the leaching of the membrane liquid phase, include (1) problems associated with the miscibility of the membrane components [15], (2) solubility of the membrane liquid phase in the aqueous phase(s) [16, 17], and (3) the composition of the aqueous phase(s) in contact with the membrane [10, 13]. Different approaches have been proposed with the aim to eliminate or minimise the effect of these three factors. Recently, Kaya et al. have demonstrated improvement of the PIM mechanical stability by doping the membrane with reduced graphene oxide (rGO) without compromising its permeability [18]. According to the authors, the addition of rGO to the membrane composition improved its structure, increased its roughness and also prevented the physical aging of the membrane. Salazar-Alvarez et al. reported on the use of ethanol as a modifier, which was added to the casting solution and resulted in better miscibility of the membrane components (i.e., di-(2-ethylhexyl)phosphoric acid (D2EHPA), tris-(2-butoxyethyl)phosphate and cellulose triacetate (CTA)) [15]. Matsuoka

et al. reduced the loss of the carrier tributyl phosphate (TBP) from the corresponding PIMs by saturating the feed solution with TBP [17]. It was also demonstrated by Cho et al. that the membrane stability could be improved by incorporating in the membrane composition a modifier with very low water solubility, such as 1-tetradecanol or 1-dodecanol [16]. The ionic strength of the aqueous feed or receiving solutions also plays a determining role in the loss of membrane liquid phase, and it has been reported by Zhang et al. that the membrane mass loss during extraction could be minimized by conditioning the PIM in an aqueous solution with the same background composition as the feed solution for a certain period of time [13]. Recently a new approach has been developed by us for improving the stability as well as the permeability of PIMs which is based on introducing an additional polymer, capable of creating a cross-linked polymer network in the presence of UV-light [19].

Cross-linking polymers are extensively used engineering materials because of their excellent mechanical and thermal stability [20]. There are two common approaches used to induce the cross-linking, i.e., thermal polymerisation or photo-initiated radical polymerisation. Radiation induced polymerisation has some advantages over heat induced polymerisation, which include high reaction rate at ambient temperature, low energy consumption and solvent free formulation [21]. There are several polymers that can be used as cross-linking agents, namely poly(ethylene glycol) dimethacrylate (PEG-DMA) [22, 23], 4-hydroxy-butyl vinyl ether (HBVE), bismaleimide (Q-bond) [24], and oxetane-acrylate [21]. PEG-DMA is among the most frequently used cross-linking polymers with numerous applications in biochemistry and medicinal chemistry [25-27]. Its capability in improving mechanical resistance under high vacuum conditions or under chemical stress is well known [28]. Engineered mechanical properties and biodegradability of this polymer make it suitable for orthopaedic tissue engineering [29].

Hence, this cross-linking polymer was chosen for the present study which focused on utilising the cross-linking polymerisation concept in the development of a more stable PIM for the extraction, transport and separation of Zn(II) with improved extraction rate and capacity. The compatibility of different base-polymers with the cross-linking polymer PEG-DMA was investigated using D2EHPA as the carrier. The long-term stability and surface morphology of the PIMs studied were also examined.

2. Experimental

2.1. Reagents and solutions

D2EHPA (97%, Aldrich, USA) as the carrier (extractant) was used as received in the preparation of all membranes. Three different polymers, i.e., poly(vinylidene fluoride-co-hexafluropropylene) (PVDF-HFP, Aldrich, USA), CTA (Acros Organics, USA) and PVC (Aldrich, USA), were tested as base-polymers. PEG-DMA (Aldrich, USA) and 2,2-dimethoxy-2-phenyl acetophenone (DMPA, Aldrich, Italy) were used as the cross-linking polymer and the initiator, respectively. NPOE (Sigma-Aldrich, Switzerland) was used as the plasticizer in the CTA- and PVC-based PIMs. The plasticizer dibutyl phthalate (DBP, Aldrich, USA) was also used for PVC-based PIM preparation only. Tetrahydrofuran (THF without stabiliser, VWR) and dichloromethane (DCM, Chem-supply) were of analytical reagent grade and were used in the preparation of the PIM casting solutions.

Zinc(II) chloride (Unilab, APS chemical limited, Australia) and hydrochloric acid (Ajax, Australia) were of analytical reagent grade and were used in the preparation of solutions for the extraction, back-extraction and transport experiments. For the selectivity studies, the following reagents were used: nickel(II) chloride (Sigma Aldrich, USA), cadmium(II) chloride (UNIVAR, Ajax chemicals, Australia), copper(II) chloride (UNIVAR, Ajax chemicals, Australia), cobalt(II) chloride (J.T. Baker chemicals, USA), and disodium hydrogen phosphate (BDH chemicals, UK). All aqueous solutions were prepared using deionised water (resistivity ≥18 MΩ cm, Millipore, Synergy185).

2.2. Membrane preparation

Cross-linked PIMs containing PVDF-HFP as the base-polymer were prepared by mixing a weighed amount of this polymer with THF in a glass jar (1 mL of solvent per 0.1 g of base-polymer), followed by stirring the mixture at 40 ^{o}C using a temperature-controlled water-bath. After complete dissolution of the base-polymer, D2EHPA was added, and the mixture was stirred once again at 40 ^{o}C until a homogeneous solution was obtained. After cooling to room temperature, PEG-DMA and DMPA were added to the solution. Since both the cross-linking polymer and the photo-initiator are light sensitive, the glass jar containing the casting solution was covered with aluminium foil and stirred for another 30 min at room temperature. The resultant PIM casting solution was cast on a clean, smooth glass plate using a homemade Teflon

casting knife [30]. The PIM casting solution was poured into the casting knife well which was subsequently pulled across the glass plate to form a thin layer of the PIM casting solution. The glass plate was covered with an aluminium tray (27.0 by 32.5 cm and 9.5 cm tall) to allow the slow evaporation of THF for a 24 h period thus assisting the formation of homogeneous PIMs.

Cross-linked PIMs containing PVC or CTA as the base-polymer were prepared by first dissolving the base-polymer in THF or DCM at room temperature under stirring until a homogenous casting solution was obtained. The remaining components, namely D2EHPA, NPOE or DBP, PEG-DMA, DMPA, were then added in this order to the casting solution and the solution was stirred at room temperature until complete dissolution of all PIM components was achieved which was followed by PIM casting as described above.

The resulting rectangular-shaped membranes (approximately 14 × 12 cm) were peeled from the glass plate. Only flexible, mechanically stable and homogeneous PIMs were considered as successful and selected to undergo UV treatment as described in Section 2.3. Non-cross-linked PIMs were prepared using the same procedure as described above, except that no PEG-DMA and DMPA were added to the PIM casting solution and no UV treatment was applied.

2.3. UV-polymerization

In order to cross-link the membranes a house-made UV-treatment box was used (Figure 1). The UV-treatment box consisted of two steel compartments. One of them contained the UV-lamp (UVP-USA, 8 W, 0.16 A, 230 V, tuned at 365 nm) (Figure 1A), and on top of it a glass plate (27×20 cm, 2 mm thickness) and a membrane holder were placed (Figure 1B). The other compartment acted as the lid of the box and accommodated an inlet and outlet for N_2 gas (Figure 1C). The membrane holder (Figure 1B) was composed of two metallic frames (25 × 19 cm each, wrapped in aluminium foil) which were used to hold the rectangular-shaped PIM. The glass plate was used to support the membrane holder over the UV lamp. The total distance between the UV lamp and the PIM was 7.3 cm. Since O_2 also absorbs UV-light at 365 nm, N_2 gas was pumped into the UV-treatment box for 15 min in order to purge the air. The UV-lamp was then switched on and the PIM was irradiated for 15 min while pumping N_2 gas [19].

(a) (b)

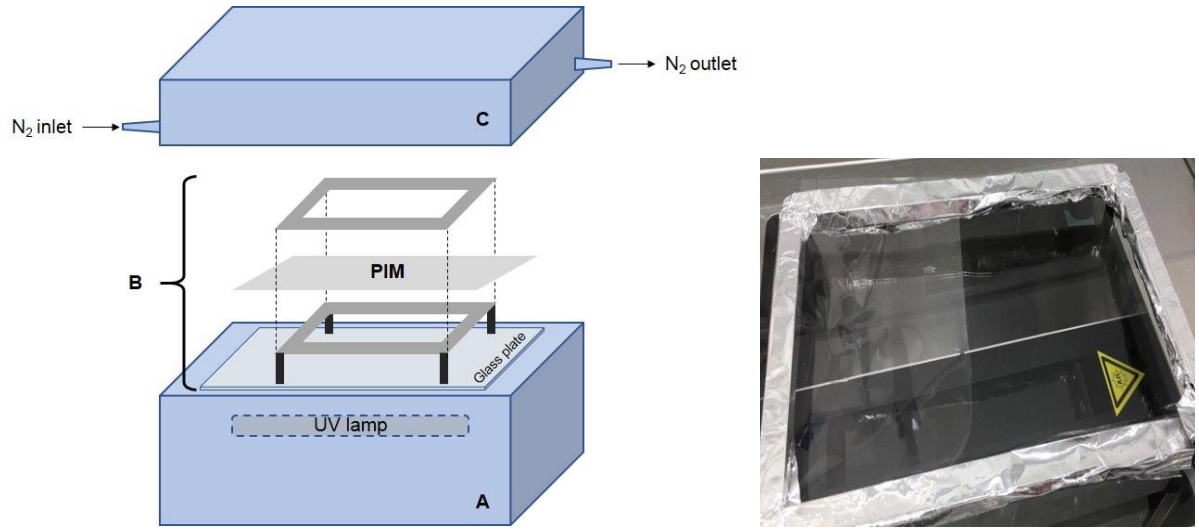

Figure 1. (a) Schematic of the UV-treatment box. (A) Compartment accommodating the UV lamp; (B) Membrane holder placed on top of a glass plate; (C) Lid of the box with a N_2 inlet and outlet. (b) Photographic image of the UV lamp compartment.

2.4. Zn(II) extraction, back-extraction and transport experiments

A 30 mg L^{-1} Zn(II) solution (prepared from $ZnCl_2$), adjusted to pH 3 using 1.0 M HCl, was used as the feed solution, and 1.0 M HCl was used as the receiving (stripping) solution for the extraction and back-extraction of Zn(II). These conditions have been adopted because they were found to be the optimal conditions for the selective and efficient extraction and back-extraction of Zn(II) using a PIM containing D2EHPA as the carrier [31]. A house-made holder, made of a 3 mm thick PVC sheet (supplied by Alternative plastics Australia Pty Ltd), was used to hold the membranes vertically inside the aqueous feed and receiving solutions to prevent the membrane from folding or attaching to the glass jar walls during the extraction and back-extraction experiments. For the extraction experiments, circular pieces of the cross-linked or non-cross-linked PIMs (3.65 cm diameter, average mass between 60 - 80 mg) were thus attached to holders and immersed in glass jars containing 100 mL of the feed solution followed by shaking at 150 rpm using an orbital shaker (Platform Mixer OM06, Ratek, Australia). For the back-extraction experiments, a similar procedure was adopted, although Zn(II)-loaded PIMs were submerged in the receiving solution instead. During the extraction and back-extraction experiments, 0.5 mL samples were collected at pre-selected time

intervals and diluted prior to the determination of the Zn(II) concentration by atomic absorption spectrometry (AAS). All the experiments were done in triplicate.

The initial flux (J_0) was calculated according to the method developed by St. John et al. [32]. An exponential decay function (Eq. (1)) was used to fit the transient Zn(II) concentration in the aqueous feed solution, and the initial flux was calculated from the first derivative (Eq. (2)) of the best exponential fit (Eq. (1)). All these calculations were executed with the help of a home-made Quick C program.

$$\Psi = a_1 + a_2\, e^{-a_3 t} \quad (1)$$

where a_1, a_2 and a_3 are the empirical coefficients of Eq. (1) best fitting the experimental data.

$$J_0 = \left(\frac{d\Psi}{dt}\right)_{t=0} = -a_2 a_3 \quad (2)$$

Transport experiments involving the simultaneous extraction and back-extraction of Zn(II) on each side of the PIM with best extraction performance were carried out in a glass transport cell consisting of two 100 mL compartments (i.e., feed and receiving compartment) separated by the PIM with a surface area exposed to the feed and receiving solutions of 18.1 cm^2 (diameter of 4.8 cm) (Figure 2). The membrane was sandwiched between the two compartments with the assistance of Teflon gaskets. Transport experiments involving feed solutions with three different Zn(II) concentrations (i.e., 27, 46 and 65 mg L^{-1} Zn(II)) and a receiving solution containing 1.0 M HCl were conducted. During the transport experiments, both the feed and receiving solutions were stirred at 1200 rpm (measured by a laser tachometer, Digitech QM1448, Jaycar, Australia) using glass stirrers and the rotation speed was monitored periodically using the tachometer. Samples of 0.5 mL were collected from the feed and receiving solutions at predetermined times and replaced with the same volume of deionised water or 1.0 M HCl, respectively. The collected samples were then diluted with deionised water and their Zn(II) concentrations were measured by AAS.

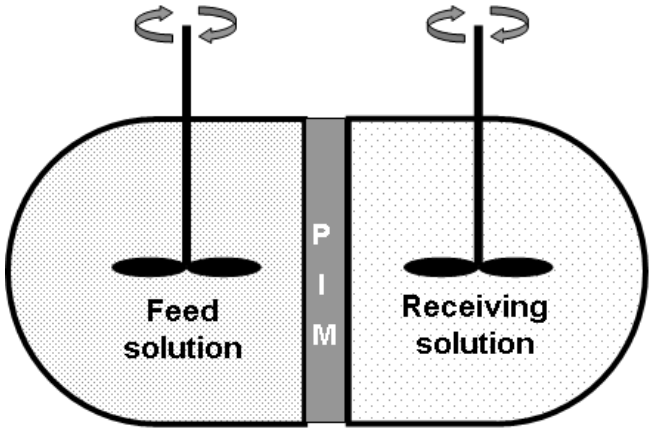

Figure 2. Schematic of the PIM transport cell.

2.5. Instrumentation

The Zn(II) concentration in all feed and receiving solutions was determined by AAS (Hitachi Z-2000 Series Polarized Zeeman, Japan) with the following settings: Zn hollow cathode lamp (Hitachi); current, 8 mA; working wavelength, 213.9 nm; burner height, 7 mm; slit width, 0.7 nm; acetylene flow rate, 1.8. L min^{-1}; and air flow rate, 15.0 L min^{-1}.

Inductively coupled plasma-optical emission spectrometry (ICP-OES) (Optima 4300 DV, PerkinElmer, USA) was used to determine the transient concentrations of Zn(II), Co(II), Cu(II), Ni(II), Cd(II), and Fe(III) in the feed solutions used in the selectivity study. The instrumental set up was: power level, 1.30 kW; coolant flow, 15.0 L min^{-1}; auxiliary flow, 0.20 L min^{-1}; nebulizer flow, 0.80 L min^{-1}; and sample aspiration rate, 1.50 mL min^{-1}.

The pH of the feed and receiving solutions was measured before and after each experiment using a combined pH/conductivity meter (SmartChem-Lab, TPS, Australia).

Membrane thickness was measured using an optical microscope (LH50A, Olympus, Japan) with a calibrated Nikon lens (Carton Optical Ind., Japan). Circular membranes were cut in half and the thickness of the cross-section was measured at ten different points for a single membrane. A similar experiment was conducted in triplicate (i.e., three different membranes for each type were studied).

The mass of each membrane was measured using an analytical balance before each extraction experiment. In the stability study, membrane mass was also measured after drying the membrane overnight following each extraction/back-extraction cycle.

Mass spectra of the feed and receiving solutions were obtained by electrospray ionisation mass spectrometry (ESI-MS) in positive mode using an Aligent 6520 Quadrupole Time of Flight (Q-ToF) Mass Spectrometer (Agilent Technologies, USA), controlled via the MassHunter software package version B.05.01. For each analysis, 1 μL of sample was injected into the carrier of 70% acetonitrile and 30% formic acid (0.1%) at a flow rate of 3 mL min^{-1}. The mass spectrometer conditions were as follows: drying gas flow rate, 7 L min^{-1}; nebuliser pressure, 40 psi; drying gas temperature, 300 °C; capillary voltage, 3500 V; fragmentor voltage, 100 V; skimmer voltage, 65 V; Oct Rf, 750 V; scan range acquired, 20 - 1200 m/z. Standard solutions were prepared by dissolving weighted amounts of PEG-DMA, D2EHPA and NPOE in acetonitrile (Ajax, Australia) and deionised water.

2.6. Surface morphology study

The surface morphology of UV-treated and non-treated PIMs was studied by atomic force microscopy (AFM, Asylum Research, Oxford Instruments). The AFM study was performed using a Si tip with force constant 1.2-29 N m^{-1}. The resonance frequency of the cantilever during the imaging was ≈ 138 kHz. The relative humidity (58-60%) and temperature (21-23 ^{o}C) of the experimental room were monitored during the imaging period. Image processing and roughness calculations were conducted with WSxM 5.0 software (Nanotech).

3. Result and discussion

3.1. Selection of the base-polymer

Although the base-polymer is not the active constituent of a PIM, it plays an important role in determining its properties as it provides the back-bone of the membrane which holds the carrier within its structure. The PIM's performance depends on the compatibility between the base-polymer, the membrane liquid phase and, in the case of cross-linked PIMs, also on the nature of the cross-linking polymer. Hence, three different base-polymers, namely PVC, CTA and PVDF-HFP, were used to cast cross-linked (mass ratio of base-polymer to cross-linking polymer of 5:5) and non-cross-linked PIMs containing 35 wt% D2EHPA as the carrier to assess their ability to form homogeneous and mechanically stable PIMs with oil-free surfaces. Due to incompatibility between the membrane components, the PIM liquid phase may exude onto the membrane surface and form tiny droplets which can be either visually observed or detected by gently wiping the membrane surface with a tissue paper. It was observed that the surfaces of the cross-linked PVC- and CTA-based PIMs were oily (i.e., unsuccessful PIMs) and the PVDF-HFP-based PIM was homogenous and with oil-free surfaces (i.e., successful PIM). Since, PIMs containing only D2EHPA and PVC are well known to produce good membranes [1], this oil formation on the PIMs' surfaces suggested an incompatibility between the polymers which is likely due to the difference in their polarities. A separate plasticizer was thus added to the cross-linked PVC- and CTA-based membranes. NPOE was chosen because it is one of the most commonly used plasticizers in PIMs due to its low viscosity (11.1 cP, 25 °C [1]) and high dielectric constant (ε_r = 24, 25 °C [1]). The cross-linked PIM with CTA and NPOE (20 wt%) was homogenous and with oil-free surfaces and was thus considered to be successful and studied further. However, the cross-linked PVC-based membrane still had an oily surface in

the presence of 20 wt% NPOE. DBP was also tested as plasticizer (ε_r = 6.58, 20 °C [1]) to cast PVC-based cross-linked membranes, although these were also oily and thus PVC-based membranes were not considered for further studies. The corresponding non-cross-linked PVC- and CTA-based PIMs were considered as successful because they were homogeneous, stable and with oil-free surfaces.

As both CTA (with NPOE) and PVDF-HFP base-polymers allowed the formation of successful cross-linked PIMs, a comparison between cross-linked and non-cross-linked PIMs was conducted with respect to their ability to extract Zn(II). The results of extraction experiments, expressed as mg of Zn(II) extracted per 1 g of PIM versus time, are presented in Figure 3. The cross-linked CTA-based PIM extracted Zn(II) at a faster rate in comparison with its non-cross-linked counterpart (Figure 3a), whereas the same was not observed for the PVDF-HFP-based membranes (Figure 3b). Moreover, the rate of extraction of Zn(II) into the cross-linked CTA-based membrane was higher than that for the cross-linked PVDF-HFP-based PIM. Therefore, CTA was selected as the base-polymer in the subsequent experiments.

The results presented in Figure 3 suggest that cross-linking affects in a different way the structure of CTA and PVDF-HFP-based PIMs. However, this structure is also strongly dependent on the PIM carrier[10]. In addition to the structural factors, the rate of extraction and transmembrane transport are also determined by the nature of the extracted chemical species-carrier adduct (e.g., ion-pair or complex) and the characteristics of the PIM liquid phase (i.e., viscosity, dielectric constant)[2, 3]. Previously reported results on the comparison of cross-linked and non-cross-linked PIMs containing PVDF-HFP as the base-polymer and Aliquat 336 as the carrier in the extraction of SCN^- showed that the cross-linked PIM performed considerably better than its non-cross-linked counterpart [19]. This phenomenon was explained by the presence of hydrophilic PEG groups whose hydration could have led to the creation of water channels within the membrane assisting the transmembrane transport of the ion-pairs of the quaternary alkylammonium cations of Aliquat 336 and SCN^-. However, in the case of the extraction and transport of the hydrophobic Zn(II)-D2EHPA complex, these water channels are unlikely to provide any advantages and hence the performance of the PVDF-HFP cross- and non-cross-linked PIMs was found to be similar (Figure 3b). However, it can be hypothesized that cross-linking of the CTA-based PIMs containing D2EHPA as carrier induces bulk or surface structural changes which are beneficial to their performance. The beneficial effects on Zn(II) extraction and transport of the surface morphology of the cross-linked CTA-based PIMs are discussed in Section 3.4.

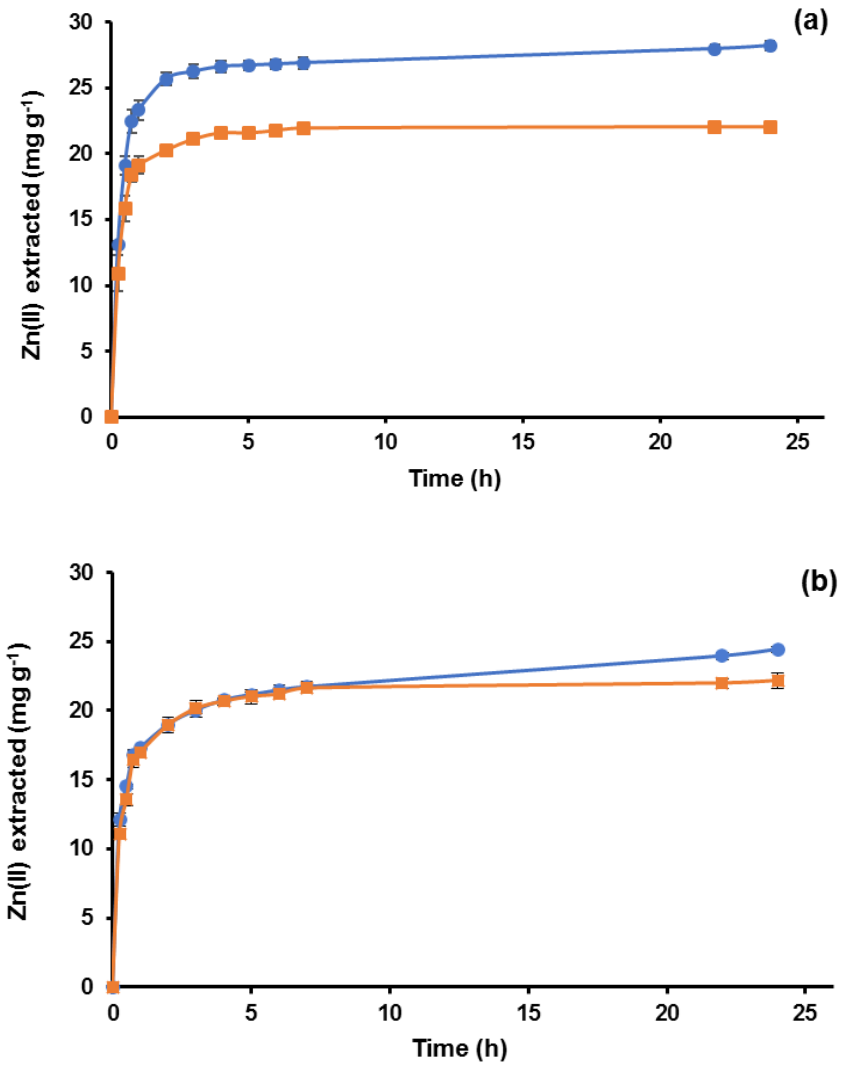

Figure 3. Transient concentration of Zn(II) extracted (expressed as mg Zn per g of PIM) into cross-linked (●) or non-cross-linked (■) PIMs composed of 35 wt% D2EHPA as the carrier (extractant) and CTA (a) or PVDF-HFP (b) as the base-polymer. Polymer ratio, 6:4; NPOE concentration in the CTA-based PIMs, 20 wt%; feed solution, 100 mL of 30 mg L^{-1} Zn(II) at pH 3; PIMs thicknesses and masses : CTA-crosslinked - 54±2 μm, 63.4 ± 4.0 g; CTA-non-crosslinked - 55±2 μm, 59.3 ± 0.4; PVDF-HFP-crosslinked - 46±3 μm, 66.6 ± 0.6 mg and PVDF-HFP-non-crosslinked - 44±3 μm, 62.2 ± 4.1 mg. Error bars, ± standard deviation (SD) based on 3 replicate experiments (n=3).

With the aim of proving that the extractant was the PIM component responsible for the extraction of Zn(II), a blank experiment was also conducted using a CTA-based cross-linked membrane with a composition identical to the one described above with the exception that no carrier (i.e., D2EHPA) was added. The result obtained (Figure S1, Supplementary Material) indicated that no Zn(II) was transferred from the solution to the PIM. Therefore, it was concluded that the transfer of Zn(II) from the solution to the PIM was the result of its extraction by the PIM carrier (i.e., D2EHPA).

3.2 Effect of CTA-based cross-linked membrane composition on Zn(II) extraction

3.2.1 Effect of the polymer ratio (CTA:PEG-DMA)

The ratio between the cross-linking polymer and the base-polymer to form the backbone of the cross-linked PIM within which the carrier was held was found to affect the properties of the corresponding PIM [19]. Therefore, it was essential to study the effect of the polymer ratio CTA:PEG-DMA in order to achieve satisfactory extraction performance. Extraction experiments were thus conducted with cross-linked PIMs with a ratio of CTA to PEG-DMA varying from 5:5 to 9:1, while maintaining all other conditions (i.e., 35 wt% D2EHPA, 20 wt% NPOE, 0.6 wt% initiator, 15 min of UV-treatment, feed solution containing 30 mg L^{-1} Zn(II) at pH 3) constant. Increasing the amount of PEG-DMA, so that it was higher than the amount of the base-polymer CTA, was found to compromise the membrane's mechanical stability. A similar observation, using PVDF-HFP as the base-polymer, was also reported by O'Bryan et al. [19]. The results obtained in extraction experiments are shown in Figure 4, where it can be observed that the PIMs with 5:5 and 6:4 polymer ratios exhibited the highest extraction rates, while the extraction rates of the other PIMs were 20% lower. The higher extraction rates for ratios 5:5 and 6:4 were probably caused by the higher degree of cross-linking. The polymer ratio 6:4 was selected for the subsequent experiments since the PIM with the polymer ratio 5:5 was slightly sticky and softer before UV-treatment in comparison with the PIMs with the former polymer ratio. It was also observed that the initial flux for the PIM with 6:4 polymer ratio was slightly higher than the one for the PIM with 5:5 polymer ratio (14.8 and 13.4 μmol m^{-2} s^{-1}, respectively).

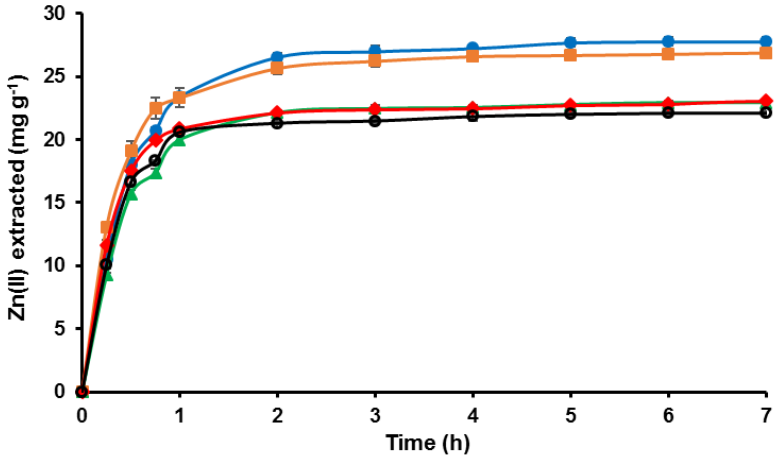

Figure 4. Effect of the ratio between CTA and PEG-DMA on the transient concentration of Zn(II) extracted into the corresponding PIM (expressed as mg Zn per g of PIM): (●) 5:5; (■) 6:4; (♦) 7:3; (▲) 8:2, and (○) 9:1. PIM composition, 35 wt% D2EHPA, 20 wt% NPOE, 0.6% initiator; feed solution, 100 mL of 30 mg L^{-1} Zn(II) at pH 3; PIMs thicknesses varied between 50 and 55 μm (Table S1, Supplementary Material). Errors bars, ± SD (n=3).

3.2.2 Effect of the membrane liquid phase composition

As mentioned in the Introduction, PIM instability is associated with the loss of membrane liquid phase. In the present study the membrane liquid phase consisted of the extractant D2EHPA and the plasticizer NPOE. Hence, it was important to study the effect of their concentrations in order to obtain a PIM composition which produced stable PIMs with good extraction capabilities. The effect of the membrane liquid phase was thus studied by casting PIMs with different concentrations of D2EHPA (35-50 wt%) and NPOE (5-20 wt%), as shown in Table 1. Those PIM compositions that produced successful membranes (i.e., homogenous, transparent and mechanically stable) were then used in the Zn(II) extraction experiments, and the performance of the corresponding PIMs was assessed according to the amount of Zn(II) extracted (Table 1).

Table 1. Effect of the membrane liquid phase composition of the cross-linked CTA-based PIM on its appearance and extractive capacity. The concentrations of the carrier (i.e., D2EHPA) and plasticizer (i.e., NPOE) were varied while keeping the polymer ratio at 6:4 (CTA:PEG-DMA) and the initiator concentration at 0.6 wt%. Successful PIMs were used in the extraction and back-extraction experiments for a 24 h period. Zn(II) concentrations in the PIMs (mg g^{-1}) at equilibrium are also presented.

PIM ID	**D2EHPA (wt%)**	**NPOE (wt%)**	**PIM's physical appearance before extraction**	**PIM's physical appearance after back-extraction**	**Zn(II) extracted at equilibrium (mg g^{-1})**
1	35	5	✓	✓	26.0 (±0.3)
2	35	10	✓	✓	24.0 (±0.3)
3	35	20	✓	✓	28.2 (±0.4)
4	40	5	✓	✓	31.6 (±0.1)
5	40	10	✓	✓	31.1 (±0.2)
6	40	20	✓	✓	28.6 (±0.3)
7	45	5	✓	Deformed and white in color	36.5 (±0.7)
8	45	10	✓	Deformed and white in color	34.5 (±0.2)
9	45	20	✓	NT	31.9 (±1.3)
10	50	5	Non-homogenous	NT	NT
11	50	10	Non-homogenous	NT	NT
12	50	20	Non-homogenous	NT	NT

✓ Successful PIM (i.e., homogenous, transparent and mechanically stable); NT, PIM not tested,

All membranes cast with 50 wt% D2EHPA (Table 1, PIMs 10, 11 and 12) were not homogenous and for that reason were not considered as successful for further study. Membranes with 35, 40 or 45 wt% D2EHPA and 5, 10 or 20 wt% NPOE (Table 1, PIMs 1 to 9) were found to be successful and were assessed for their ability to extract Zn(II). PIMs with 45 wt% D2EHPA and with 5 or 10 wt% NPOE (Table 1, PIMs 7 and 8) were more efficient in extracting Zn(II) than the remaining successful PIMs. It was observed that, after back-extraction with 1.0 M HCl solution (i.e., receiving solution), these PIMs started to become opaque. It was assumed that the PIM opaqueness could be related to the presence of insoluble Zn(II)-DEHP adducts in the membrane as this was observed for PIMs with higher extractant concentrations. The PIMs containing 40 wt% D2EHPA and 5 or 10 wt% NPOE (Table 1, PIMs 4 and 5), and 45 wt% D2EHPA and 20 wt% NPOE (Table 1, PIM 9) were all able to extract about 31 mg of Zn(II) per g of membrane. PIMs 4 and 5 exhibited the same extraction efficiency as PIM 9 but contained lower concentrations of D2EHPA and NPOE and therefore were selected for the subsequent stability study.

3.3 Stability study

Both PIMs 4 and 5 (Table 1) were used in 5 consecutive extraction and back-extraction experiments (i.e., 5 cycles) to assess their long-term stability. It was observed that after the second cycle, PIM 4 started to become opaque as a precipitate started to form on the PIM's surface, whereas no such formation was observed for PIM 5 throughout the 5 cycles. Therefore, PIM 5 was selected as the PIM composition with best extraction performance for further studies in which its stability was compared with that of non-cross-linked PIMs.

The superior stability of cross-linked PIMs containing PVDF-HFP as the base-polymer and Aliquat 336 as the extractant in comparison with the corresponding non-cross-linked PIMs has been demonstrated earlier by the Kolev group in 5 consecutive extraction/back-extraction experiments [19]. Similarly, the cross-linked CTA-based PIM (PIM 5, Table 1) and its non-cross-linked counterpart were used in five consecutive extraction/back-extraction experiments, and their stability was compared in terms of extraction rate and amount of Zn(II) extracted. In each case back-extraction was very fast and virtually complete stripping of Zn(II) from the loaded membrane was observed (Figures S2 and S3, Supplementary Material). Figure 5 shows all five extraction curves for each membrane. The extraction performance of the non-cross-linked PIM (Figure 5b) decreased by 31%, whereas this decrease for the cross-linked PIM was

only 7% (Figure 5a). In addition, the non-cross-linked PIM (i.e., 40 wt% D2EHPA, 10 wt% NPOE and 50 wt% CTA) started to become physically deformed (i.e., wrinkled around the edges) and opaque after the second cycle (Figure S4, Supplementary Material) due to the accumulation of a precipitate. It was hypothesized that this precipitate was the leached-out Zn-D2EHPA complex which was confirmed by AAS measurements indicating the presence of Zn in the precipitate. Hence, it was concluded that the cross-linked PIM showed superior extraction efficiency and stability in comparison with the non-cross-linked PIM.

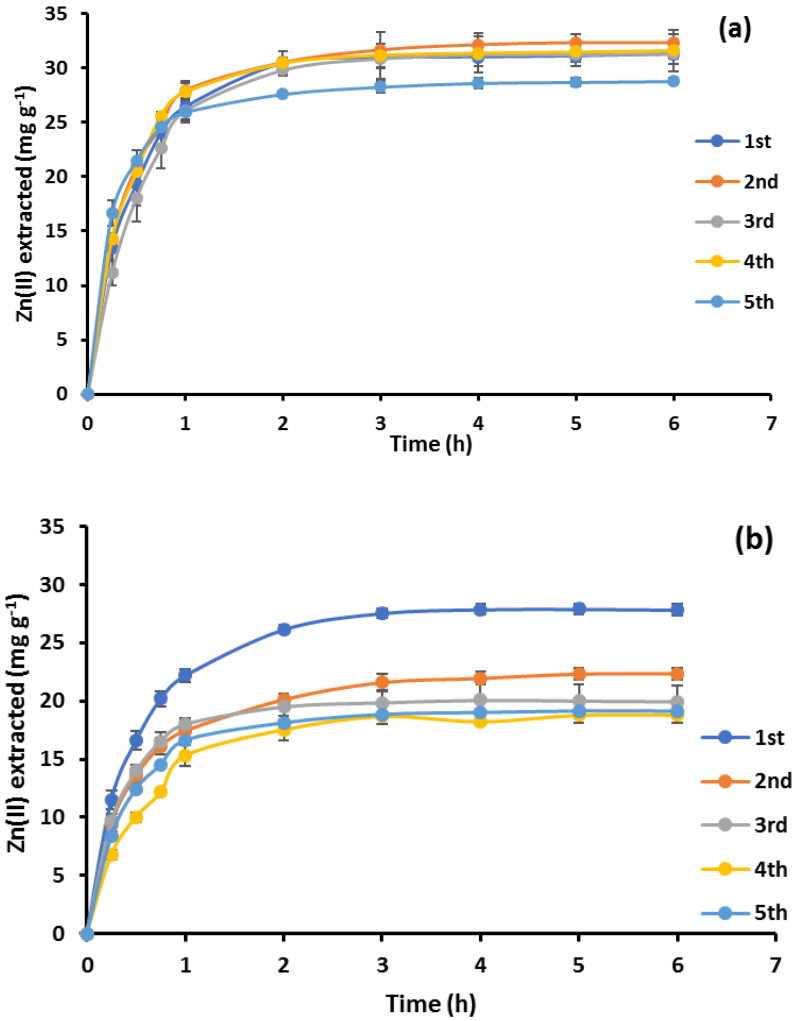

Figure 5. Transient Zn(II) concentrations in a cross-linked (a) and a non-cross-linked (b) CTA-based PIM (mg Zn(II) per g PIM) for five consecutive extraction experiments. D2EHPA concentration, 40 wt%; NPOE concentration, 10 wt%; polymers ratio, 6:4; initiator concentration, 0.6 wt%; feed solution, 100 mL of 30 mg L^{-1} Zn(II) at pH 3; receiving solution, 1.0 M HCl. Error bars, ± SD (n=3).

It was also observed that in the second extraction experiment the cross-linked PIM extracted a slightly higher amount of Zn(II) (32.3 mg g^{-1}) than in the first extraction experiment (31.2 mg g^{-1}) despite a 12% mass loss after the first extraction/back-extraction cycle. With the aim of finding an explanation for this observation, the feed and receiving solutions after the first and second cycles were analyzed by mass spectrometry and the corresponding spectra are shown in Figure 6a. The mass spectrum of the feed solution after the first extraction experiment showed peaks with high intensity at 441, 485 and 529 (m/z), which corresponded to the presence of PEG-DMA (Figure 6a). The difference between two consecutive peaks is 44 (m/z) which corresponds to the mass of a PEG unit. Therefore, it can be concluded that peaks at 441, 485, 529, 573 and 617 (m/z) refer to PEG-DMA with different number of PEG units. Peaks at 323 (protonated D2EHPA $(D2EHPA+H)^{+}$) and 645 (m/z) (protonated D2EHPA dimer $(D2EHPA\text{-}D2EHPA)+H)^{+}$.) were also identified, corresponding to the presence of D2EHPA, although their intensity was significantly lower than that of the PEG-DMA peaks. In the feed solution after the second extraction experiment, no PEG-DMA peaks were observed and the D2EHPA peaks were still present as in the feed solution after the first extraction experiment (Figure 6b).

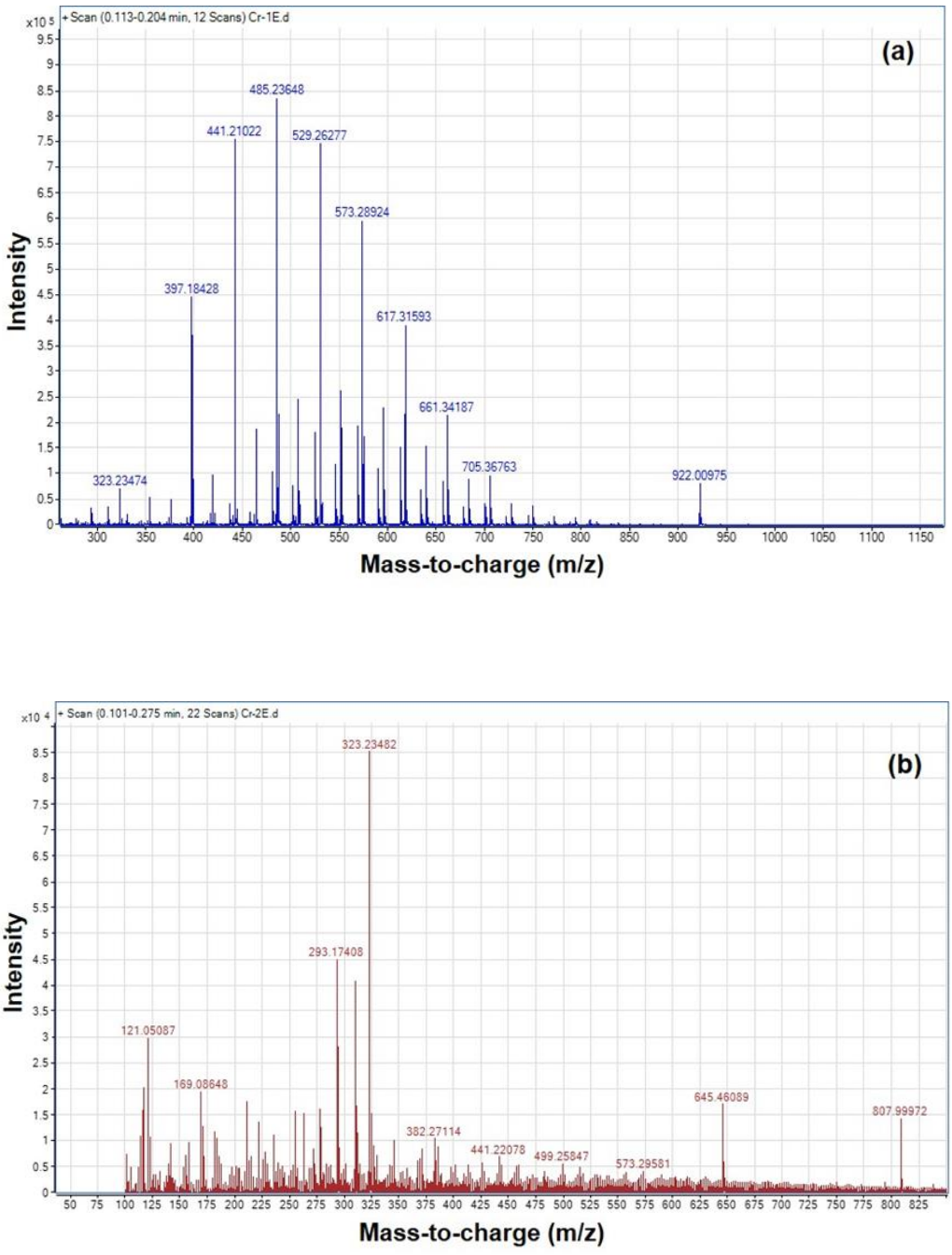

Figure 6. Mass spectra of the feed solution after the first (a) and second (b) extraction experiments involving the same cross-linked membrane (PIM 5, Table 1).

It should be noted that no peaks corresponding to either PEG-DMA or D2EHPA were observed in the mass spectra of the back-extraction solutions, and no peaks related to NPOE were identified in any of the solutions. This analysis indicated that the mass loss of 12% recorded after the first cycle was mostly due to the loss of un-crosslinked PEG-DMA present in the membrane. The loss of PEG-DMA during Zn(II) extraction can be avoided by washing the

membrane with a mildly acidic solution (to prevent D2EHPA loss by reducing its solubility) before its use in extraction/transport experiments. It was assumed that the un-crosslinked PEG-DMA impeded to some extent the extraction of Zn(II) and, therefore, its loss to the feed solution in the first cycle resulted in a higher initial flux value (i.e., 1.2×10^{-5} and 1.5×10^{-5} mol m^{-2} s^{-1} for the 1st and 2nd cycles, respectively) and a slightly higher amount of Zn(II) extracted despite the fact a small amount of D2EHPA was lost (about 2%) in the first cycle. From the second cycle onwards, there was no loss of PEG-DMA as cross-linked PEG-DMA chains are less susceptible to get solubilised in the aqueous phase. However, small amounts of D2EHPA (i.e., 2-3%) leached into the feed solution during each subsequent cycle (Figure 7), which was most likely responsible for the relatively small decrease in the amount of Zn(II) extracted in each subsequent cycle (i.e., 32.3 mg in the 1st cycle versus 28.8 mg Zn(II) g^{-1} in the 5th cycle).

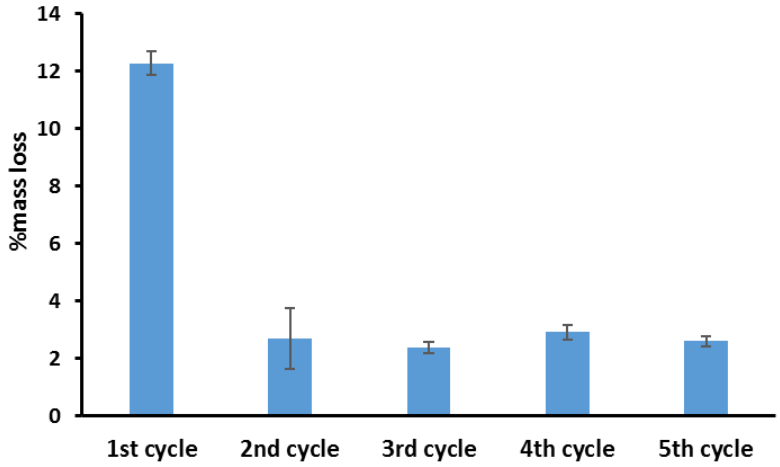

Figure 7. Percentage mass loss of a cross-linked CTA-based PIM (PIM 5) during the stability study (i.e., five consecutive extraction and back-extraction cycles). Error bars, ± SD (n=3).

3.4. Surface morphology analysis

3.4.1 Cross-linked vs. non-cross-linked CTA-based PIMs

Due to good extraction efficiency and stability, the surface morphology of the cross-linked PIM 5 (Table 1) and its non-cross-linked counterpart (i.e., 40 wt% D2EHPA, 10% NPOE and 50% CTA) was studied using AFM. Typical constant force AFM topographs are shown in Figure 8. There are distinguishable morphological differences between the cross-linked and non-cross-linked membranes.

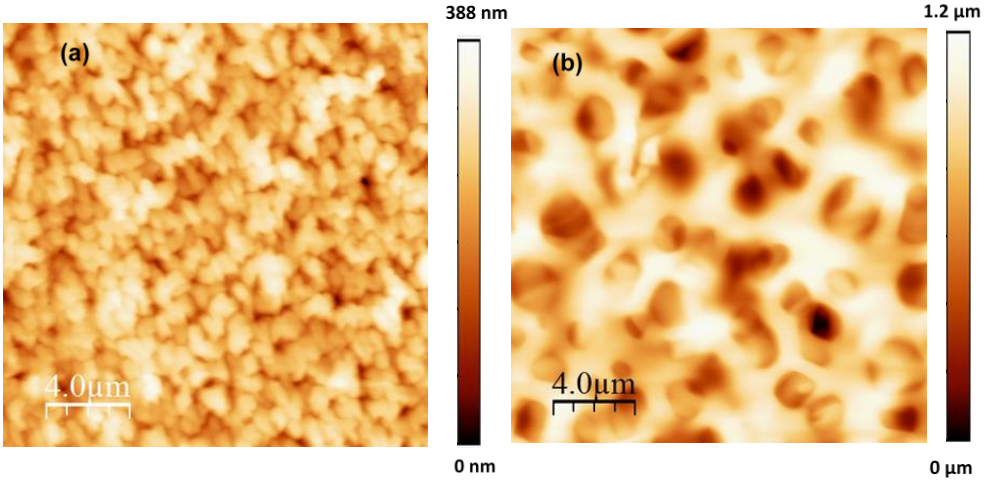

Figure 8. Constant force AFM topographs of a cross-linked (a) and non-cross-linked (b) membrane (cross-linked PIM composition: 40 wt% D2EHPA, 10 wt% NPOE, polymers ratio 6:4, 0.6 wt% initiator; non-cross-linked PIM composition: 40 wt% D2EHPA, 10 wt% NPOE, 50 wt% CTA).

Figure 8a clearly shows that the cross-linked PIM exhibits granular like features and the corresponding voids between the granules are as deep as 400 nm relative to their tops, whereas the non-cross-linked membrane appears as a smooth film with deeper dents (as deep as 1200 nm) in comparison with the cross-linked PIM. In order to assess the surface area of the membranes, the granule/void density was calculated, and is shown in Table 2 and Figure 9. For the non-cross-linked membrane, 11 voids per 100 μm^2 were found in which approximately 10% of the voids were around 800-900 nm, and the remaining varied from 250-500 nm (Table 2; Figure 9b). On the other hand, in the cross-linked membrane about four times more voids were identified, well distributed throughout the PIM surface, with an average depth of 150-250 nm (Table 2; Figure 9a). Even though the cross-linked PIM's voids were shallower than those of its non-cross-linked counterpart, they provided a larger effective surface area compared to the cross-linked PIM due to their much higher number which resulted in higher PIM flexibility and extraction rate in comparison with the non-cross-linked PIM (Figure 3a).

Table 2. Analysis of the PIM voids in the AFM topographs of the cross-linked and non-cross-linked PIMs.

Type of PIM	Number of voids (per 100 μm^2)	Area covered by the voids (μm^2)
Cross-linked PIM (PIM 5)	48	20
Non-cross-linked PIM	11	27

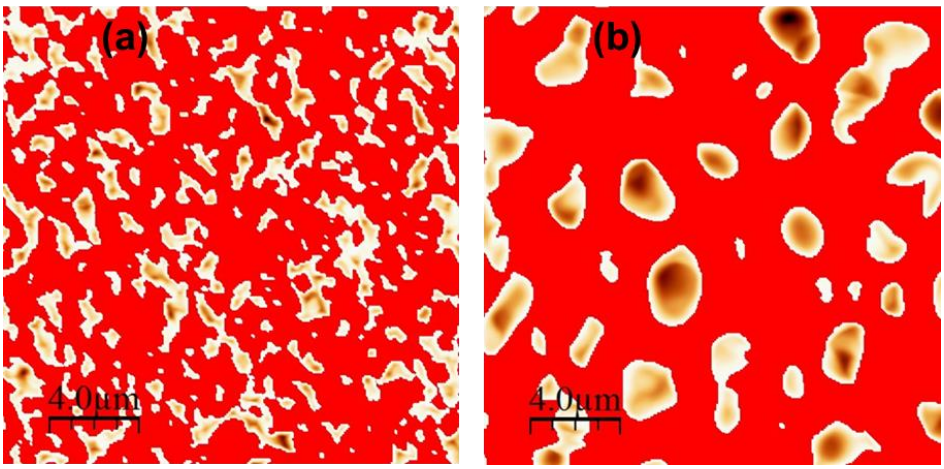

Figure 9. Contrast saturated AFM topographs of a cross-linked (a) and non-cross-linked (b) membrane. The voids present in cross-linked and non-cross-linked membranes are clearly visible (cross-linked PIM composition: 40 wt% D2EHPA, 10 wt% NPOE, polymers ratio 6:4, 0.6 wt% initiator; non-cross-linked PIM composition: 40 wt% D2EHPA, 10 wt% NPOE, 50 wt% CTA).

3.4.2 Effect of the amount of plasticizer on the surface morphology of the cross-linked CTA-based PIMs

In general, the role of the plasticizer in PIMs is to penetrate the base-polymer chains and decrease the intermolecular forces, leading to a decrease in the glass transition temperature of the polymer which results in a more flexible membrane. Hence, the plasticizer concentration in the membrane is important: if it is too low the membrane will be too rigid and if it is too high the membrane will be too soft and mechanically unstable, and moreover the plasticizer tends to exude to the membrane surface. In order to assess the effect of the plasticizer

concentration on the surface morphology of cross-linked membranes, PIMs containing 40 wt% D2EHPA and 5, 10 or 20 wt% NPOE (Table 1, PIMs 4, 5 and 6), were imaged by AFM (Figures 10a-10c). The AFM topographs show that the three PIMs mentioned above are morphologically similar and consist of interconnected granules. However, the size of the granules gradually decreased as the NPOE concentration in the membrane was increased as a result of more NPOE penetrating the polymer chains thus making them slightly more flexible which resulted in smoother PIM surfaces and higher initial flux values (Figure 10d).

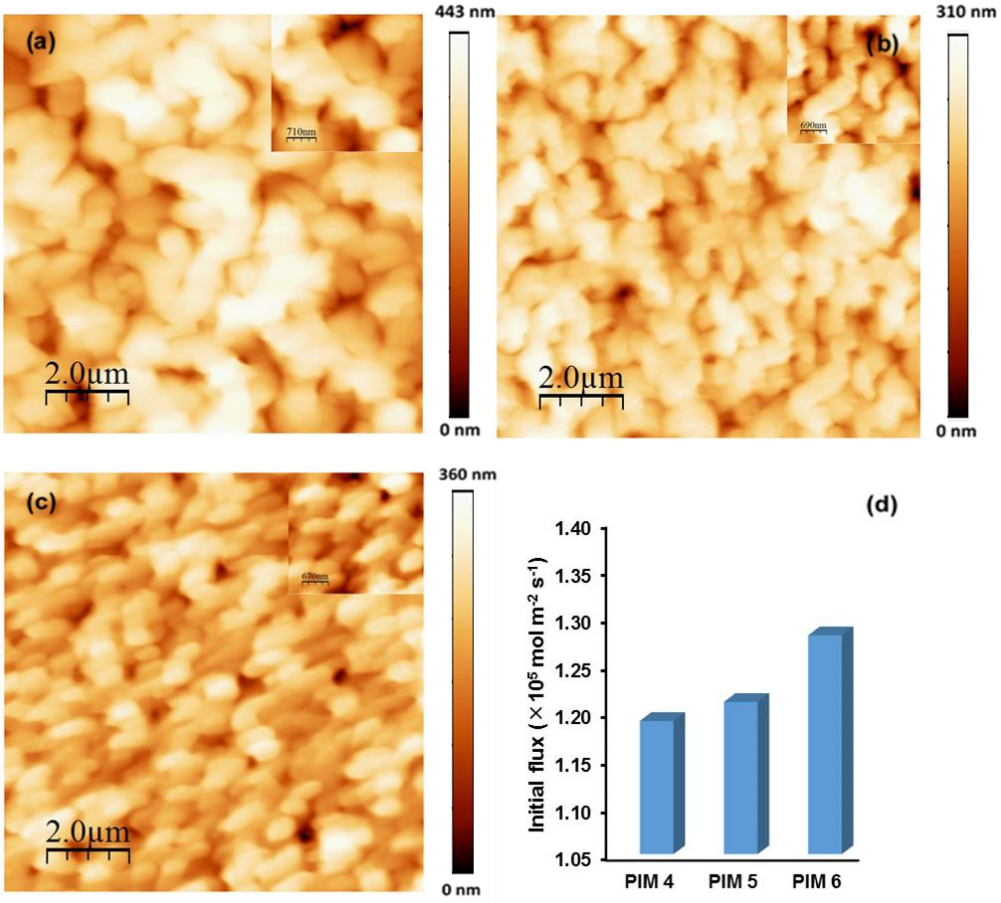

Figure 10. Constant force AFM topographs of cross-linked membranes containing different NPOE concentrations: (a) 5 wt%, (b) 10 wt% and (c) 20 wt%, and the corresponding initial flux values (d). D2EHPA concentration, 40 wt% D2EHPA; polymers ratio (CTA:PEG-DMA), 6:4; initiator (DMPA) concentration, 0.6 wt%.

3.5. Interference study

In environmental or industrial waters common base metal ions, such as Cd(II), Co(II), Ni(II), and Fe(III), will also be present along with Zn(II). Therefore, selectivity is a very important parameter for assessing the suitability of the newly developed PIM for environmental or industrial applications.

An interference study was conducted using the cross-linked CTA-based PIM (PIM 5, Table 1), which provided a good extraction performance and the best long-term stability. This PIM was thus immersed in 100 mL of synthetic feed solution containing Zn(II), Co(II), Ni(II), Cd(II), and Cu(II) at 30 mg L^{-1} concentration each and pH 3. Figure 11a clearly indicates that Zn(II) was preferentially extracted into the membrane with minimal interference from the other base metal ions. Since these base metal ions can also be present at concentrations higher than that of Zn(II), the selectivity of the newly developed cross-linked PIM was also assessed when the concentrations of the interferents were five times higher than the Zn(II) concentration (i.e., feed solution containing 30 mg L^{-1} Zn(II) and 150-160 mg L^{-1} Co(II), Ni(II), Cd(II), and Cu(II) each). Even under these conditions the interference was relatively insignificant (Figure 11b). These results confirmed the high selectivity of the CTA/D2EHPA cross-linked PIM towards Zn(II), showing that Zn(II) could be extracted selectively in the presence of a mixture of different base metal ions commonly present in environmental and industrial waters.

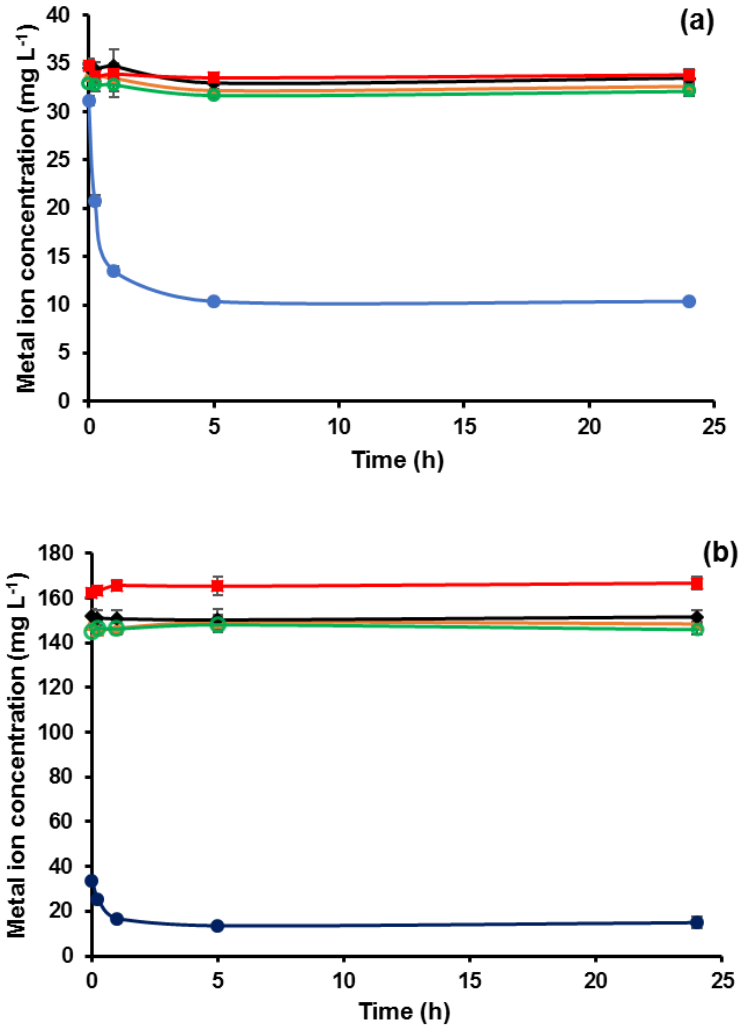

Figure 11. Transient concentrations of (●) Zn(II), (■) Cd(II), (▲) Co(II), (♦) Cu(II), and (○) Ni(II) in the feed solutions at pH 3 in which the potential interfering metal ions have the same concentration as Zn(II) (a) or have a concentration five times higher than that of Zn(II) (b). Cross-linked PIM composition, 40 wt% D2EHPA, 10 wt% NPOE, CTA:PEG-DMA 6:4, 0.6 wt% initiator; feed solution, 100 mL of 30 mg L^{-1} of each metal ion (a) and 30 mg L^{-1} Zn(II) and 150-160 mg L^{-1} for each interferent (b).

Fe(III) is commonly present in industrial and environmental waters and has been reported to interfere with Zn(II) extraction when using D2EHPA-based PIMs [31]. In the same study the Fe(III) interference was successfully eliminated by adding disodium hydrogen phosphate (Na_2HPO_4) to the feed solution in a 1:3 mole ratio (Fe(III):Na_2HPO_4) in order to precipitate Fe(III) and thus avoid its extraction by the PIM. The same approach was applied in the present study. The results obtained confirmed the Fe(III) interference in the absence of Na_2HPO_4, and

also demonstrated that in the presence of Na_2HPO_4 the interference of Fe(III) could be eliminated and Zn(II) could be extracted to the same extent as if Fe(III) were not present (Figure 12).

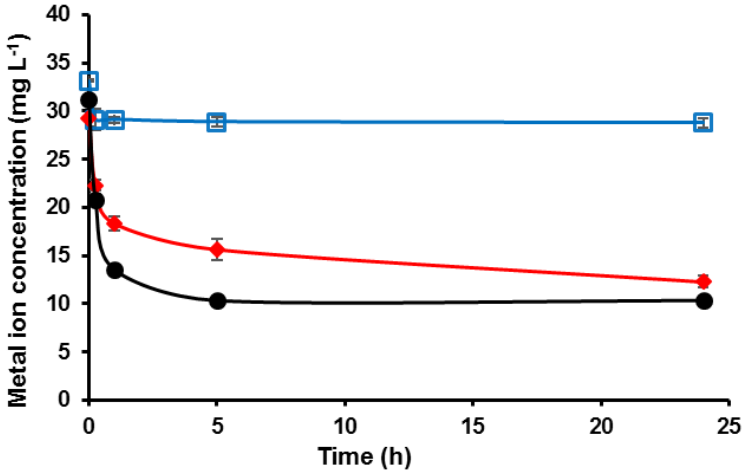

Figure 12. Transient concentrations of Zn(II) (□) and Fe(III) (◆) in a feed solution containing 30 mg L^{-1} of each ion, and of Zn(II) (●) in a feed solution of the same Fe(III) and Zn(II) composition in the presence of Na_2HPO_4. Cross-linked PIM composition, 40 wt% D2EHPA, 10 wt% NPOE, CTA : PEG-DMA 6:4, 0.6 wt% initiator. Error bars, ± SD (n=3).

3.6. Transport of Zn(II)

One of the main advantages of PIM-based separation over conventional solvent extraction stems from the possibility of conducting the extraction and back-extraction processes at the feed and receiving sides of the PIM, respectively, simultaneously. This capability of PIMs, in combination with their facilitated transmembrane mass transport mechanism [1, 2], allows the complete transport of the target chemical species (in this case Zn(II)) from the feed to the receiving solution. To demonstrate this capability of PIM-based separation, transport experiments were carried out using the cross-linked PIM with best extraction performance which was composed of 40 wt% D2EHPA, 10 wt% NPOE, and CTA:PEG-DMA 6:4, and 0.6 wt% initiator. Feed solutions containing 27, 46 or 65 mg L^{-1} Zn(II) at pH 3 and receiving solutions containing 1.0 M HCl were used in these experiments. The transient Zn(II) concentrations in the feed and receiving solutions, shown in Figure 13, clearly indicate that the newly developed cross-linked membrane is capable of practically completely (i.e., 98.9±0.9 %, 93.6±1.0 % and 97.2±2.1 % for initial Zn(II) concentrations of 27, 46 and 65 mg L^{-1},

respectively) transporting Zn(II) from the feed solution to the receiving solution in about 3 h under the experimental conditions used. The thickness of the membrane decreased insignificantly from 55±2 μm to 52±2 μm after completing the transport experiments which was, most likely, due to the leaching of un-crosslinked PEG-DMA from the membrane into the adjacent aqueous phases.

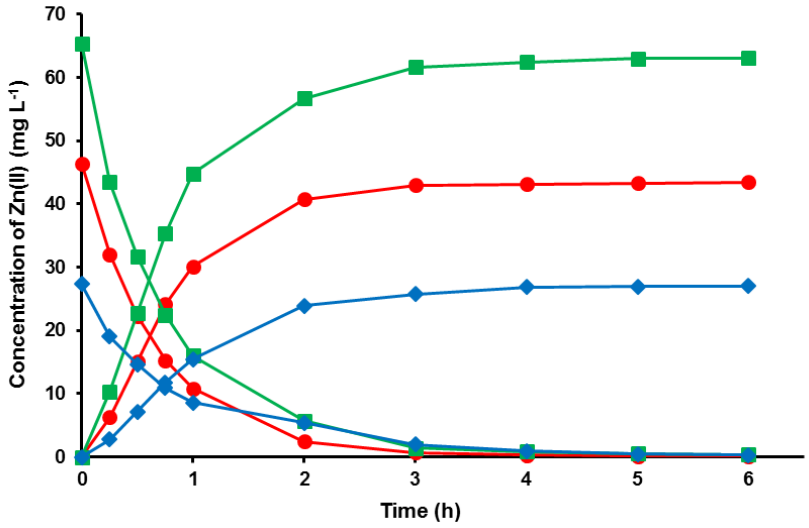

Figure 13. Transient Zn(II) concentrations in the feed solutions (100 mL) containing initially 65 (■), 46 (●) and 27 (◆) mg L^{-1} of Zn(II) at pH 3 and in the respective receiving solutions (100 mL) during transport experiments using the cross-linked CTA-based PIM with D2EHPA concentration of 40 wt%, NPOE concentration of 10 wt%, polymers ratio of 6:4, and initiator concentration of 0.6 wt%. The receiving solution contained 1.0 M HCl. Transport experiments were performed in duplicate.

4. Conclusions

On the basis of the results obtained it was concluded that depending on the nature of the base polymer and cross-linking polymer, cross-linked PIMs can exhibit superior stability, extraction rate and extractive capacity compared to their non-cross-linked counterparts.

A screening of the base-polymers PVC, CTA and PVDF-HFP for their suitability in preparing cross-linked PIMs was performed. Of these, PVC showed to be unsuitable for cross-linking with PEG-DMA due to polymer incompatibility. Successful cross-linked PIMs were prepared

with both PVDF-HFP and CTA, however, the CTA-based PIM provided superior Zn(II) extraction performance in comparison to both the cross-linked PVDF-HFP-based PIM and its CTA-based non-cross-linked counterpart. The effect of the concentrations of both the carrier D2EHPA and plasticizer NPOE in the cross-linked CTA-based PIM was studied, and the membrane composed of 40 wt% D2EHPA, 10 wt% NPOE, 0.6 wt% DMPA with a base-polymer to cross-linking polymer mass ratio of 6:4 was found to have the highest extraction rate in addition to showing very good stability over five consecutive extraction/back-extraction cycles. Limited mass loss of the PIM was observed during the first cycle which was proven by mass spectrometric analysis of the feed solution to be due to the loss of un-crosslinked PEG-DMA. The stability of the cross-linked CTA-based PIM was shown to be significantly superior compared to its non-cross-linked counterpart. It also exhibited high selectivity for Zn(II) at pH 3 in the presence of other commonly encountered in industrial and environmental waters base metal ions at concentrations 5 times higher than that of Zn(II).

AFM surface imaging of both cross-linked and non-cross-linked CTA-based PIMs showed that the cross-linked PIM surface displayed a large number of shallow voids and these voids became smaller in size as the NPOE concentration was increased, while the non-cross-linked PIMs contained a small number of deeper voids. The specific surface area of the cross-linked PIM was found to be larger than that of its non-cross-linked counterpart which could explain the faster rate of extraction with cross-linked PIMs.

The PIM with best extraction performance transported practically completely Zn(II) from a feed solution at pH 3 to a receiving solution containing 1.0 M HCl which involved simultaneous extraction of Zn(II) at the PIM/feed solution interface, its back-extraction at the PIM/receiving solution interface and facilitated transport of Zn(II) across the membrane.

References

[1] M.I.G.S. Almeida, R.W. Cattrall, S.D. Kolev, Recent trends in extraction and transport of metal ions using polymer inclusion membranes (PIMs), J. Membr. Sci., 415-416 (2012) 9-23.

[2] L. Nghiem, P. Mornane, I. Potter, J. Perera, R. Cattrall, S. Kolev, Extraction and transport of metal ions and small organic compounds using polymer inclusion membranes (PIMs), J. Membr. Sci., 281 (2006) 7-41.

[3] C. Fontàs, R. Tayeb, M. Dhahbi, E. Gaudichet, F. Thominette, P. Roy, K. Steenkeste, M.-P. Fontaine-Aupart, S. Tingry, E. Tronel-Peyroz, Polymer inclusion membranes: The concept of fixed sites membrane revised, J. Membr. Sci., 290 (2007) 62-72.

[4] M. Baczynska, M. Regel-Rosocka, M.T. Coll, A. Fortuny, A.M. Sastre, M. Wisniewski, Transport of Zn(II), Fe(II), Fe(III) across polymer inclusion membranes (PIM) and flat sheet supported liquid membranes (SLM) containing phosphonium ionic liquids as metal ion carriers, Separation Science and Technology, 51 (2016) 2639-2648.

[5] H.P. Duan, Z.Z. Wang, X.H. Yuan, S.X. Wang, H. Guo, X.J. Yang, A novel sandwich supported liquid membrane system for simultaneous separation of copper, nickel and cobalt in ammoniacal solution, Sep Purif Technol, 173 (2017) 323-329.

[6] H.P. Duan, S.X. Wang, X.J. Yang, X.H. Yuan, Q. Zhang, Z.J. Huang, H. Guo, Simultaneous separation of copper from nickel in ammoniacal solutions using supported liquid membrane containing synergistic mixture of M5640 and TRPO, Chemical Engineering Research & Design, 117 (2017) 460-471.

[7] K. Staszak, A. Wojciechowska, M.T.A. Reis, I. Wojciechowska, K. Wieszczycka, M.R.C. Ismael, J.M.R. Carvalho, Recovery of zinc(II) from chloride solutions using pseudo-emulsion based hollow fiber strip dispersion with pyridineketoxime extractants, Sep Purif Technol, 177 (2017) 152-160.

[8] K. Wieszczycka, M. Regel-Rosocka, K. Staszak, A. Wojciechowska, M.T.A. Reis, M.R.C. Ismael, M.L.F. Gameiro, J.M.R. Carvalho, Recovery of zinc(II) from chloride solutions using pseudo-emulsion based hollow fiber strip dispersion (PEHFSD) with 1-(3-pyridyl)undecan-1-one oxime or tributylphosphate, Sep Purif Technol, 154 (2015) 204-210.

[9] F.J. Alguacil, Non-dispersive extraction of gold(III) with ionic liquid Cyphos IL101, Sep Purif Technol, 179 (2017) 72-76.

[10] M. Baczynska, M. Waszak, M. Nowicki, D. Przadka, S. Borysiak, M. Regel-Rosocka, Characterization of Polymer Inclusion Membranes (PIMs) Containing Phosphonium Ionic Liquids as Zn(II) Carriers, Industrial & Engineering Chemistry Research, 57 (2018) 5070-5082.

[11] M. Ulewicz, E. Radzyminska-Lenarcik, Application of polymer and supported membranes with 1-decyl-4-methylimidazole for pertraction of transition metal ions, Sep. Sci. Technol., 49 (2014) 1713-1721.

[12] D. Kogelnig, A. Regelsberger, A. Stojanovic, F. Jirsa, R. Krachler, B.K. Keppler, A polymer inclusion membrane based on the ionic liquid trihexyl(tetradecyl)phosphonium chloride and PVC for solid–liquid extraction of Zn(II) from hydrochloric acid solution, Monatshefte für Chemie - Chemical Monthly, 142 (2011) 769-772.

[13] L.L. Zhang, R.W. Cattrall, M. Ashokkumar, S.D. Kolev, On-line extractive separation in flow injection analysis based on polymer inclusion membranes: a study on membrane stability and approaches for improving membrane permeability, Talanta, 97 (2012) 382-387.

[14] M. Ulewicz, J. Szczygelska-Tao, J.F. Biernat, Selectivity of Pb(II) transport across polymer inclusion membranes doped with imidazole azothiacrown ethers, J. Membr. Sci., 344 (2009) 32-38.

[15] G. Salazar-Alvarez, A.N. Bautista-Flores, E.R.D. Miguel, M. Muhammed, J. de Gyves, Transport characterisation of a PIM system used for the extraction of Pb(II) using D2EHPA as carrier, J. Membr. Sci., 250 (2005) 247-257.

[16] Y. Cho, C. Xu, R.W. Cattrall, S.D. Kolev, A polymer inclusion membrane for extracting thiocyanate from weakly alkaline solutions, J. Membr. Sci., 367 (2011) 85-90.

[17] H. Matsuoka, M. Aizawa, S. Suzuki, Uphill transport of uranium across a liquid membrane, J. Membr. Sci., 7 (1980) 11-19.

[18] A. Kaya, C. Onac, H.K. Alpoguz, S. Agarwal, V.K. Gupta, N. Atar, A. Yilmaz, Reduced graphene oxide based a novel polymer inclusion membrane: Transport studies of Cr(VI), J. Mol. Liq., 219 (2016) 1124-1130.

[19] Y. O'Bryan, Y.B. Truong, R.W. Cattrall, I.L. Kyratzis, S.D. Kolev, A new generation of highly stable and permeable polymer inclusion membranes (PIMs) with their carrier immobilized in a crosslinked semi-interpenetrating polymer network. Application to the transport of thiocyanate, J. Membr. Sci., 529 (2017) 55-62.

[20] K.A. Walker, L.J. Markoski, G.A. Deeter, G.E. Spilman, D.C. Martin, J.S. Moore, Cross-linking chemistry for high-performance polymer networks, Polymer, 35 (1994) 5012-5017.

[21] C. Decker, Recent developments in photoinitiated radical polymerization, Macromolecular Symposia, 143 (1999) 45-63.

[22] K.Y. Suh, R. Langer, J. Lahann, A novel photodefinable reactive polymer coating and its use for microfabrication of hydrogel elements, Adv. Mater., 16 (2004) 1401-1405.

[23] T. Fourniols, L.D. Randolph, A. Staub, K. Vanvarenberg, J.G. Leprince, V. Preat, A. des Rieux, F. Danhier, Temozolomide-loaded photopolymerizable PEG-DMA-based hydrogel for the treatment of glioblastoma, J. Control. Release, 210 (2015) 95-104.

[24] C. Decker, F. Morel, S. Jonsson, S. Clark, C. Hoyle, Light-induced polymerisation of photoinitiator-free vinyl ether maleimide systems, Macromol. Chem. Phys., 200 (1999) 1005-1013.

[25] K. Arcaute, B. Mann, R. Wicker, Stereolithography of spatially controlled multi-material bioactive poly (ethylene glycol) scaffolds, Acta biomaterialia, 6 (2010) 1047-1054.

[26] S. Bäckström, J. Benavente, R.W. Berg, K. Stibius, M.S. Larsen, H. Bohr, C. Hélix-Nielsen, Tailoring properties of biocompatible PEG-DMA hydrogels with UV light, Materials Sciences and Applications, 3 (2012) 425.

[27] T.-J. Jeon, N. Malmstadt, J.J. Schmidt, Hydrogel-encapsulated lipid membranes, Journal of the American Chemical Society, 128 (2006) 42-43.

[28] S. Petralito, R. Spera, S. Pacelli, M. Relucenti, G. Familiari, A. Vitalone, P. Paolicelli, M.A. Casadei, Design and development of PEG-DMA gel-in-liposomes as a new tool for drug delivery, Reactive and Functional Polymers, 77 (2014) 30-38.

[29] S. He, M.J. Yaszemski, A.W. Yasko, P.S. Engel, A.G. Mikos, Injectable biodegradable polymer composites based on poly (propylene fumarate) crosslinked with poly (ethylene glycol)-dimethacrylate, Biomaterials, 21 (2000) 2389-2394.

[30] Y.Y.N. Bonggotgetsakul, R.W. Cattrall, S.D. Kolev, Recovery of gold from aqua regia digested electronic scrap using a poly (vinylidene fluoride-co-hexafluoropropene) (PVDF-HFP) based polymer inclusion membrane (PIM) containing Cyphos (R) IL 104, J. Membr. Sci., 514 (2016) 274-281.

[31] S.D. Kolev, Y. Baba, R.W. Cattrall, T. Tasaki, N. Pereira, J.M. Perera, G.W. Stevens, Solid phase extraction of zinc(II) using a PVC-based polymer inclusion membrane with di(2-ethylhexyl)phosphoric acid (D2EHPA) as the carrier, Talanta, 78 (2009) 795-799.

[32] A.M. St John, R.W. Cattrall, S.D. Kolev, Determination of the initial flux of polymer inclusion membranes, Separation and Purification Technology, 116 (2013) 41-45.

5. Supplementary material

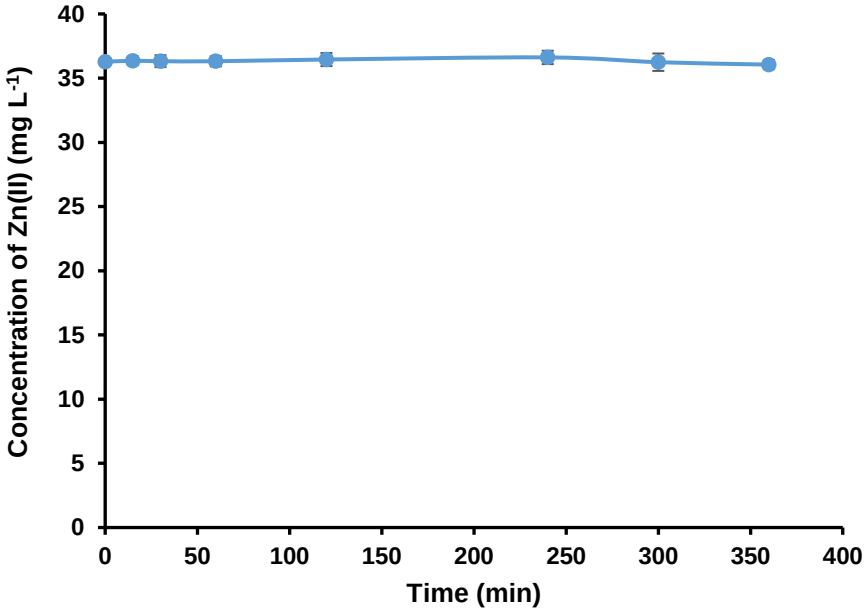

Figure S1. Concentration of Zn(II) in the feed solution during the extraction experiment involving a cross-linked membrane containing no carrier (i.e., 20 wt% NPOE, 79.4 wt% CTA and PEG-DMA at a 6:4 ratio, 0.6 wt% initiator).

Table S1. Thickness data of PIMs having different CTA:PEG-DMA ratios, 35wt% D2EHPA, 20 wt% NPOE and 0.6 wt% initiator.

CTA:PEG-DMA ratio	5:5	6:4	7:3	8:2	9:1
Thickness± SD (n=10) (µm)	50±5	55±2	55±3	52±2	55±3
Initial flux (J_0) (µmol m^{-2} s^{-1})	13.4	14.8	11.9	12.7	12.1

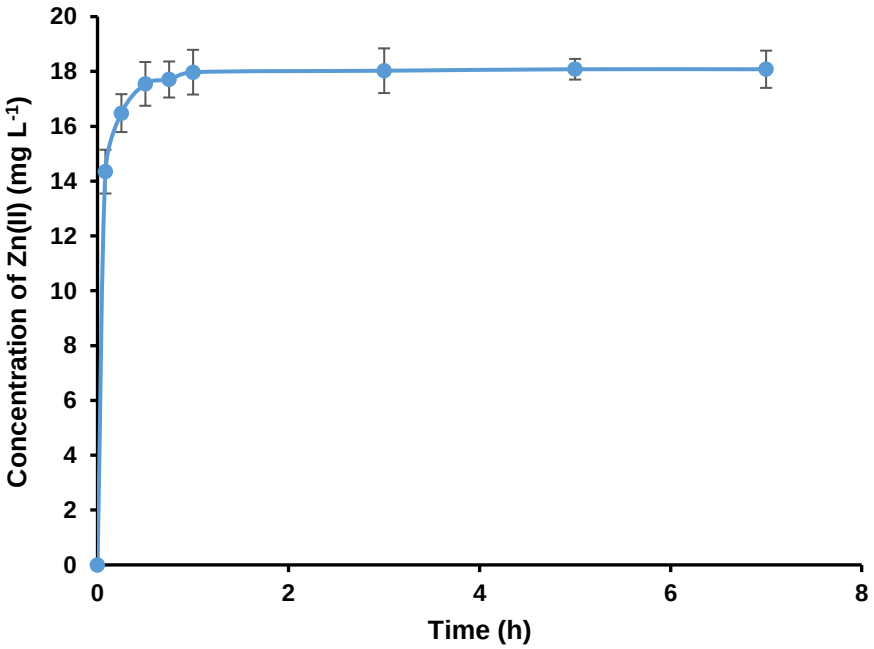

Figure S2. Concentration of Zn(II) in the receiving solution during a back-extraction experiment. PIM composition, 40 wt% D2EHPA, 10 wt% NPOE, 0.6% initiator; receiving solution, 1.0 M HCl. Error bars, ± SD (n=3).

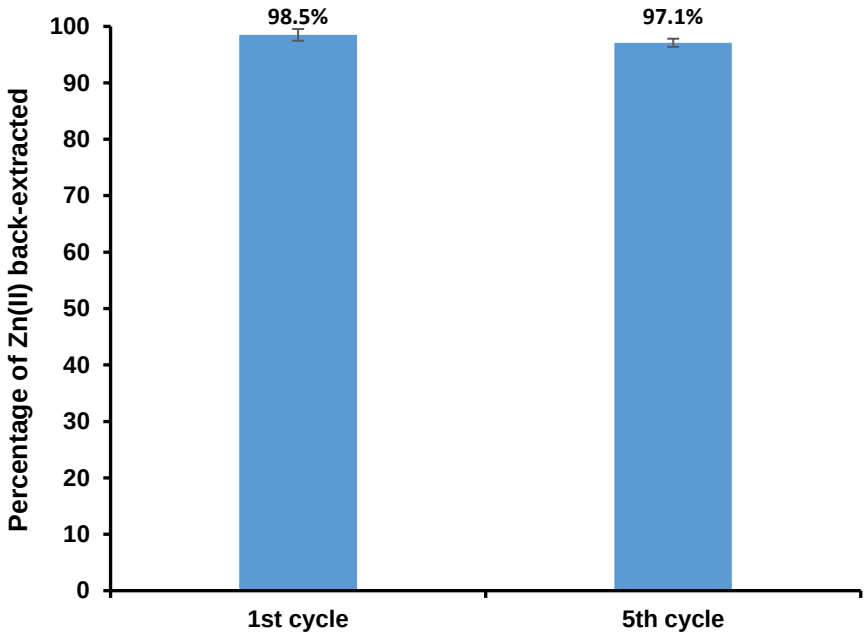

Figure S3. Percentage of Zn(II) back-extracted into the receiving solution during five consecutive extraction/back-extraction experiments. PIM composition, 6:4 polymer ratio, 40 wt% D2EHPA, 10 wt% NPOE, 0.6% initiator; receiving solution, 1.0 M HCl. Error bars, ± SD (n=3).

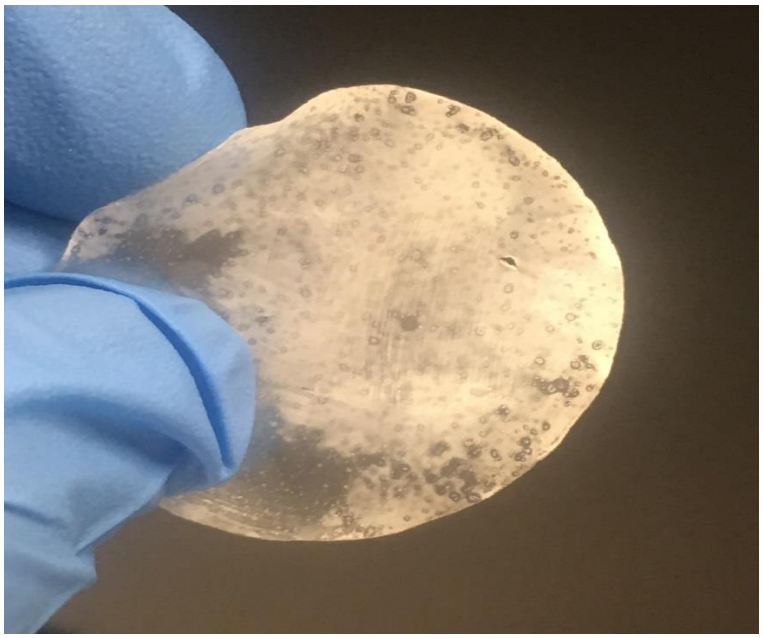

Figure S4. Photographic image of a non-cross-linked PIM (40 wt% D2EHPA, 10 wt% NPOE and 50 wt% CTA) after the second extraction/back-extraction cycle.

Chapter 3

Improving the performance of polymer inclusion membranes by cross-linking their polymeric backbone

1. Introduction

The increasing interest in polymer inclusion membranes (PIMs) has established them as environmentally friendly materials for applications in chemical analysis [1] as well as in extraction-based separation processes [2]. The analytical applications of PIMs include their use as the sensing membranes in ion-selective electrodes and optodes [2, 3]. Separation based on the use of PIMs has emerged as a less expensive, safer and environmentally friendlier alternative to conventional solvent extraction of both metallic or non-metallic species [4]. The separation of heavy metals is becoming more important nowadays due to their environmental effects associated with globalisation and industrialisation. Toxic metals are released into the environment in numerous ways. Fossil fuel combustion, sewage waste, vehicle emissions, discarded batteries, mining activities, tanneries, and metallurgy are examples of the major sources of heavy metal pollution of aquatic systems [5-8]. Several methods have been reported for the treatment of waters polluted with heavy metals, namely, ion exchange [9], co-precipitation [10], solvent extraction [11], and membrane-based separation [12].

PIMs are a type of liquid membranes generally composed of a base polymer and an extractant which sometimes they may also incorporate a plasticizer or a modifier. Poly(vinyl chloride) (PVC) [13, 14] and cellulose triacetate (CTA) [15] are the most commonly used base polymers. However, there is a recent trend in using other base polymers, such as poly(vinylidene fluoride) (PVDF) [16] and poly(vinylidene fluoride-co-hexafluoropropylene) (PVDF-HFP) [17, 18]. The base polymer acts as the skeleton of the membrane and holds the membrane liquid phase consisting of the extractant (often referred to as carrier) and a plasticizer or a modifier, if used, within its entangled chains. Aliquat 336 (a mixture of quaternary alkylammonium chlorides with the dominant species being trioctylmethylammonium chloride), di-(2-ethylhexyl)phosphoric acid (D2EHPA), bis(2,4,4-trimethylpentyl)phosphinic acid (Cyanex 272), trihexyl(tetradecyl)phosphonium bis(2,4,4-trimethylpentyl)phosphinate (Cyphos® IL 104), and tetrahydroxycalix[4]arene (Calix[4]arene) are a few examples of PIM extractants [4,

19-21]. The extractant is usually a complexing agent or an ion-exchanger which forms a complex or an ion-pair with the species of interest and the corresponding adduct is transported across the PIM which involves simultaneous extraction and back-extraction on the corresponding sides of the membrane. PIMs are characterized usually by lower rate of leaching of the membrane liquid phase into the adjacent aqueous phase compared to supported liquid membranes, which are the most frequently used liquid membranes at present. Notwithstanding this advantage, PIM extraction efficiency in terms of amount extracted and rate of extraction needs to be improved further in order to make them suitable for industrial applications [22, 23]. Different approaches for improving the membrane performance have been reported and they include modification of the membranes by the addition of reduced graphene oxide [24] or the incorporation of a cross-linking polymer in the membrane skeleton [18]. For instance, O'Bryan et al. [18] have demonstrated that a cross-linked PIM could transport thiocyanate across the membrane faster than its non-cross-linked counterpart.

The most efficient method for generating highly cross-linked polymers is based on UV irradiation of a multifunctional monomer in the presence of a suitable photo-initiator [25, 26]. The advantages of photoinduced polymerisation over thermal cross-linking, such as solvent free processing and energy efficiency, make it suitable for the coating industry, photolithography, microelectronics, and the manufacturing of paints, composite materials, dental restorative formulations, and adhesives [27-29]. Different types of monomers including acrylate, vinylether, epoxide, and maleimide have been extensively used for UV-curing in a variety of applications [25, 30-32]. Ali Kara et al. have demonstrated the possibility of using poly(ethylene glycol) dimethacrylate (PEGDMA) beads in heavy metal removal. In their work, PEGDMA was copolymerised with vinyl imidazole to allow the removal of Cd(II), Hg(II) and Pb(II) [33]. Methacrylate based cryogels [34], monoliths [35] and microspheres [36] have also been reported for heavy metal removal. PEGDMA has also been used by us as a cross-linking polymer in PIMs for enhancing the extraction/transport efficiency of thiocyanate [18] and Zn(II) [37]. In both studies the cross-linked PIMs showed superior extraction/transport performance in comparison with the corresponding non-cross-linked PIMs. Apart from improving the rate of separation, cross-linking agent with polyethylene glycol (PEG) unit could improve the biofouling resistant activity of cross-linked PIMs as PEGs are known to play a role of bactericidal agent[38, 39]. Waheed et. al. [40] and Hassanien et. al. [41] have demonstrated anti-bacterial property of the membrane prepared using PEG along with cellulose acetate polymer. Maleimide resins possess high tensile strength and modulus, excellent

chemical and corrosion resistance, as well as good stability at elevated temperatures [42]. These advantages increase the applicability of maleimide resins in electronic and aerospace engineering. Vinyl ethers are highly reactive monomers and extensive curing can be achieved in a very short time [30]. The low odour and non-irritating nature of this type of monomers makes them suitable for different UV-curing applications, such as protective coating [43]. Low shrinkage, great impact strength and high adhesion of the UV-cured polymer are also some of the advantages which make vinyl ethers popular cross-linking polymer [30, 44].

In Chapter 2 it was demonstrated that the cross-linking polymer PEGDMA and the initiator DMPA can be used to prepare successful cross-linked PIMs composed of PVDF-HFP or CTA as the base polymer and Aliquat 336 [18] or D2EHPA [37] as the extractant. Hence, in the present study we aimed to explore the applicability of frequently used cross-linking polymers and photo-initiators for the preparation of cross-linked PIMs. The suitability of the photo-initiator studied was examined by fabricating cross-linked PVC-based membrane (without extractant) which contained PEGDMA, poly (ethylene glycol) divinyl ether (PEGDVE), or N-ethyl maleimide (NEM) as the cross-linking polymer. This was followed by the optimization of the cross-linking conditions, for the fabrication not only of PVC-based membranes, but also of membranes containing CTA or PVDF-HFP as the base polymer. The extractant D2EHPA or Aliquat 336 was then included in the membrane compositions. Cross-linked PIMs, containing either D2EHPA or Aliquat 336, were prepared under the optimal conditions established earlier and their extraction performance was compared with that of their non-cross-linked counterparts by using Zn^{2+} or SCN^- as model target species, respectively.

2. Experimental

2.1. Reagents and solutions

Poly(vinylidene fluoride-co-hexafluropropylene) (PVDF-HFP, Aldrich, USA), cellulose triacetate (CTA, Acros Organics, USA) and poly(vinyl chloride) (PVC, Aldrich, USA) were used as base polymers. Poly(ethylene glycol) dimethylacrylate (PEGDMA, Aldrich, USA), poly(ethylene glycol) divinyl ether (PEGDVE, Aldrich, USA) and N-ethylmaleimide (NEM, Aldrich, USA) were incorporated into the membranes as cross-linking polymers. Three different photo-initiators, namely 2,2-dimethoxy-2-phenyl acetophenone (DMPA, Aldrich, Italy), triarylsulfonium hexafluorophosphate salts (TASHFP in 50% propylene carbonate,

Aldrich, USA, note: in membranes using TASHFP, the wt% value refers to that in the casting solution) and triphenylphosphine oxide (TPO, Aldrich, USA), were tested for their ability to induce cross-linking in the membranes studied. Analytical grade tetrahydrofuran without stabiliser (THF, VWR) and dichloromethane (DCM, Chem-Supply, Australia) were used to dissolve the PIM components. The extractants D2EHPA (97%, Aldrich, USA) and Aliquat 336 (Aldrich, USA) were used as received. 2-Nitropheny octyl ether (NPOE) (Sigma-Aldrich, Switzerland) was used as a plasticizer in the CTA-based PIMs.

2.2. Membrane preparation

Cross-linked PIMs containing PVDF-HFP, CTA or PVC as the base polymer were prepared by following the procedure described previously [37]. A weighed amount of each polymer was dissolved in either THF (for PVDF-HFP and PVC) or DCM (for CTA) in a glass jar. In the case of PVDF-HFP, the polymer and solvent mixture was stirred at 50 ^{o}C in a temperature-controlled water-bath until the polymer was completely dissolved and then the solution was cooled down to room temperature. The dissolution of PVC or CTA in THF or DCM, respectively, was performed at room temperature. The extractant D2EHPA or Aliquat 336 was added to the polymer solution which was further stirred until a homogeneous solution was obtained. This was followed by the addition of the cross-linking polymer (PEGDMA, PEGDVE, or NEM) and photo-initiator (DMPA or TASHFP). Since both cross-linking polymers and the photo-initiators are light sensitive, the glass jar containing the PIM mixture was covered with an aluminum foil and stirred for 30 min at room temperature. The resultant PIM casting solution (containing PVDF-HFP, CTA or PVC) was cast on a clean and smooth glass plate using a homemade Teflon casting knife [18]. A rectangular PIM (approximately 14 by 12 cm) was formed after slow evaporation of the solvent for approximately 24 h [23]. In the case of CTA-based PIMs, the plasticizer NPOE was also added to the casting solution (10 wt%). The same procedure was applied for the preparation of cross-linked membranes without extractant or plasticizer.

After casting, the membranes were removed from the glass plate, and their physical appearance was evaluated. Only membranes or PIMs that were visually homogeneous and flexible were considered to be successfully cast and were thus selected to be cross-linked by UV irradiation as described in Section 2.3. The UV treatment step was not applied for the preparation of non-

cross-linked PIMs, and moreover no cross-linking polymer or initiator was added to the corresponding casting solutions.

2.3. UV polymerization

The cross-linking of the successful homogeneous membranes was performed by following the procedure described previously by us [37]. The membranes were placed inside a UV-treatment box containing a UV-lamp (UVP-USA, 8 W, 0.16 A, 230 V) tuned at 365 nm. Any O_2 present inside the UV-treatment box was purged with N_2 for 15 min prior to the start of the UV polymerization process when UV lamp was turned on. PIMs were irradiated with UV-light for different time periods in N_2 atmosphere, maintained by continuously pumping N_2 through the UV-treatment box.

2.4. Extraction experiments

Circular segments of the cross-linked or non-cross-linked PIMs (3.65 cm diameter) were cut from flat sheet membranes fabricated by the casting knife. A homemade membrane holder made of a 3 mm in thickness PVC sheet [37], was used to hold each circular membrane segment inside a glass jar containing 100 mL of aqueous feed solution while the glass jar was being continuously shaken at 150 rpm on an orbital shaker (Platform Mixer OM 06, Ratek, Australia).

A 30 mg L^{-1} Zn(II) feed solution, prepared from $ZnCl_2$ (Unilab, APS Chemicals, Australia) and adjusted to pH 3 using 1 M HCl solution was used in the Zn^{2+} extraction experiments. During each extraction experiment, 0.5 mL of the feed solution was withdrawn at pre-selected times and the Zn(II) concentration was determined by atomic absorption spectrometry (AAS).

The SCN^- extraction experiments were conducted using a 30 mg L^{-1} SCN^- feed solution, which was prepared from KSCN (VWR, Australia), and the sampling throughout the experiments was performed as described above. After appropriate dilution, the SCN^- concentration in the collected samples was determined as the red coloured $[FeSCN]^{2+}$ complex by a flow injection analysis system with spectrophotometric detection, described by Cho et al. [45]. It is important to note that all membranes used in the SCN^- extraction experiments were conditioned prior to use, by immersing each membrane in 100 mL of 1.0 M $NaNO_3$ solution for 20 h while shaking

the solution at 150 rpm on an orbital shaker. This conditioning resulted in exchanging the chloride ion of Aliquat 336 for a nitrate ion [45].

The initial flux (J_0) was calculated by Eq. (1) which is the first derivative of an exponential decay function (Eq. (2)) whose empirical coefficients were determined by fitting it to the transient Zn^{2+} or SCN^- concentrations in the corresponding aqueous feed solutions during extraction [46]. A home-made Quick C program was used for conducting curve fitting using a simplex optimization algorithm [46].

$$J_0 = \left(\frac{d\Psi}{dt}\right)_{t=0} = -a_2 a_3 \quad (1)$$

$$\Psi = a_1 + a_2\, e^{-a_3 t} \quad (2)$$

where a_1, a_2 and a_3 are the empirical coefficients and Ψ is the transient Zn^{2+} or SCN^- concentration in the aqueous feed solution.

2.5. Instrumentation

The cross-linking conditions, such as the UV irradiation time and the effectiveness of the photo-initiators, were monitored using attenuated total reflectance Fourier transform infrared spectroscopy (ATR-FTIR) (Spectrum 100, PerkinElmer, USA).

An atomic absorption spectrometer (Hitachi Z-2000 Series Polarized Zeeman, Japan) was used for determining the concentration of Zn(II) in the aqueous feed solution samples under the following conditions: Zn hollow cathode lamp (Hitachi, Japan); current, 8 mA; working wavelength, 213.9 nm; burner height, 7 mm; slit width, 0.7 nm; acetylene flow rate, 1.8 L min^{-1}, air flow rate, 15.0 L min^{-1}.

Mass spectrometric measurements (6520 Accurate-Mass Q-TOF LC/MS, Agilent Technologies, USA coupled to an Agilent autosampler, 1200 Series) were performed with electrospray ionization in the positive mode under the following conditions: drying gas flow rate, 7 L min^{-1}; nebuliser pressure, 40 psi; drying gas temperature, 300 °C; capillary voltage, 4000 V; skimmer voltage, 65 V; scan range acquired, 100-2000 m/z. Each analysis involved the injection of 1 µL of sample (feed solution dissolved in acetonitrile (HPLC grade, Sigma, USA)) into the carrier solvent stream of 70% acetonitrile (HPLC grade, Sigma, USA) in 0.1% formic acid (HPLC grade, Sigma, USA) flowing at 0.3 mL min^{-1}.

3. Results and discussion

3.1. Selection of the initiator for the cross-linking polymerization

Although there are reports in the literature describing the types of initiators that can be used with a specific type of cross-linking polymer [42, 47], to the best of our knowledge, an assessment of the optimal cross-linking conditions and the appropriate initiator to be used in a mixed polymeric system containing a base polymer and a cross-linking polymer have not yet been reported.

In general, cross-linking polymerization proceeds via two basic pathways, namely, cationic polymerization or free radical polymerization. Different types of photo-initiators are required to initiate each of the photopolymerization mechanisms [47]. In the present study, three photo-initiators were selected: DMPA, a very efficient and frequently used free radical photo-initiator for methacrylate-based cross-linking [32]; TPO, known to act as a free radical photo-initiator for different types of cross-linking polymers [42]; and TASHFP, commonly used in cationic polymerisation processes [48].

Two cross-linking polymers (i.e., PEGDMA and PEGDVE) and one cross-linking monomer (i.e., NEM) were selected for testing along with the three photo-initiators discussed above. PVC was chosen as the base polymer for the initial assessment of the suitability of the photo-initiators studied because it is readily available, and it is one of the most commonly used base polymers in PIMs. PVC-based membranes were thus prepared using the three cross-linking agents (polymers/monomers) mixed separately with the three different photo-initiators to determine the effectiveness of the photo-initiators in initiating the cross-linking processes in the mixed polymeric membrane systems studied. All these membranes were composed of a 6:4 base polymer to cross-linking polymer weight ratio and contained 2 wt% photo-initiator. The polymers ratio was selected on the basis of our previous study [37]. After casting the membranes, they were irradiated with UV-light for 15 min and then analysed by ATR-FTIR to assess the effectiveness of the photo-initiator. The results are described in the following sections for each cross-linking polymer.

3.1.1. PEGDVE cross-linking

PEGDVE is a bifunctional vinyl ether oligomer which is very reactive and generally undergoes fast cationic polymerisation in the presence of a photogenerated protonic acid [49]. The degree of polymerisation of PEGDVE in the membranes using the three initiators was assessed by monitoring the change in the transmittance percentage (%T) (Figure 1) of the inverted peak at 1621 cm^{-1} which corresponds to the C=C stretching frequency of the vinyl ether double bond present in PEGDVE [50]. Cross-linking of PEGDVE proceeds via the formation of a new C-C bond and subsequent conversion of alkene to alkane in PEGDVE (i.e., C=C to C-C) (Figure 2). Thus, the %T at 1621 cm^{-1} increases as the cross-linking process progresses. Figure 1 shows that only TASHFP was effective in photo-initiating the cross-linking of PEGDVE. A small increase in %T was observed for the DMPA initiated membrane, indicating a lower degree of cross-linking. Based on these results, TASHFP was selected as the most efficient photo-initiator for preparing PEGDVE-based cross-linking membranes.

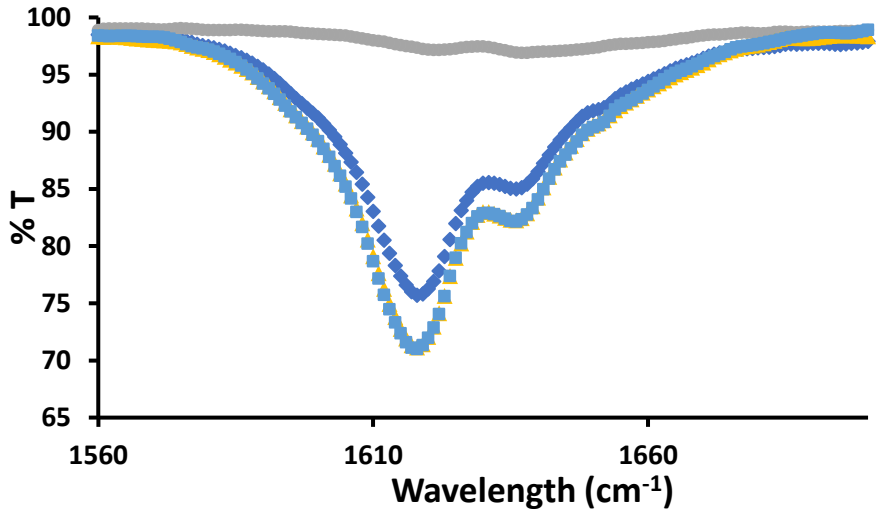

Figure 1. ATR-FTIR spectra of the PEGDVE membranes containing PVC as the base polymer (6:4 PVC:PEGDVE mass ratio) and 2 wt% of one of the following photo-initiators: (◆) DMPA, (●) TASHFP, (■) TPO. Membrane (▲) did not contain a photo-initiator and was not UV irradiated. UV-irradiation time was 15 min.

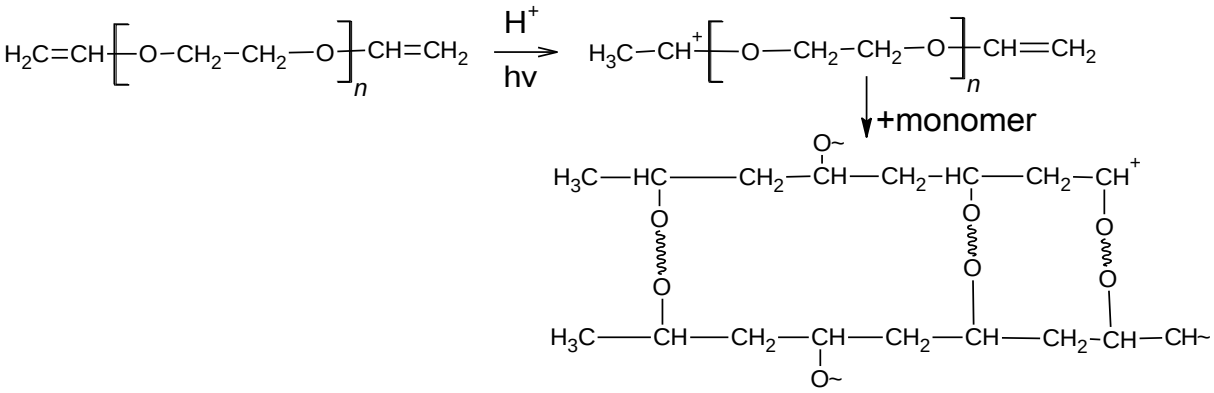

Figure 2. Cross-linking of PEGDVE.

3.1.2. PEGDMA cross-linking

PEGDMA has been used in the preparation of cross-linked PIMs previously, and it is known to undergo radical polymerisation upon UV-irradiation [19]. As reported in Chapter 2, the membrane performance improved significantly after cross-linking using DMPA as the photo-initiator [37]. However, to the best of our knowledge, other initiators have not been tested in either PEGDMA-based polymeric membranes or PIMs. Hence, the three different initiators studied were applied for cross-linking a PVC membrane with PEGDMA. The effectiveness of these initiators was assessed by monitoring the change in %T of the ATR-FTIR peak at 1637 cm^{-1} (Figure 3). This peak corresponds to the stretching frequency of C=C bonds in the PEGDMA acrylate groups (Figure 4), and the consequent shift of the C=O stretching frequency in this group to a higher wavenumber (i.e., from 1716 cm^{-1} to 1728 cm^{-1}) as a result of the loss of conjugation of the C=O moiety with the adjacent C=C moiety after cross-linking [51].

The results shown in Figure 3 indicate that only the DMPA and TASHFP were successful in initiating cross-linking via the radical-mediated pathway. As the degree of cross-linking increased, the C=C bonds of the acrylate groups were converted to C-C bonds and subsequently formed new links to acrylate groups of adjacent PEGDMA units via C-C bonding (Figure 4). Although TASHFP has a preference to act as a cationic initiator, it has been reported that it can induce radical cross-linking as well [52, 53]. In this case TASHFP decomposes in the presence of UV-irradiation thus forming intermediate aryl radicals which may induce radical-assisted polymerisation. Hence, both initiators (i.e., DMPA and TASHFP) were selected for further optimisation studies.

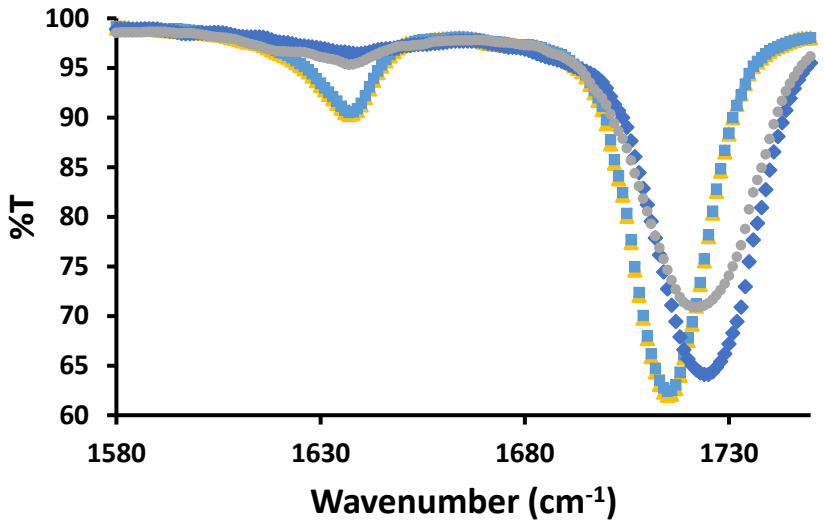

Figure 3. ATR-FTIR spectra of the PEGDMA membranes containing PVC as the base polymer (6:4 PVC:PEGDMA mass ratio) and 2 wt% of one of the following photo-initiators: (◆) DMPA, (●) TASHFP, (■) TPO. Membrane (▲) did not contain a photo-initiator and was not UV irradiated. UV-irradiation time was 15 min.

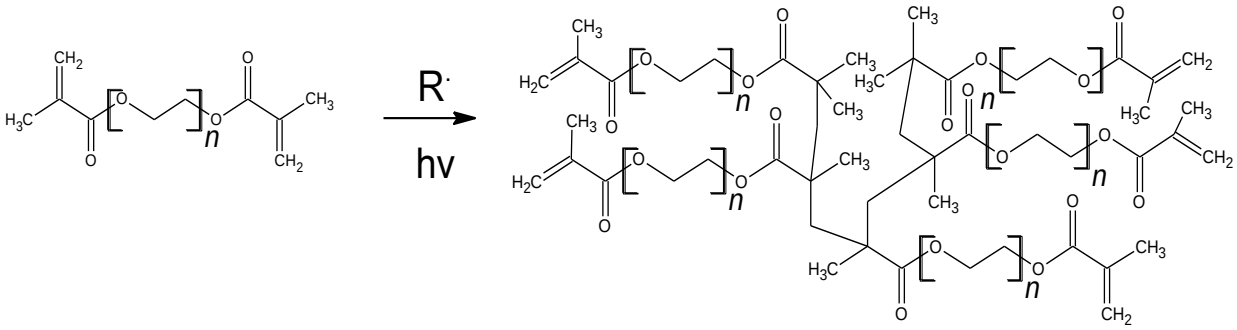

Figure 4. Cross-linking of PEGDMA (R· refers to a radical).

3.1.3. NEM cross-linking

Maleimide derivatives and their polymers are well known for their thermal stability as well as their electron withdrawing properties due to the presence of a five membered rigid ring [54]. Maleimide molecules are commonly used for radical assisted cross-linking although it has also been reported that N-substituted maleimide monomers can undergo homo-polymerisation even when they are exposed to UV-radiation in the absence of an initiator, provided that the monomer contains easily abstractable hydrogen atoms [25]. The extent of cross-linking of

NEM using the three photo-initiators studied was assessed on the basis of the IR peak at 698 cm^{-1} as proposed by Decker et. al. [25], and the results are shown in Figure 5. The characteristic peak at 698 cm^{-1} is due to the =C-H bending vibration of the maleimide monomer [55]. It can be observed that only DMPA was effective in cross-linking NEM and was thus chosen for further optimisation studies. This result also supports the radical cross-linking mechanism for the NEM molecule (Figure 6). The reason why TASHFP was not able to initiate cross-linking could be related to the faster decomposition of the intermediate radical to some other product which suppressed the radical capture by NEM units. The TPO initiator also did not provide effective cross-linking which could have been most likely due to the lower photon intensity of the UV-light or to some other experimental conditions that may need to be modified (e.g., addition of a modifier such as diallylbisphenol A) [42].

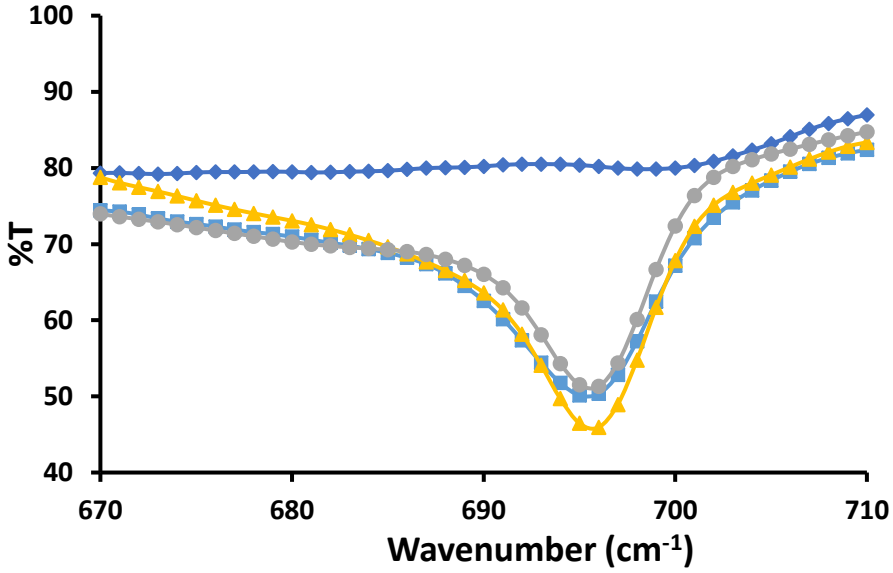

Figure 5. ATR-FTIR spectra of the NEM membranes, containing PVC as the base polymer (6:4 PVC:NEM weight ratio) and 2 wt% of one of the following photo-initiators: (◆) DMPA, (●) TASHFP, (■) TPO. Membrane (▲) did not contain a photo-initiator and was not UV irradiated. UV-irradiation time was 15 min.

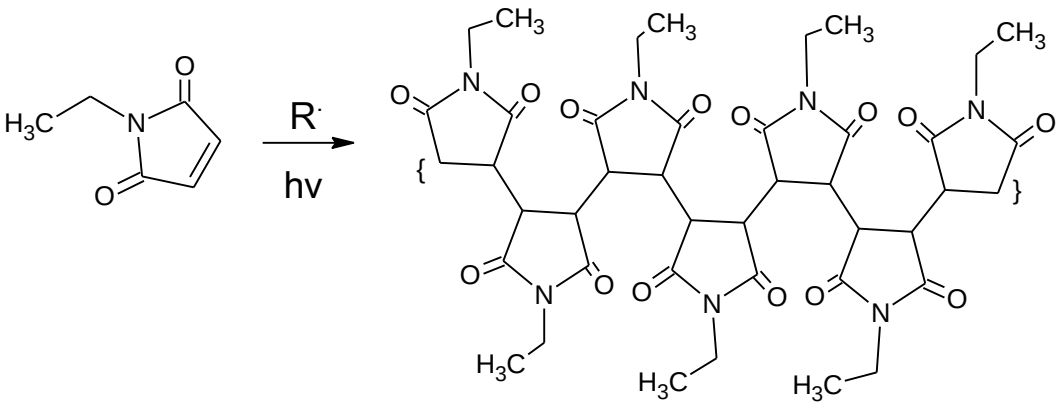

Figure 6. Cross-linking of NEM (R· refers to a radical).

3.2. Optimization of the cross-linking conditions for PVC, CTA and PVDF-HFP-based membranes

The polymerisation reactions used in this study consist of three main steps: initiation, propagation and termination. The initiation reaction depends on the intensity of light as well as the absorption properties of the photo-initiator (i.e., molar absorptivity). The photo-initiator plays a key role in the light-induced polymerisation as it controls both the reaction rate and the depth of cure profile within the sample [28]. The rate of initiation is directly proportional to the quantum yield (Φ) of formation of the initiating species (i.e., radical or cation). The propagation of the reaction in mixed polymeric systems, with or without an extractant, depends on the spatiotemporal distribution of both the light intensity and the photo-initiator [32] as well as on the nature of the base polymers involved. The three most commonly used base polymers in PIMs (i.e., PVC, CTA and PVDF-HFP) and the three cross-linking polymers selected in this study (i.e., PEGDVE, PEGDMA and NEM) were used to prepare different membranes without an extractant, and each membrane was optimised in terms of the concentration of the photo-initiator and the UV-irradiation time. In optimising the concentrations of the photo-initiators, selected earlier for further studies (i.e., DMPA and TASHEP), and the UV-irradiation time by varying these parameters consideration was given to minimising the amounts of the photo-initiators used as well as the time of irradiation without compromising the membranes' physical appearance.

DMPA-initiated membranes were prepared using 1, 2 and 4 wt% of the photo-initiator, whereas 2, 4 and 8 wt% photo-initiator was used for TASHFP-initiated membranes because preliminary experiments indicated that the minimal concentration of TASHFP for achieving cross-linking was 2 wt%. The resulting membranes were irradiated by UV-light for 1, 5 and 15 min. If the 15-min irradiation produced a better result than shorter irradiation times, the membranes were irradiated for a further 15 and 30 min to verify if the cross-linking had been completed. All the UV-irradiated (cross-linked) and non-UV-irradiated membranes free of photo-initiator were analysed by ATR-FTIR by comparing the intensities of the characteristic IR peaks at 1637 cm^{-1} (PEGDMA), 1617 cm^{-1} (PEGDVE) and 697 cm^{-1} (NEM) similarly as performed in the previous section (Table S1, Table S2, Table S3, Figure S1 and Figure S2).

3.2.1 PVC-based membranes

The optimal cross-linking conditions found for PVC-based cross-linked membranes are presented in Figure 7. For the PVC-PEGDMA-DMPA membrane, 1% DMPA and 5-min UV-irradiation provided optimal cross-linking conditions. In case of the PVC-PEGDMA-TASHFP membrane, 15-min UV-irradiation produced higher degree of cross-linking than 1 and 5 min, and so the membrane was irradiated for a further 15 and 30 min. This demonstrated that 30-min irradiation was the minimum time required for maximum cross-linking of the membrane using TASHFP as photo-initiator. A possible reason for the need of a longer irradiation time and higher photo-initiator concentration in the case of TASHFP mediated cross-linking could be the partial decomposition of the TASHFP radical. However, this was not the case when TASHFP was used to initiate the cross-linking of PEGDVE which followed the cationic cross-linking pathway.

In the case of the PVC-PEGDVE-TASHFP membrane, it was noticed that the membrane turned yellow when irradiated for 5 and 15 min irrespective of the photo-initiator concentration. This colouration was probably caused by the by-product (Eq. S1) formed in the photodecomposition of the photo-initiator [51, 56, 57]. Similar type of coloured hydrogel formation has been also reported by Tucker et.al.[56]. Only the 1-min irradiated membrane did not change its appearance. Comparing the ATR-FTIR spectra of all the 1-min irradiated membranes, the 8 wt% TASHFP membrane was found to exhibit the highest degree of cross-linking. The same result for the PVC-NEM-DMPA membrane was achieved at 2 wt% DMPA and 15-min UV-irradiation. Irradiation for a further 15 and 30 min did not improve the degree of cross-linking.

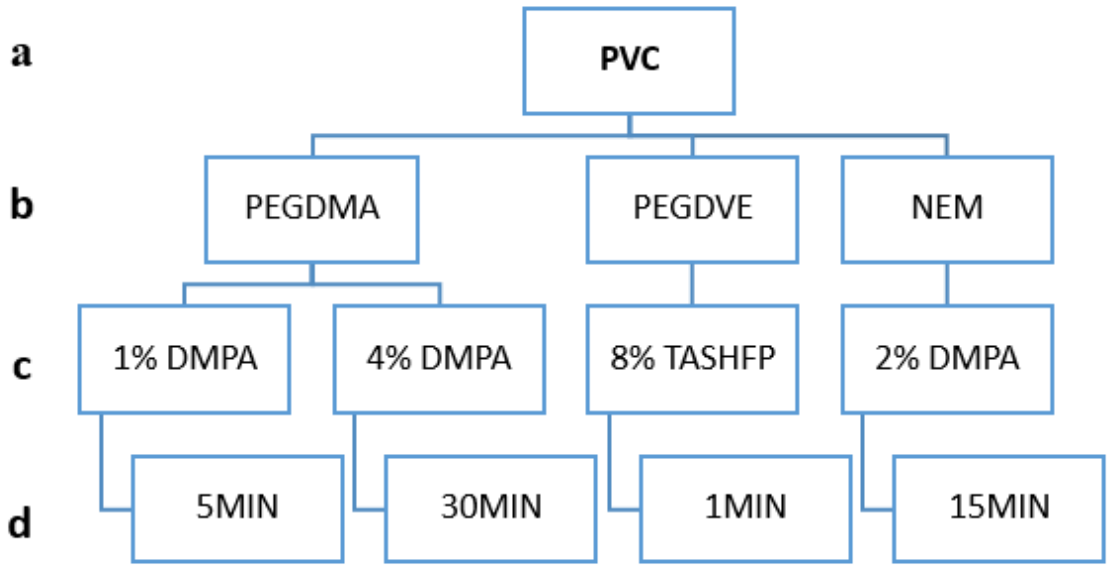

Figure 7. Flowchart representing the optimum cross-linking conditions for PVC-based membranes. (a) base polymer; (b) cross-linking agent (i.e., PEGDMA and PEGDVE polymers and NEM monomer); (c) optimum concentration of photo-initiator; (d) optimum UV-treatment time. Mass ratio of base polymer to cross-linking agent, 6:4.

3.2.2. PVDF-HFP-based membranes

The optimum cross-linking conditions for the PVDF-HFP-based membranes are presented in Figure 8. DMPA initiated cross-linking of PEGDMA was comparatively faster with PVDF-HFP as the base polymer than with PVC. This suggested that the transport of the initiating radical across the PVDF-HFP-based membrane was faster than in its PVC-based counterpart. However, cross-linking of the PVDF-HFP-PEGDMA membrane with 2 wt% TASHFP required approximately the same time to reach completion as in the case of the PVC-PEGDMA membrane (i.e., 30 min).

The same yellow colouration, obtained for the PVC-based membrane, was also observed when the PVDF-HFP-PEGDVE-TASHFP membrane was irradiated for 5 and 15 min. To achieve optimum cross-linking without any colouration, 1 min irradiation and 8 wt% TASHFP were required. The optimal conditions for complete cross-linking of NEM were 5-min irradiation

and 4 wt% DMPA. This was faster than in the case of the PVC-based membrane though a higher concentration of the photo-initiator was required (Figures 7 and 8).

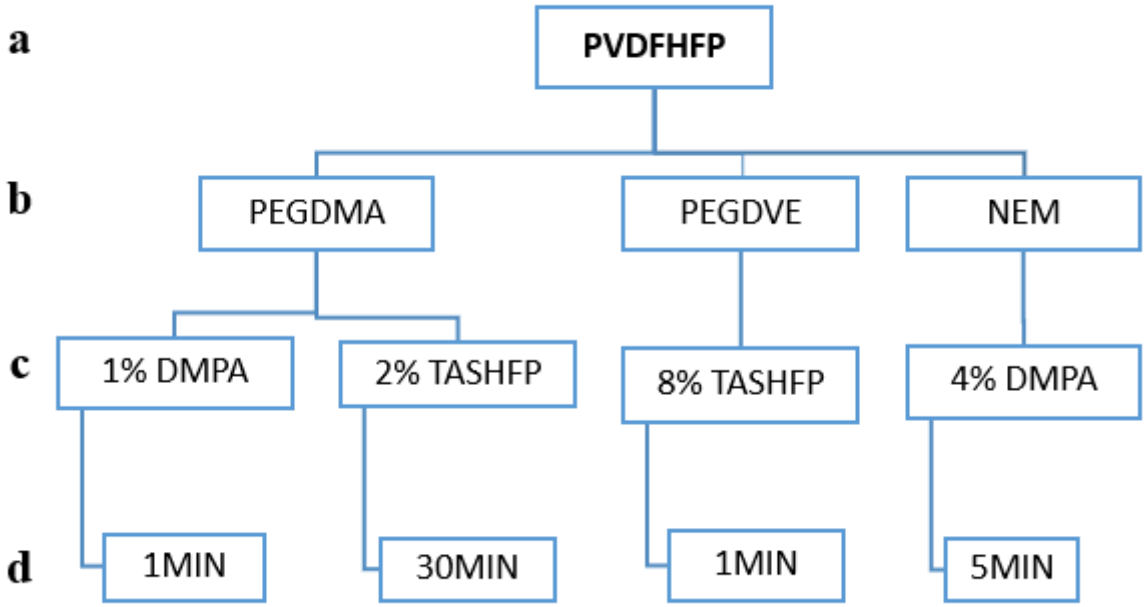

Figure 8. Flowchart representing the optimum cross-linking conditions for PVDF-HFP-based membranes. (a) base polymer; (b) cross-linking agent (i.e., PEGDMA and PEGDVE polymers and NEM monomer); (c) optimum concentration of photo-initiator; (d) optimum UV-treatment time. Mass ratio of base polymer to cross-linking agent, 6:4.

3.2.3. CTA-base membranes

The optimum cross-linking conditions for the CTA-based membranes are presented in Figure 9. Due to the higher viscosity of the casting solution of CTA in dichloromethane the cross-linking rate in the corresponding membranes was relatively slow and therefore in most cases a higher concentration of photo-initiator and a longer UV-irradiation time was required to complete the cross-linking process within 30 min. In the case of DMPA, a 30-min irradiation time and 4 wt% DMPA were required to complete the cross-linking of PEGDMA while in the case of TASHFP an even higher concentration of the photo-initiator (i.e., 8 wt%) was required to achieve the same result if the UV irradiation time was to be kept at 30 min.

For PEGDVE, optimum cross-linking was obtained by using 8 wt% TASHFP and an irradiation time of 15 min. Also, no colouration was observed for the PEGDVE cross-linked

membranes. The cross-linked membranes, when NEM was used as the cross-linking monomer, were not successful as NEM crystallised and exuded from the membranes during their overnight drying.

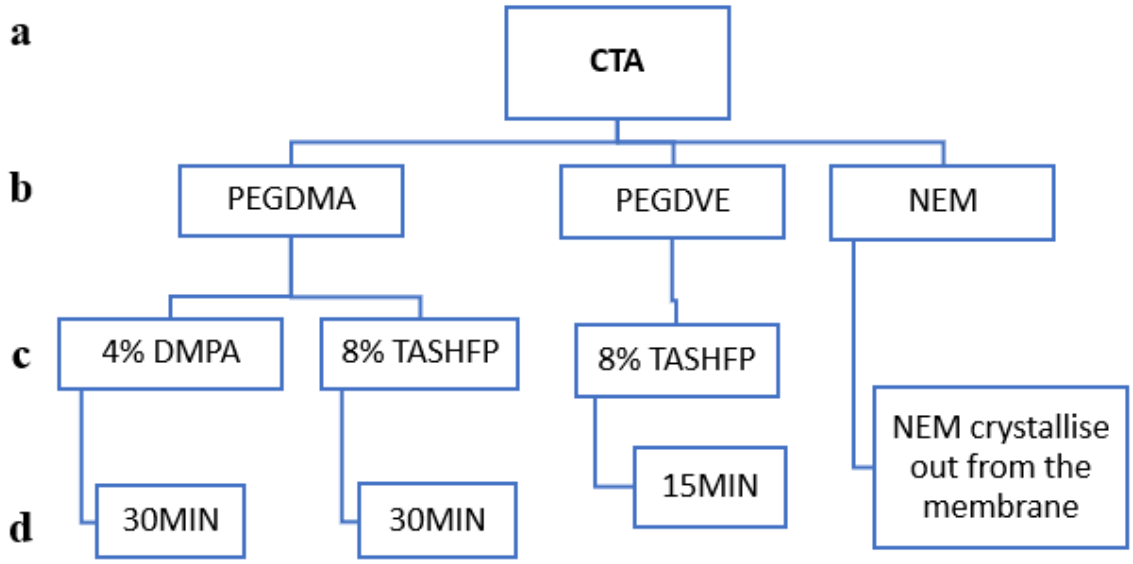

Figure 9. Flowchart representing the optimum cross-linking conditions for CTA-based membranes. (a) base polymer; (b) cross-linking agent (i.e., PEGDMA and PEGDVE polymers and NEM monomer); (c) optimum concentration of photo-initiator; (d) optimum UV-treatment time. Mass ratio of base polymer to cross-linking agent, 6:4.

3.3. Physical appearance of the membranes after incorporation of different extractants

In the study described earlier, the optimisation was carried out without including any extractant in the membrane composition. Such extractants would have complicated the IR spectra of the cross-linking agents which were used to monitor the cross-linking process [18]. Therefore, extractants were introduced into the membrane casting solutions to fabricate PIMs only after the optimisation conditions for cross-linking had been established. Hence, PIMs were prepared by using the optimal cross-linking conditions regarding the concentration of the photo-initiator and the UV-irradiation time while keeping the base polymer to cross-linking polymer ratio at 6:4 and incorporating 30 wt% of D2EHPA or Aliquat 336. In the case of PIMs containing CTA

as the base polymer, 10 wt% NPOE was added as a plasticizer because otherwise these PIMs were too very rigid. The homogeneity of the membranes was visually assessed (Table 1).

Table 1. Physical appearance of PVC, PVDF-HFP, and CTA-based cross-linked PIMs containing 30 wt% D2EHPA or Aliquat 336 as the extractant. CTA-based PIMs also contained 10 wt% NPOE as a plasticizer.

Extractant	**Cross-linking agents and photo-initiators**				**Base polymer**
	PEGDMA		**PEGDVE**	**NEM**	
	DMPA	**TASHFP**	**TASHFP**	**DMPA**	
D2EHPA	Oily membrane surface	Oily membrane surface	Oily membrane surface	Oily membrane surface	PVC
Aliquat 336	Homogeneous membrane	White precipitate formation in the casting solution	White precipitate formation	Homogeneous membrane	
D2EHPA	Homogeneous membrane	Homogeneous membrane	Homogeneous membrane but very soft before cross-linking	Homogeneous membrane	PVDF-HFP
Aliquat 336	Homogeneous membrane	White solution formation	White precipitate formation in the casting solution	Homogeneous membrane	
D2EHPA	Homogeneous membrane	Homogeneous membrane	Oily membrane surface	Not prepared as NEM crystallised on the membrane's surface	CTA
Aliquat 336	Homogeneous membrane	Homogeneous membrane	Homogeneous membrane		

It can be observed that in total 13 successful homogeneous cross-linked PIMs were obtained. All D2EHPA-PVC-based PIMs tested and the D2EHPA-CTA-based PIM with PEGDVE and TASHFP were inhomogeneous with oily surfaces and were deemed unsuitable for extraction studies. In addition, during the membrane preparation involving Aliquat 336, a white precipitate was formed when TASHFP was added to the THF casting solution containing the base polymer, Aliquat 336 and the cross-linking agent. It was found that the white precipitate was also formed when only Aliquat 336 and TASHFP were dissolved in THF. Interestingly, this was not observed when CTA was used as the base polymer. Since the use of CTA involves the use of DCM as solvent rather than THF, it was assumed that the compound forming the precipitate was soluble in DCM but not in THF. This was confirmed by collecting a filtered sample of the white precipitate which dissolved in DCM.

The possible reaction between TASHFP and Aliquat 336 is described by Eq. (3) where TAS^+ and $R_3CH_3N^+$ are the triarylsulfonium and Aliquat 336 cations, respectively, and HFP^- is the hexafluorophosphate anion. This reaction product was confirmed using mass spectrometric analysis in the positive ion mode of a solution of the white precipitate in acetonitrile (Figure 10).

$$TAS^+HFP^- + R_3CH_3N^+Cl^- \rightarrow TAS^+Cl^- + R_3CH_3N^+HFP^- \quad (3)$$

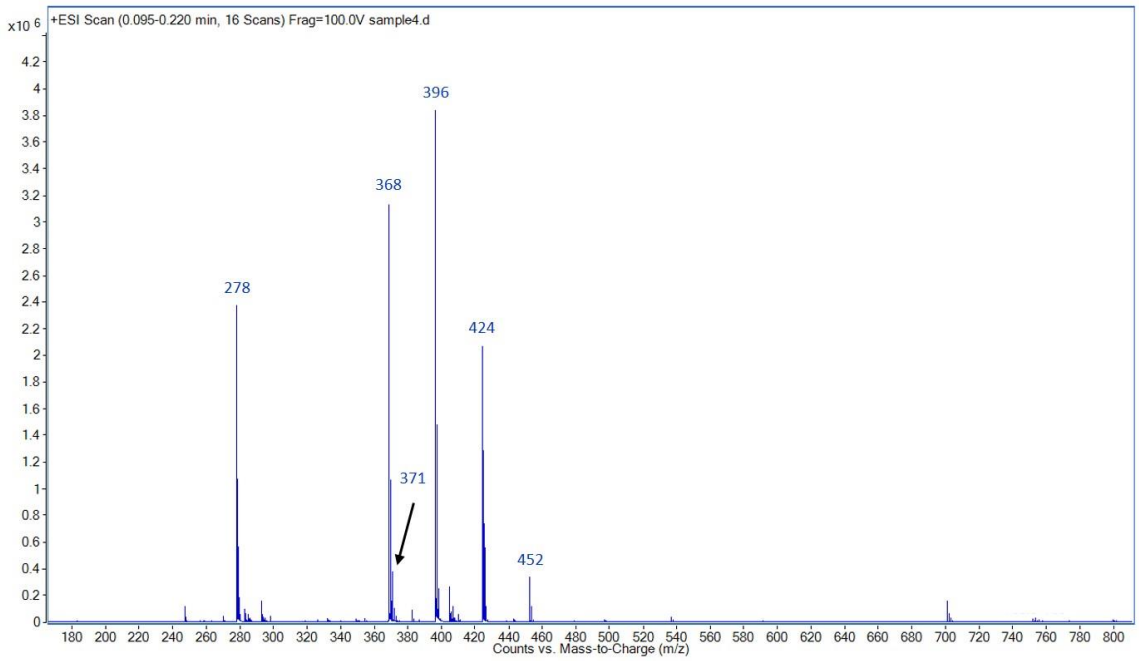

Figure 10. Mass spectrum in the positive mode of an acetonitrile solution of the white precipitate formed in the reaction between Aliquat 336 and TASHFP.

The peaks at m/z values of 368, 396, 424, and 452 are characteristic of the four major quaternary ammonium cations of Aliquat 336 [58] while those at m/z values of 278 ($C_{36}H_{28}S_3^{2+}$) and 371 ($C_{24}H_{19}S_2^{+}$) correspond to the two arylsulfonium cations that exist in TASHFP as received from the supplier. It should be noted that Zhuravlev et al. have also reported the formation of white precipitates of quaternary ammonium hexafluorophosphates [59].

3.4. Extraction experiments

The extraction performance of all homogeneous cross-linked PIMs obtained as part of this study (Table 1) was compared with that of their non-cross-linked counterparts. In the case of the D2EHPA-based PIMs the extracted species was Zn^{2+} since such PIMs have been used successfully in the extraction of this metallic cation [13, 60, 61]. Aliquat 336-based PIMs are capable of extracting the SCN^- ion efficiently [17, 18] and therefore this anion was used in comparing the extraction performance of the Aliquat 336-based cross-linked and non-cross-linked PIMs studied. In each case, extraction was carried out for 6 h using 3.65 cm PIM discs containing 30 wt% of extractant and 10 wt% NPOE in the case of CTA-based PIMs. The

amount extracted was then calculated as 'mg' of extracted species per 'g' of PIM. The corresponding extraction curves are shown in Figure 11. The extraction results are summarized in Table 2.

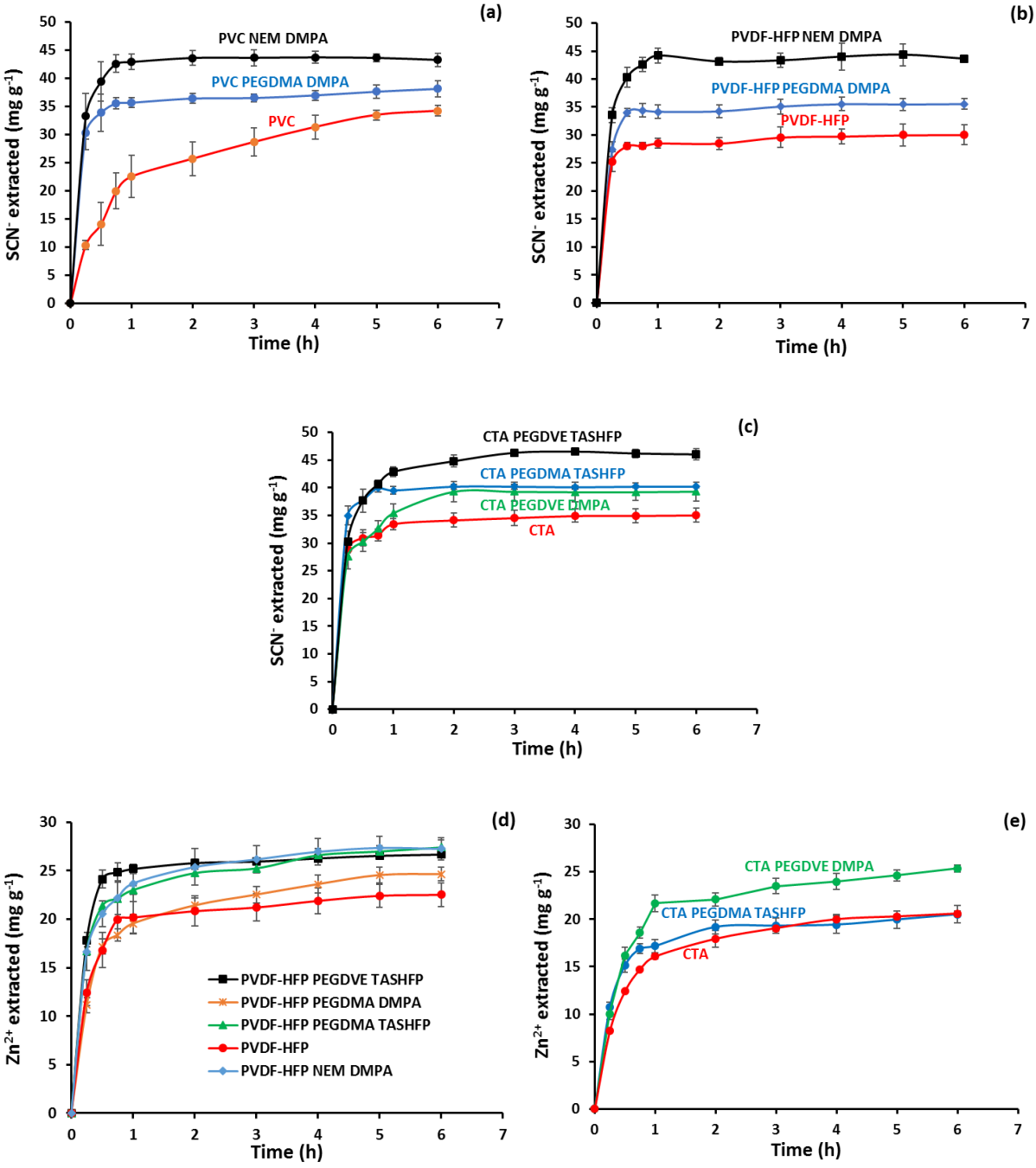

Figure 11. Transient concentrations of SCN^- (a, b, c) and Zn^{2+} (d, e) during extraction experiments involving PIMs 1-3 (a); 4-6 (b); 7-10 (c), 11-15 (d); and 16-18 (e). PIM compositions and experimental conditions as in Table 2. Error bars = ±standard deviation (n=3).

Table 2. Concentration of Zn^{2+} and SCN^- (± standard deviation, n=3) in circular sections (3.65 cm in diameter) of the homogeneous cross-linked PIMs, developed as part of this study (Table 1) after a 6-h extraction period from 100 mL feed solutions containing initially 30 mg L^{-1} Zn^{2+} or SCN^- (×, not present).

PIM ID	Base polymer	Cross-linking polymer	Initiator	Extractant (30 wt%)	Analyte	Plasticizer (10 wt%)	Amount of extracted Zn^{2+}/SCN^- (mg g^{-1})	$J_0 \times 10^6$ (mol m^{-2} s^{-1})
1	PVC	PEGDMA	DMPA	Aliquat 336	SCN^-	×	38.1±1.4	39.1±3.4
2		NEM	DMPA				43.3±2.1	49.5±2.9
3		×	×				34.1±0.9	4.63±1.53
4	PVDF-HFP	PEGDMA	DMPA	Aliquat 336	-	×	35.5±1.0	44.9±2.7
5		NEM	DMPA		SCN^-		43.6±0.5	52.2±0.9
6		×	×				30.0±1.7	31.1±3.8
7	CTA	PEGDMA	DMPA	Aliquat 336	SCN^-	NPOE	39.3±1.7	18.8±2.5
8		PEGDMA	TASHFP				40.2±0.2	47.3±4.3
9		PEGDVE	TASHFP				46.1±1.0	35.8±0.4
10		×	×				35.0±1.2	19.9±2.3
11	PVDF-HFP	PEGDMA	DMPA	D2EHPA	Zn^{2+}	×	24.7±0.7	12.3±0.9
12		NEM	DMPA				27.3±1.1	15.1±3.0
13		PEGDMA	TASHFP				27.4±0.8	17.0±0.7
14		PEGDVE	TASHFP				26.7±0.2	24.1±1.3
15		×	×				22.5±1.2	7.8±0.8
16	CTA	PEGDMA	DMPA	D2EHPA	Zn^{2+}	NPOE	25.3±0.4	12.5±0.6
17		PEGDMA	TASHFP				20.5±0.9	13.7±0.4
18		×	×				20.6±0.3	6.54±0.12

All cross-linked PIMs exhibited higher initial fluxes (especially the PVC-based PIMs) than the corresponding non-cross-linked PIMs with the exception of PIM 7 whose initial flux was similar to that of the relevant non-cross-linked membrane (i.e., PIM 10).

All Aliquat 336- based cross-linked membranes extracted a larger amount of SCN^- over a 6 h period than the corresponding non-cross-linked membranes (12 to 45% more). The PIM, composed of Aliquat 336, NPOE, CTA, PEGDVE and TASHFP (PIM 9) was the best performing Aliquat 336-based membrane in terms of extraction performance. In the case of the D2EHPA-based membranes, up to 23% more Zn^{2+} was extracted over 6 h into the cross-linked PIMs compared to the non-crossed-linked ones. Only PIM 17 (i.e., composed of D2EHPA, NPOE, CTA, PEGDMA, and TASHFP) showed no improvement in comparison to the amount of Zn^{2+} extracted by the corresponding non-cross-linked membrane. However, its initial flux was twice as high as that of the non-cross-linked membrane.

4. Conclusions

PVC, CTA and PVDF-HFP-based cross-linked membranes were fabricated using the cross-linking agents PEGDMA, PEGDVE or NEM and the photo-initiators TASHFP, TPO or DMPA to select the optimal cross-linking conditions for the base polymers studied. The effectiveness of the photo-initiators listed above was assessed with the PVC-based membranes containing PEGDMA, PEGDVE or NEM as cross-linking agent. The results have shown that both DMPA and TASHFP are effective for initiating cross-linking of PEGDMA while TASHFP is effective for PEGDVE and DMPA for NEM. The concentration of initiator and time of UV irradiation were then studied not only for the PVC-based membranes, but also for the PVDF-HFP- and CTA-based membranes. Different optimal cross-linking conditions were established for each of the three most common base polymers used, thus indicating that the optimal cross-linking conditions are base polymer dependent.

The optimal cross-linked conditions resulting in homogeneous membranes were used for the fabrication of PIMs incorporating either D2EHPA or Aliquat 336 as the extractant. These results clearly demonstrated that cross-linking the polymer backbone of PIMs containing either D2EHPA or Aliquat 336 enhanced their extraction performance in terms of the amount of Zn^{2+} or SCN^- extracted and the rate of extraction in comparison with their non-cross-linked counterparts.

References

[1] M.I.G.S. Almeida, R.W. Cattrall, S.D. Kolev, Polymer inclusion membranes (PIMs) in chemical analysis - A review, Anal. Chim Acta, 987 (2017) 1-14.

[2] M.I.G.S. Almeida, R.W. Cattrall, S.D. Kolev, Recent trends in extraction and transport of metal ions using polymer inclusion membranes (PIMs), J. Membr. Sci., 415-416 (2012) 9-23.

[3] J.A. López-López, C. Mendiguchía, J.J. Pinto, C. Moreno, Liquid membranes for quantification and speciation of trace metals in natural waters, TrAC Trends in Analytical Chemistry, 29 (2010) 645-653.

[4] L. Nghiem, P. Mornane, I. Potter, J.M. Perera, R.W. Cattrall, S.D. Kolev, Extraction and transport of metal ions and small organic compounds using polymer inclusion membranes (PIMs), J. Membr. Sci., 281 (2006) 7-41.

[5] L. Friberg, G.F. Nordberg, V.B. Vouk, Handbook on the toxicology of metals, Elsevier/North-Holland Biomedical Press, Amsterdam; New York 1979.

[6] P. Galiatsatou, M. Metaxas, V. Kasselouri-Rigopoulou, Adsorption of zinc by activated carbons prepared from solvent extracted olive pulp, J. Hazard. Mater., 91 (2002) 187-203.

[7] S.E. Bailey, T.J. Olin, R.M. Bricka, D.D. Adrian, A review of potentially low-cost sorbents for heavy metals, Water Res., 33 (1999) 2469-2479.

[8] B. Hu, X. Jia, J. Hu, D. Xu, F. Xia, Y. Li, Assessment of heavy metal pollution and health risks in the soil-plant-human system in the Yangtze River Delta, China, Int. J. Environ. Res. Public Health, 14 (2017).

[9] A. Dabrowski, Z. Hubicki, P. Podkoscielny, E. Robens, Selective removal of the heavy metal ions from waters and industrial wastewaters by ion-exchange method, Chemosphere, 56 (2004) 91-106.

[10] S. Verbych, M. Bryk, G. Chornokur, B. Fuhr, Removal of copper(II) from aqueous solutions by chitosan adsorption, Sep. Sci. Technol., 40 (2005) 1749-1759.

[11] N.E. Belkhouche, M. Amine Didi, D. Villemin, Separation of nickel and copper by solvent extraction using di-2 ethylhexylphosphoric acid-based synergistic mixture, Solvent Extr. Ion Exch., 23 (2005) 677-693.

[12] N.S.W. Zulkefeli, S.K. Weng, N.S. Abdul Halim, Removal of heavy metals by polymer inclusion membranes, Curr. Pollut. Rep., 4 (2018) 84-92.

[13] S.D. Kolev, Y. Baba, R.W. Cattrall, T. Tasaki, N. Pereira, J.M. Perera, G.W. Stevens, Solid phase extraction of zinc(II) using a PVC-based polymer inclusion membrane with di(2-ethylhexyl)phosphoric acid (D2EHPA) as the carrier, Talanta, 78 (2009) 795-799.

[14] C.F. Croft, M.I.G.S. Almeida, R.W. Cattrall, S.D. Kolev, Separation of lanthanum(III), gadolinium(III) and ytterbium(III) from sulfuric acid solutions by using a polymer inclusion membrane, J. Membr. Sci., 545 (2018) 259-265.

[15] O. Kebiche-Senhadji, L. Mansouri, S. Tingry, P. Seta, M. Benamor, Facilitated Cd(II) transport across CTA polymer inclusion membrane using anion (Aliquat 336) and cation (D2EHPA) metal carriers, J. Membr. Sci., 310 (2008) 438-445.

[16] L. Guo, Y. Liu, C. Zhang, J. Chen, Preparation of PVDF-based polymer inclusion membrane using ionic liquid plasticizer and Cyphos IL 104 carrier for Cr (VI) transport, J. Membr. Sci., 372 (2011) 314-321.

[17] Y. O'Bryan, R.W. Cattrall, Y.B. Truong, I.L. Kyratzis, S.D. Kolev, The use of poly(vinylidenefluoride-co-hexafluoropropylene) for the preparation of polymer inclusion membranes. Application to the extraction of thiocyanate, J. Membr. Sci., 510 (2016) 481-488.

[18] Y. O'Bryan, Y.B. Truong, R.W. Cattrall, I.L. Kyratzis, S.D. Kolev, A new generation of highly stable and permeable polymer inclusion membranes (PIMs) with their carrier immobilized in a crosslinked semi-interpenetrating polymer network. Application to the transport of thiocyanate, J. Membr. Sci., 529 (2017) 55-62.

[19] L.J.L. Zhang, R.W. Cattrall, M. Ashokkumar, S.D. Kolev, On-line extractive separation in flow injection analysis based on polymer inclusion membranes: A study on membrane stability and approaches for improving membrane permeability, Talanta, 97 (2012) 382-387.

[20] B.N. Mahanty, P.K. Mohapatra, D.R. Raut, D.K. Das, P.G. Behere, M. Afzal, W. Verboom, Polymer inclusion membrane containing a diglycolamide-functionalized calix[4]arene for actinide ion uptake and transport, J. Membr. Sci., 516 (2016) 194-201.

[21] C. Fontàs, R. Tayeb, M. Dhahbi, E. Gaudichet, F. Thominette, P. Roy, K. Steenkeste, M.-P. Fontaine-Aupart, S. Tingry, E. Tronel-Peyroz, Polymer inclusion membranes: The concept of fixed sites membrane revised, J. Membr. Sci., 290 (2007) 62-72.

[22] M. Ulewicz, E. Radzyminska-Lenarcik, Application of polymer and supported membranes with 1-decyl-4-methylimidazole for pertraction of transition metal ions, Sep. Sci. Technol., 49 (2014) 1713-1721.

[23] N. Kavitha, K. Palanivelu, Recovery of copper(II) through polymer inclusion membrane with di (2-ethylhexyl) phosphoric acid as carrier from e-waste, J. Membr. Sci., 415-416 (2012) 663-669.

[24] A. Kaya, C. Onac, H.K. Alpoguz, S. Agarwal, V.K. Gupta, N. Atar, A. Yilmaz, Reduced graphene oxide based a novel polymer inclusion membrane: Transport studies of Cr(VI), J. Mol. Liq., 219 (2016) 1124-1130.

[25] C. Decker, C. Bianchi, S. Jönsson, Light-induced crosslinking polymerization of a novel N-substituted bis-maleimide monomer, Polymer, 45 (2004) 5803-5811.

[26] K.A. Walker, L.J. Markoski, G.A. Deeter, G.E. Spilman, D.C. Martin, J.S. Moore, Crosslinking chemistry for high-performance polymer networks, Polymer, 35 (1994) 5012-5017.

[27] E. Andrzejewska, Photopolymerization kinetics of multifunctional monomers, Prog. Polym. Sci., 26 (2001) 605-665.

[28] C. Decker, Recent developments in photoinitiated radical polymerization, Macromol. Symp., 143 (1999) 45-63.

[29] R.S. Davidson, Exploring the science, technology and applications of U.V. and E.B. curing, SITA Tecnology Limited, 1999.

[30] C. Decker, C. Bianchi, D. Decker, F. Morel, Photoinitiated polymerization of vinyl ether-based systems, Prog. Org. Coat., 42 (2001) 253-266.

[31] C. Decker, T. Nguyen Thi Viet, H. Pham Thi, Photoinitiated cationic polymerization of epoxides, Polym. Int., 50 (2001) 986-997.

[32] V. Mucci, C. Vallo, Efficiency of 2, 2-dimethoxy-2-phenylacetophenone for the photopolymerization of methacrylate monomers in thick sections, J. Appl. Polym. Sci., 123 (2012) 418-425.

[33] A. Kara, L. Uzun, N. Besirli, A. Denizli, Poly(ethylene glycol dimethacrylate-n-vinyl imidazole) beads for heavy metal removal, J. Hazard. Mater., 106 (2004) 93-99.

[34] K. Tekin, L. Uzun, Ç.A. Şahin, S. Bektaş, A. Denizli, Preparation and characterization of composite cryogels containing imidazole group and use in heavy metal removal, React. Funct. Polym., 71 (2011) 985-993.

[35] L. Uzun, D. Türkmen, E. Yılmaz, S. Bektaş, A. Denizli, Cysteine functionalized poly(hydroxyethyl methacrylate) monolith for heavy metal removal, Colloids and Surfaces A: Physicochemical and Engineering Aspects, 330 (2008) 161-167.

[36] E. Uguzdogan, E.B. Denkbas, E. Ozturk, S.A. Tuncel, O.S. Kabasakal, Preparation and characterization of polyethyleneglycolmethacrylate (PEGMA)-co-vinylimidazole (VI) microspheres to use in heavy metal removal, J. Hazard. Mater., 162 (2009) 1073-1080.

[37] B. Hoque, M.I.G.S. Almeida, R.W. Cattrall, T.G. Gopakumar, S.D. Kolev, Effect of cross-linking on the performance of polymer inclusion membranes (PIMs) for the extraction, transport and separation of Zn(II), J. Membr. Sci., 589 (2019) 11.

[38] T.M. Nalawade, K. Bhat, S.H. Sogi, Bactericidal activity of propylene glycol, glycerine, polyethylene glycol 400, and polyethylene glycol 1000 against selected microorganisms, J. Int. Soc. Prev. Community. Dent., 5 (2015) 114.

[39] O.H. Robertson, E.M. Appel, T.T. Puck, H.M. Lemon, M.H. Ritter, A study of the bactericidal activity in vitro of certain glycols and closely related compounds, Int. J. Infect. Dis., (1948) 124-137.

[40] S. Waheed, A. Ahmad, S.M. Khan, T. Jamil, A. Islam, T. Hussain, Synthesis, characterization, permeation and antibacterial properties of cellulose acetate/polyethylene glycol membranes modified with chitosan, Desalination, 351 (2014) 59-69.

[41] A.M. Hassanien, M.A. El-Hashash, M.A. Mekewi, D.B. Guirguis, A.M. Ramadan, Fabrication of Polyvinyl Alcohol/Cellulose Acetate (PVA/CA/PEG) Antibacterial Membrane for Potential Water Purification Application, Hydrol. Current. Res., 4 (2013).

[42] M. Abadie, Y. Xiong, F. Boey, UV photo curing of N, N′-bismaleimido-4, 4′-diphenylmethane, Eur. Polym. J., 39 (2003) 1243-1247.

[43] C. Decker, F. Morel, S. Jönsson, S. Clark, C. Hoyle, Light-induced polymerisation of photoinitiator-free vinyl ether/maleimide systems, Macromol. Chem. Phys., 200 (1999) 1005-1013.

[44] J.P. Fouassier, J. Lalevée, Photochemical production of interpenetrating polymer networks; simultaneous initiation of radical and cationic polymerization reactions, Polymers-Basel, 6 (2014) 2588-2610.

[45] Y. Cho, C. Xu, R.W. Cattrall, S.D. Kolev, A polymer inclusion membrane for extracting thiocyanate from weakly alkaline solutions, J. Membr. Sci., 367 (2011) 85-90.

[46] A.M. St John, R.W. Cattrall, S.D. Kolev, Determination of the initial flux of polymer inclusion membranes, Sep Purif Technol, 116 (2013) 41-45.

[47] C. Decker, Photoinitiated crosslinking polymerisation, Prog. Polym. Sci., 21 (1996) 593-650.

[48] A. Mackintosh, A. Kuehne, R. Pethrick, B. Guilhabert, E. Gu, C. Lee, M. Dawson, G. Heliotis, D. Bradley, Novel polymer systems for deep UV microlens arrays, J. Phys. D-Appl. Phys., 41 (2008) 094007.

[49] J. Crivello, D. Conlon, Aromatic bisvinyl ethers: A new class of highly reactive thermosetting monomers, Journal of Polymer Science Part A: Polymer Chemistry, 21 (1983) 1785-1799.

[50] T. Nishikubo, T. Iizawa, A. Yoshinaga, M. Nitta, Study of photopolymers, 15. Polymerization of ethylene glycol divinyl ether and photocrosslinking reaction of its polymer, Die Makromolekulare Chemie, 183 (1982) 789-799.

[51] S. Bäckström, J. Benavente, R.W. Berg, K. Stibius, M.S. Larsen, H. Bohr, C. Hélix-Nielsen, Tailoring properties of biocompatible PEG-DMA hydrogels with UV light, Materials Sciences and Applications, 3 (2012) 425.

[52] E. Yoshida, Selective controlled/living photoradical polymerization of glycidyl methacrylate, using a nitroxide mediator in the presence of a photosensitive triarylsulfonium salt, Polymers-Basel, 4 (2012) 1580-1589.

[53] E. Yoshida, Elucidation of acceleration mechanisms by a photosensitive onium salt for nitroxide-mediated photocontrolled/living radical polymerization, Open J. Poly. Chem., 4 (2014) 47.

[54] K. Onimura, M. Matsushima, K. Yamabuki, T. Oishi, Synthesis and properties of N-substituted maleimides conjugated with 1, 4-phenylene or 2, 5-thienylene polymers, Polym. J., 42 (2010) 290.

[55] R.-H. Lin, W.-H. Lu, C.-W. Lin, Cure reactions in the blend of cyanate ester with maleimide, Polymer, 45 (2004) 4423-4435.

[56] R.M. Tucker, B.W. Parcher, E.F. Jones, T.A. Desai, Single-Injection HPLC Method for Rapid Analysis of a Combination Drug Delivery System, AAPS PharmSciTech, 13 (2012) 605-610.

[57] J.V. Crivello, J.H.W. Lam, Triarylsulfonium salts as photoinitiators of free radical and cationic polymerization, J. Polym. Sci. Pt. C-Polym. Letters, 17 (1979) 759-764.

[58] G. Argiropoulos, R.W. Cattrall, I.C. Hamilton, R. Paimin, Determination of the quaternary ammonium ion components of Aliquat 336 by electrospray mass spectrometry, Anal. Chim Acta, 360 (1998) 167-169.

[59] O. Zhuravlev, V. Nikol'skii, L. Voronchikhina, Thermal stability of quaternary ammonium hexafluorophosphates and halides, Russ. J. Appl. Chem., 86 (2013) 824-830.

[60] M.I.G.S. Almeida, C. Chan, V.J. Pettigrove, R.W. Cattrall, S.D. Kolev, Development of a passive sampler for Zinc(II) in urban pond waters using a polymer inclusion membrane, Environmental Pollution, 193 (2014) 233-239.

[61] F. Nitti, M.I.G.S. Almeida, R. Morrison, R.W. Cattrall, V.J. Pettigrove, R.A. Coleman, S.D. Kolev, Development of a portable 3D-printed flow-through passive sampling device free of flow pattern effects, Microchemical Journal, 143 (2018) 359-366.

5. Supplementary material:

Table S1. Optimisation of cross-linking conditions for PVC based membrane.

wt% of Initiator	% Transmittance (%T)					Cross-lniking agent and initiator
	1min UV	5min UV	15min UV	30min UV	NO UV	
1% DMPA	93.14	**94.15**	94.20	×	89.17	PEG-DMA and DMPA
2% DMPA	×	×	94.02	×		
4% DMPA	×	×	94.20	×		
2% TASHFP	×	×	92.78	×	91.21	PEG-DMA and TASHFP
4% TASHFP	91.21	91.78	94.31	**95.59**		
8% TASHFP			94.35	×		
2% TASHFP	93.24	Membrane turned to yellow colour		×	73.22	PEG-DVE and TASHFP
4% TASHFP	96.50			×		
8% TASHFP	**97.83**			×		
1% DMPA	×	×	58.84	×	45.93	NEM and DMPA
2% DMPA	56.46	58.45	**74.79**	74.21		
4% DMPA	×	×	74.79	×		

× Not analysed, **Highlighted** value stand for optimised condition.

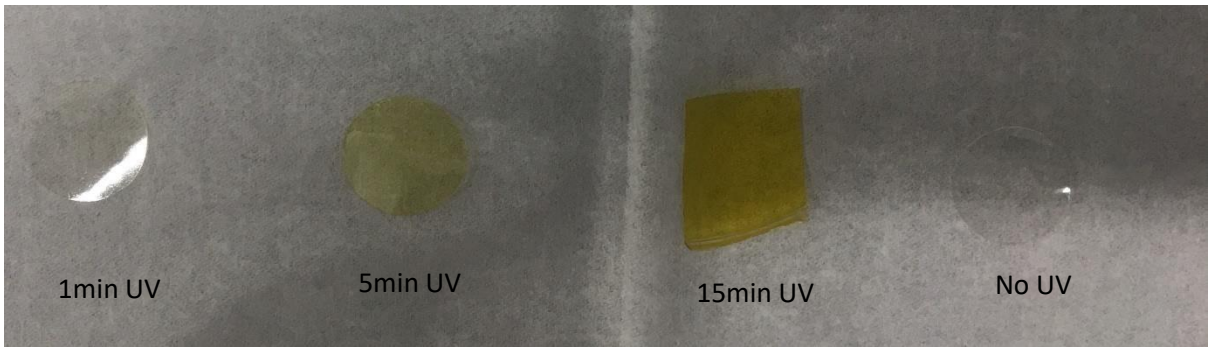

Figure S1. Coloration of PVC based membrane upon longer UV-irradiation.

Table S2. Optimisation of cross-linking conditions for PVDF-HFP based membrane.

wt% of Initiator	% Transmittance (%T)					Cross-lniking agent and initiator
	1min UV	5min UV	15min UV	30min UV	NO UV	
1% DMPA	**97.97**	97.97	98.03	×	92.37	PEG-DMA and DMPA
2% DMPA	×	×	97.70	×		
4% DMPA	×	×	97.76	×		
2% TASHFP	91.37	93.43	96.37	**97.67**	91.01	PEG-DMA and TASHFP
4% TASHFP	×	×	96.51	×		
8% TASHFP	×	×	96.22	×		
2% TASHFP	93.49	Membrane turned to yellow colour		×	76.63	PEG-DVE and TASHFP
4% TASHFP	96.85			×		
8% TASHFP	**98.11**			×		
1% DMPA	×	×	68.37	×	39.01	NEM and DMPA
2% DMPA	×	×	74.97	×		
4% DMPA	65.36	**79.86**	79.87	×		

× Not analysed, **Highlighted** value stand for optimised condition.

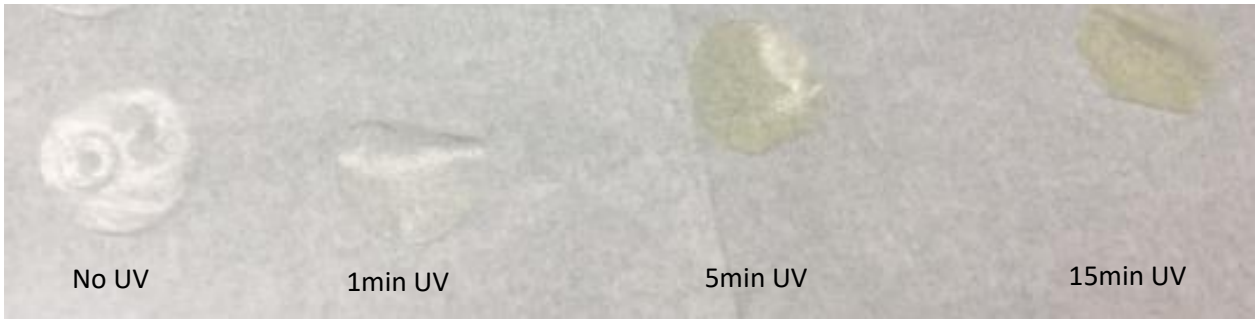

Figure S2. Coloration of PVDF-HFP based membrane upon longer UV-irradiation.

Table S3. Optimisation of cross-linking conditions for CTA based membrane.

wt% of Initiator	% Transmittance (%T)					Cross-lniking agent and initiator
	1min UV	5min UV	15min UV	30min UV	NO UV	
1% DMPA	×	×	94.25	93.99	89.05	PEG-DMA and DMPA
2% DMPA	×	×	94.35	94.81		
4% DMPA	×	×	94.59	**96.77**		
2% TASHFP	×	×	89.92	×	87.85	PEG-DMA and TASHFP
4% TASHFP	×	×	90.43	×		
8% TASHFP	87.85	89.58	91.22	**94.20**		
2% TASHFP	×	×	95.92	×	72.94	PEG-DVE and TASHFP
4% TASHFP	×	×	96.20	×		
8% TASHFP	87.85	92.86	**96.48**	96.46		

× Not analysed, **Highlighted** value stand for optimised condition.

Photo-chemical decomposition of TASHFP initiator

$$Ar_3S^+X^- \longrightarrow \left[Ar_3S^+X^-\right]^*$$

$$\left[Ar_3S^+X^-\right]^* \longrightarrow Ar_2S + Ar^\bullet + S$$

$$Ar_2S^+ + YH \longrightarrow Ar_2S^+ - H + Y$$

$$Ar_2S^+ - H \longrightarrow Ar_2S + H^+$$

$$2\,Ar^\bullet \longrightarrow Ar - Ar$$

$$Ar^\bullet + YH \longrightarrow ArH + Y^\bullet \qquad \text{(Eq S1)}$$

Chapter 4

Enhancing polymer inclusion membrane efficiency in gold recovery from electronic waste by membrane cross-linking

1. Introduction

The rapid growth in the electronics industry has created a new type of waste material which has been termed Waste Electrical and Electronic Equipment (WEEE). WEEE can contain environmentally undesirable components such as polychlorinated biphenyls, lead, mercury, tin, cadmium, and hexavalent chromium [1]. Electronic waste is of major concern due to several significant issues including the increasing rate and volume of materials disposed of in landfills, the toxicity of some of the materials present in this type of waste and the variability in regulatory requirements regarding disposal methods. However, WEEE does not only contain the above mentioned pollutants, but it also incorporates precious metals such as gold, silver and palladium [2, 3]. For example, it has been reported that mobile phones and computer circuit boards can contain gold in higher amounts than those in natural ores (i.e., 397 g ton^{-1}) [4-6]. Thus, the proper treatment of WEEE, can not only protect the environment, but it can also be a source of precious metals.

Different methods such as cementation, ion-exchange, solvent extraction, biosorption, and physical adsorption have been reported for recovering precious metals from electronic waste [7]. Park and Fray have reported a step by step process of recovering gold, silver and palladium by removing copper, aluminium, tin, lead, zinc, nickel, iron, and non-metallic components [8]. For the recovery of gold, solvent extraction was used. Gurung et al. proposed a tannin-based adsorbent, named bisthiourea - persimmon tannin or “BTU-PT gel”, for the selective recovery of precious metals from the acidic leach liquor from spent mobile phone circuit boards [9]. Agarwal et al. have described a Donnan dialysis technique using an anion exchange pore filled membrane to recover gold from electronic waste [10]. Rocchetti et al. have summarised the technologies available for the recycling of printed circuit boards [3], by reviewing the respective international patents published between 1990 and 2017. Many techniques have been proposed to recover precious metals from WEEE, although there is a need for greener and sustainable processes.

Polymer inclusion membranes (PIMs) are a relatively new type of liquid membranes which have been used in the development of a promising separation technology which follows the same working principles as solvent extraction, while having their organic liquid phase (i.e., extractant, often referred to as carrier and plasticizer/modifier) retained within the entangled chains of a base polymer. Moreover, PIM-based separation does not require the use of large volumes of toxic solvents like in solvent extraction, thus making it a greener and safer alternative [11, 12]. Although this type of liquid membranes was initially used as the sensing element in ion-selective electrodes in the mid twentieth century [13], recently it has been mainly applied for the extraction, transport and separation of metallic and non-metallic species [11, 14]. PIMs have also been reported to be able to extract and transport Au(III). For instance, Rodríguez de San Miguel et al. have reported a PIM containing Kelex 100 (7-(4-ethyl-1-methyloctyl)-8-hydroxyquinoline) suitable for Au(III) separation [15]. Under the optimal conditions (i.e., Au(III) in 1 M HCl as feed solution and 0.1 M NaCl as receiving solution), the membrane showed adequate stability with almost no loss in transport efficiency until the 15th cycle. In a separate study, ω-Thiocaprolactam was used by Núñez et al. [16] as an extractant for the selective recovery of gold from a chloride feed solution containing copper and mercury. However, only about 70% recovery was achieved using a PIM made of cellulose triacetate (CTA), 2-nitrophenyl octyl ether (NPOE) and ω-thiocaprolactam-based and a potassium iodide–hydrochloric acid aqueous receiving solution. Long alkyl chain alcohols, such as 1-octanol, 1-decanol, and 1-dodecanol, were also used in transporting Au(III) through a CTA-based PIM [17]. The effect of chain length on the transport efficiency was investigated and described by a contour surface ternary diagram. Dodecanol-based PIMs showed better stability due to the lower water solubility of 1-dodecanol in comparison with 1-octanol and 1-decanol. The above mentioned research only involved the use of synthetic solutions, although real applications on the Au(III) recovery from WEEE digests have also been reported [6]. Kubota et al. developed a N-[N,N-di(2-ethylhexyl)aminocarbonylmethyl] glycine-based PIM for the recovery of gold from discarded mobile phones [6], and recent research in our laboratory has used a Cyphos® IL 104-based PIM to selectively separate Au(III) from electronic scrap digested in aqua regia [18, 19]. However, it was established that the transport rate across the PIM decreased when the feed solution consisted of electronic waste digest [19].

To improve the extraction and transport performance of PIMs, Kolev group have recently reported on the development of a new generation of PIMs in which the carrier is immobilized in a cross-linked semi-interpenetrating polymer network [20, 21]. These cross-linked PIMs

have shown to have superior performance for the extraction and transport of thiocyanate and Zn(II) using Aliquat 336 and di-(2-ethylhexyl)phosphoric acid (D2EHPA) as the extractant, respectively. It was thus of interest to examine if cross-linked PIMs would have superior performance than their non-cross-linked counterparts for the recovery of Au(III) from digests of electronic waste.

Thus, the present chapter describes the development of a cross-linked Cyphos® IL 104-based PIM for the recovery of Au(III) from electronic waste digests in aqua regia. Different types of cross-linking agents (i.e., polymers or monomers) were examined, namely acrylate, vinyl ether and maleimide, as well as different base polymers. The surface morphology of the successful cross-linked PIMs was assessed, and the stability of those that showed better performance than the non-cross-linked PIMs was studied.

2. Experimental

2.1. Reagents and solutions

For the preparation of PIMs, Cyphos® IL104 (STREM chemical Inc., USA) was used as the carrier, poly(vinylidene fluoride-co-hexafluropropylene) (PVDF-HFP, Aldrich, USA), CTA (Acros Organics, USA) or poly(vinyl chloride) (PVC, Aldrich, USA) was used as the base polymer and 2-nitrophenyl octyl ether (NPOE) was used as the plasticizer (in CTA-based PIMs only). For the cross-linking, poly(ethylene glycol) dimethylacrylate (PEGDMA, Aldrich, USA), poly(ethylene glycol) divinyl ether (PEGDVE, Aldrich, USA) or N-ethylmaleimide (NEM, Aldrich, USA) was used as the crosslinking agent, and 2, 2-dimethoxy-2-phenyl acetophenone (DMPA, Aldrich, Italy) and triarylsulfonium hexafluorophosphate salt (TASHFP, Aldrich, USA) were tested for their suitability as photo-initiators to induce cross-linking in the membranes. Tetrahydrofuran (THF, analytical grade, without stabilizer, VWR, Australia) or dichloromethane (DCM, Chem-Supply, Australia) was used as received to dissolve the PIM components.

Feed solutions were prepared using gold(III) chloride trihydrate (≥99.9%, Sigma Aldrich) and hydrochloric acid (32%, Ajax, Australia), and the receiving solutions contained sodium sulfite anhydrous (Chem-Supply, Australia). Hydrochloric acid and nitric acid (70%, Ajax, Australia) were used in the preparation of aqua regia. Deionised water was used for the preparation of all solutions (resistivity ≥18 MΩ cm, Millipore, Synergy185).

2.2. Membrane preparation

Cross-linked PIMs were prepared following the procedure described previously by us [21]. Firstly, weighed amounts of PVDF-HFP, PVC or CTA were dissolved using an appropriate organic solvent (THF for PVDF-HFP and PVC, and DCM for CTA; 10 mL of solvent per 1 g of base polymer). In the case of PVDF-HFP, the mixture was heated with stirring at 50 ^{o}C using a temperature-controlled water-bath until the complete dissolution of the base polymer. In the case of PVC and CTA, the dissolution occurred at room temperature. Cyphos® IL 104 and NPOE (the latter in the case of CTA-based PIMs only) were then added to the solution at room temperature and stirred until a homogeneous solution was obtained. The cross-linking agent and the photo-initiator were then added, and the jar was covered with aluminium foil as both the cross-linking agent and the photo-initiator were light sensitive. The casting solution was stirred for another 30 min at room temperature and then cast on a clean glass plate using a casting knife [20]. The glass plate was covered with an aluminium tray and left overnight to allow the solvent to evaporate slowly. The resulting membrane was peeled from the glass plate and irradiated with UV-light inside a UV-treatment box containing a UV-lamp (UVP-USA, 8 W, 0.16 A, 230 V) tuned at 365 nm. The box was purged with nitrogen for 15 min to remove all oxygen and the nitrogen flow was continued while irradiating the membranes [21]. Non-cross-linked membranes were prepared as described above, except that no cross-linking agent or photo-initiator were added to the casting solution, and no UV-irradiation was applied.

2.3. Extraction experiments

Extraction experiments were conducted using circular segments (3.65 cm in diameter) of the cross-linked or non-cross-linked membranes, which were attached to homemade holders (as shown in Chapter 1) made of a 3-mm PVC sheet, in order to hold the membranes inside the glass jars containing 100 mL of feed solution. The solutions were shaken continuously at 150 rpm using an orbital shaker (Platform Mixer OM06, Ratek, Australia). A solution containing 100 mg L^{-1} Au(III) in 2.5 M HCl was used as the feed solution. During the extraction experiments, 0.5 mL samples were collected at preselected time intervals, and the Au(III) concentration was determined by atomic absorption spectrometry (AAS). The percentage of Au(III) extracted (%E) was calculated following the Eq (1).

$$\%E=([Au(III)]_i-[Au(III)]_f)/[Au(III)]_i, \quad (1)$$

where subscripts *i* and *f* refer to the initial and final Au(III) concentrations in the feed solution, respectively. All extraction experiments were conducted in triplicate.

2.4. Transport experiments

Transport experiments were conducted in a two compartment transport cell, where each compartment was fitted with a glass stirrer and the membrane was sandwiched between the compartments (contact surface area of 18.1 cm^2) [21]. The feed solution consisted of 100 mL of 100 mg L^{-1} Au(III) in 2.5 M HCl or in digested aqua regia, or 100 mL of electronic waste digest. The receiving solution was 100 mL of 0.5 M Na_2SO_3. The Au(III) concentrations in both the feed and receiving solutions at preselected times were determined by removing 0.5 mL aliquots, followed by analysis using AAS. All transport experiments were carried out in duplicate, unless mentioned otherwise.

2.5. Instrumentation

The concentration of Au(III) was determined using AAS (Hitachi Z-2000 Series Polarized Zeeman, Japan). The concentrations of Ni(II), Al(III), Co(II), Cu(II), Zn(II), and Cr(III) in the electronic waste digest were determined by inductively coupled plasma-optical emission spectrometry (ICP-OES, Optima 4300 DV, PerkinElmer, USA).

The surface morphology of the cross-linked and non-cross-linked membranes was imaged by atomic force microscopy (AFM, Oxford Instruments Asylum Research, USA). Raw images were processed using the WSxM 5.0 software (Nanotec Electronica, Spain) [22]. The respective settings have been previously described [21].

The thickness of the cross-linked and non-cross-linked PIMs was measured using an optical microscope (LH50A, Olympus, Japan) with a calibrated Nikon lens (Carton Optical Ind., Japan). A rectangular piece of membrane was cut from the middle of the cast PIM and the thickness of the cross-section was measured at twenty-five different points.

2.6. Digestion of electronic waste

Aqua regia was prepared with concentrated HCl and HNO_3 in a 3:1 volume ratio. The resultant solution was then heated at 100 ^oC for 6 h as described by Bonggotgetsakul et. al. [19] and allowed to cool down to room temperature. Aqua regia digested in this way had a total acidity of 6 mol L^{-1} and will be denominated as digested aqua regia.

The gold coated electronic components from two mobile phones were digested in 150 mL of aqua regia by heating at 300 ^oC for 2 h. After cooling, the digested solution was then filtered. The filtrate was diluted with digested aqua regia and used for the Au(III) recovery transport experiment. This solution will be referred to as electronic waste digest.

3. Results and discussion

3.1. Selection of base polymer, cross-linking polymer/monomer and photo-initiator

The optimal conditions for cross-linking of PVC, CTA and PVDF-HFP based membranes using the cross-linking polymers PEGDMA and PEGDVE, the cross-linking monomer NEM, and the photo-initiators DMPA and TASHFP, were studied previously [23]. Since, to the best of our knowledge, a cross-linked Cyphos® IL 104-based PIM has never been reported before, an initial study was carried out to examine the compatibility of Cyphos® IL 104 with different base polymer/cross-linking agent/photo-initiator combinations (Table 1), selected on the basis of the earlier study mentioned above, where the base polymer to cross-linking agent ratio was 6:4 [23].

Table 1. Physical appearance of cross-linked Cyphos® IL 104-based PIMs containing 30 wt% extractant and different base polymers, cross-linking agents and photo-initiators (base polymer : cross-linking agent ratio = 6:4). CTA-based membranes also contained 10 wt% NPOE. Cross-linked PIMs were considered successful if homogenous.

Cross-linking agent and photo-initiator				**Base polymer**
PEGDMA		**PEGDVE**	**NEM**	
DMPA	**TASHFP**	**TASHFP**	**DMPA**	
Oily surface (a)	Oily surface (b)	Oily surface (c)	Not cast*	PVC
Successful membrane (PIM1)	Successful membrane (PIM2)	Successful membrane (PIM3)	Not cast*	PVDF-HFP
Oily surface (d)	Oily surface (e)	Successful membrane (PIM4)	Not cast*	CTA

Cross-linking conditions: PIM 1, 1 wt% DMPA, 1 min UV-treatment; PIM 2, 2 wt% TASHFP, 30 min UV-treatment; PIM 3, 8 wt% TASHFP, 1 min UV-treatment; PIM 4, 8 wt% TASHFP, 15 min UV-treatment. PIMs with oily surface contain 1 wt% (a), 4 wt% (b), 8 wt% (c), 4 wt% (d), and 8 wt% (e) photo-initiator.

* PIM not cast because the casting solution was pink.

It was observed that when NEM was mixed with Cyphos® IL 104 in THF, the solution became pink. NEM is known to form a pink coloured compound with a number of different compounds such as imidazole, histidine-derivatives, or cysteine by interacting with the lone electron pair of their N or S atoms [24]. It can be expected that NEM reacts with Cyphos® IL 104 because of the presence of a P atom with a lone electron pair. This result indicated that Cyphos® IL 104 could not be used with any maleimide-based cross-linking agents to produce cross-linked PIMs. In regard to the remaining cross-linking agent/photo-initiator combinations, it was observed that the PVC-based cross-linked PIMs had oily surfaces and were thus considered unsuccessful. For PVDF-HFP-based cross-linked PIMs, all cross-linking agent/photo-initiator combinations produced homogeneous membranes (PIM 1, 2 and 3, Table 1). When using CTA as the base polymer, only the membrane with the cross-linking polymer PEGDVE and the

photo-initiator TASHFP (PIM 4, Table 1) was homogenous, while the remaining had oily surfaces. Hence, PIMs 1, 2, 3, and 4 (Table 1) were selected for further studies.

3.2. Extraction of Au(III)

Conventional Cyphos® IL 104-based PIMs have been reported earlier for the Au(III) extraction using PVC or PVDF-HFP as the base polymer [18, 19]. Using such PIMs the extraction of Au(III) proceeds through the formation of the $[P]^+[AuCl_4]^- \cdot H^+[PO_2]^-$ adduct extracted into the membrane, where $[P]^+$ and $[PO_2]^-$ represent the trihexyl(tetradecyl)phosphonium and bis(2,4,4-trimethylpentyl) phosphinate ions of Cyphos® IL 104, respectively [18]. In the present study, the performance of the four successful cross-linked membranes listed in Table 1 in the extraction of Au(III) was compared with that of the corresponding non-cross-linked PIMs. The transient Au(III) extraction curves for the PIMs mentioned above, expressed as percentage of Au(III) extracted versus time, are shown in Figure 1. It can be observed that the cross-linked PVDF-HFP-based PIMs extracted greater amounts of Au(III) (i.e., between 62 and 68% vs 51%) and at higher rates than their non-cross-linked counterparts (Table 2). The CTA-based cross-linked membrane extracted marginally higher amount of Au(III) (i.e., 58% versus 54%) and at a similar rate of extraction as its non-cross-linked PIM counterpart (Table 2). Based on these results only PVDF-HFP-based PIMs were selected for the subsequent Au(III) transport studies, although the surface morphology of all membranes was evaluated.

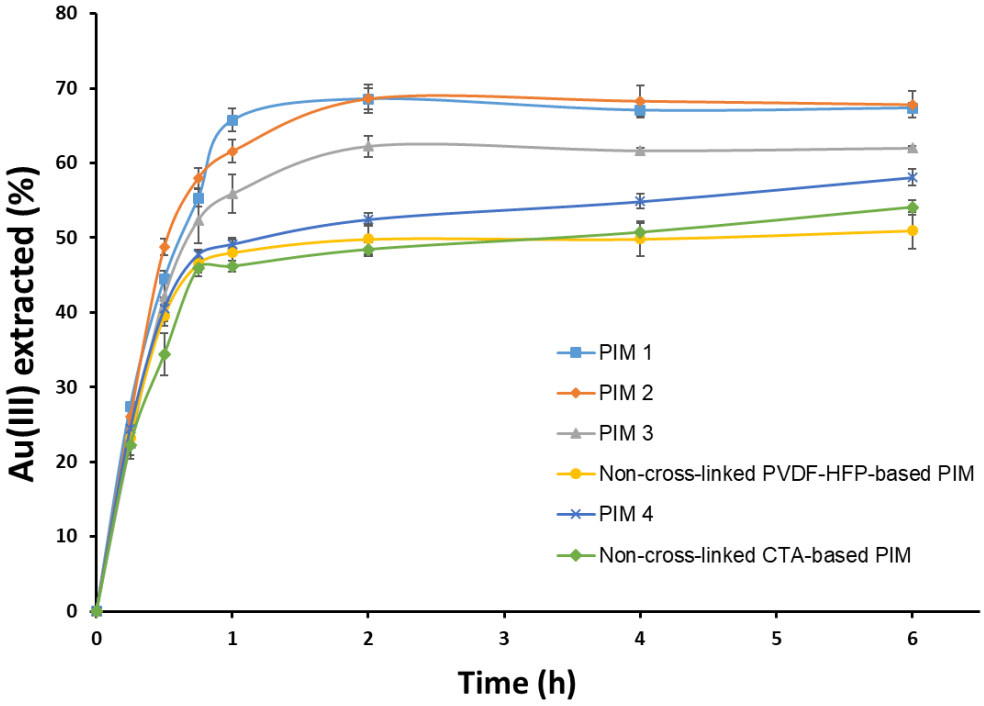

Figure 1. Transient percentage of Au(III) extracted into the successful Cyphos® IL 104-based cross-linked PIMs (Table 1) and their respective non-cross-linked counterparts. (■) PIM 1, (◆) PIM 2, (▲) PIM 3, (●) PVDF-HFP non-cross-linked PIM, (×) PIM 4, and (◆) CTA non-cross-linked PIM. Feed solution, 100 mg L^{-1} Au(III) and 2.5 M HCl. Detailed compositions of the PIMs are presented in Table 1.

Table 2. Amount of Au(III) extracted by cross-linked Cyphos® IL 104-based PIMs (PIM 1 to 4, Table 1) and their non-cross-linked counterparts (Figure 1) after 6 h, and the respective initial flux values.

PIM ID	Au(III) extracted after 6 h ($mg\ L^{-1}$)	Initial flux × 10^6 ($mol\ m^{-2}\ s^{-1}$)
PIM 1	67.4 ± 0.7	14.6 ± 0.5
PIM 2	67.8 ± 1.8	14.5 ± 1.1
PIM 3	62.0 ± 0.4	12.3 ± 1.4
PVDF-HFP non-cross-linked PIM	51.0 ± 2.4	12.0 ± 0.2
PIM 4	58.1 ± 1.1	11.7 ± 1.2
CTA non-cross-linked PIM	54.1 ± 0.9	13.0 ± 0.5

3.3. PIMs surface morphology

It has been reported that cross-linking increases the PIM's surface area in comparison with the respective non-cross-linked membrane [21].

Hence, the surface morphology of the successful Cyphos® IL 104-based cross-linked PIMs mentioned above and their non-cross-linked counterparts was assessed using AFM in the constant force mode. Topography images of the CTA-based cross-linked and non-cross-linked PIMs (Figures 2a and 2b, respectively) show very similar surface profiles with some tortuosity at very low Z scale (35.3 and 43.4 nm, respectively). This similarity in surface morphology can potentially explain the similar extraction performance of these two membranes. On the other hand, the topographic images of cross-linked PVDF-HFP-based PIMs presented in Figures 2c to 2e are very different from their respective non-cross-linked counterpart (Figure 2f). Moreover, it can be seen that the surface of PIM 2 (Figure 2d) contains a large number of well distributed indentations, whereas the surfaces of PIM 1 and PIM 3 (Figures 2c and 2e) contain less but deeper indentations (Z scale: 156.9 vs. 409.6 and 252.2 nm, respectively) looking like hillocks. In contrast, the non-cross-linked PVDF-HFP-based PIM shows a much smoother surface with barely any crests or void features in comparison with the respective cross-linked ones.

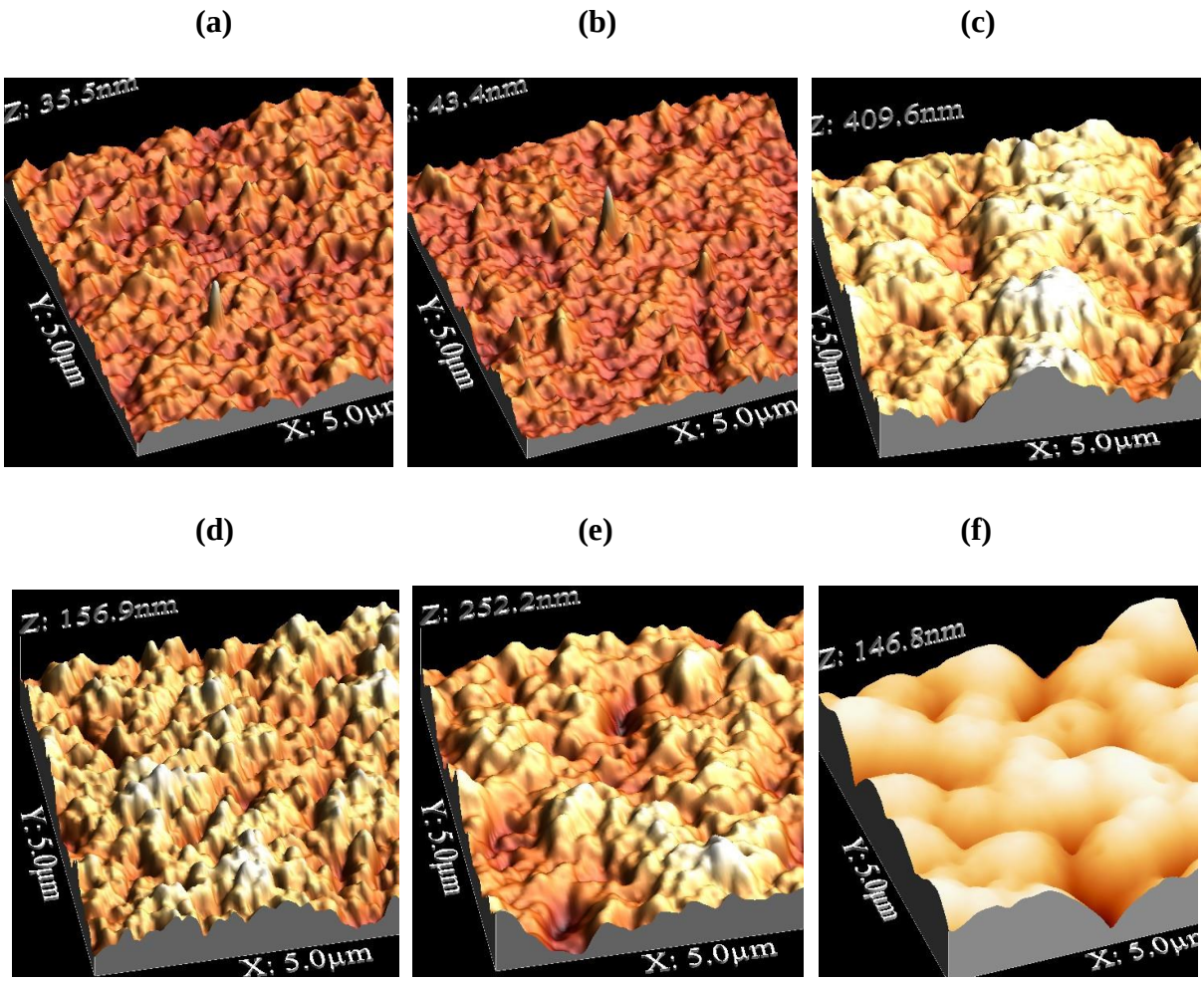

Figure 2. Constant force AFM topographic images of the CTA and PVDF-HFP cross-linked membranes and their respective non-cross-linked PIMs. (a) PIM 4 (Table 1), (b) CTA non-cross-linked PIM, (c) PIM 1, (d) PIM 2, (e) PIM 3 (Table 1), (f) PVDF-HFP non-cross-linked PIM.

In order to determine the surface area of the PVDF-HFP-based PIMs, the contrast saturated images of the respective AFM images (Figures 2c to 2f) were produced and are presented in Figures 3a to 3d. The area covered by the indentations on PIM 2 (Figure 3b) was 1.5 and 2.7 times higher than that on PIM 1 (Figure 3a) and PIM 3 (Figure 3c), respectively (72.0±1.3% vs 46.8±3.7% and 26.2±4.8%, respectively). This difference in the microstructure may be due to the fast cross-linking process of PEGDMA and PEGDVE in the presence of the photo-initiator DMPA and TASHFP, respectively (PIM 1 and PIM 3, 1 min UV-treatment), compared to the cross-linking of PEGDMA by the photoinitator TASHFP (PIM 2, 30 min UV-treatment). Moreover, in case of the PVDF-HFP non-cross-linked PIM (Figure 2f) only 8.3±1.8% of the

area was covered by indentations (Figure 3d). These observations reveal that PVDF-HFP cross-linked PIMs have a larger surface area than the corresponding non-cross-linked membrane, and this may be the underlying reason why PVDF-HFP cross-linked PIMs show superior extraction performance.

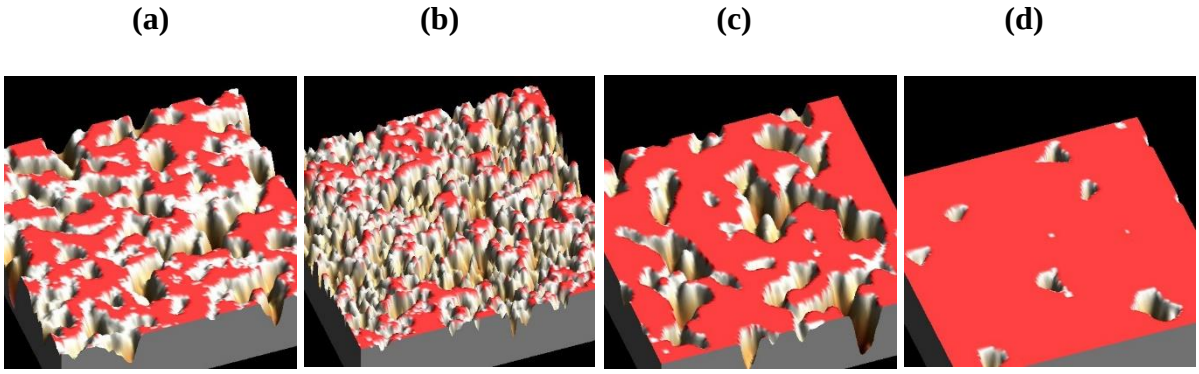

Figure 3. Contrast saturated AFM topographic images of the PVDF-HFP cross-linked membranes: (a) PIM 1, (b) PIM 2, (c) PIM 3 (Table 1), and (d) respective non-cross-linked PIM, highlighting the indentations present in the membranes (represented by the white and yellow colour).

3.4. Transport of Au(III) from HCl solution

The transport of Au(III) across each of the three successful PVDF-HFP cross-linked PIMs mentioned above along with their non-cross-linked counterpart was studied using a feed solution containing Au(III) and 2.5 M HCl and a 0.5 M Na_2SO_3 receiving solution. Bonggotgetsakul et al. have demonstrated that Na_2SO_3 was the most efficient stripping agent out of a wide range of stripping agents studied [19]. Moreover, they have also confirmed that the extraction of Au(III) from HCl solutions by Cyphos® IL 104 and its back-extraction by Na_2SO_3 take place according to Eqns. (1) and (2), respectively:

$$[P]^+[PO_2]^-_{PIM} + H^+[AuCl_4]^-_{FS} \rightleftarrows [P]^+[AuCl_4]^- \cdot H^+[PO_2]^-_{PIM} \quad (1)$$

$$[P]^+[AuCl_4]^- \cdot H^+[PO_2]^-_{PIM} + 3SO_3^{2-}{}_{RS} + H_2O \rightleftarrows [P]^+[PO_2]^-_{PIM} + [Au(SO_3)_2]^{3-}{}_{RS} + \\ + 3H^+_{RS} + 4Cl^-_{RS} + SO_4^{2-}{}_{RS} \quad (2)$$

where $[P]^+$ and $[PO_2]^-$ refer to the trihexyl(tetradecyl)phosphonium cation and the bis(2,4,4-trimethylpentyl)phosphinate anion of the extractant Cyphos® IL 104, respectively, and *PIM*, *FS* and *RS* refer to the membrane phase and the feed and receiving solutions, respectively.

The transient Au(III) concentrations in both the feed and receiving solutions are shown in Figure 4. The results obtained show that the cross-linked PIMs transported Au(III) significantly faster than their non-cross-linked counterpart, with PIM 1 and PIM 2 (Table 1) achieving close to 100% transport of Au(III) into the receiving solution in 4 h, whereas the non-cross-linked PIM achieved only 59% of transport within the same time period, and had not reached 100% transport even after 8 h.

It is interesting to note that PIM 3 which used PEGDVE as the cross-linking agent had only transported about 85% of the Au(III) into the receiving solution when the transport system reached equilibrium. However, it was noticed that, when the Au(III) feed solution was contacted with PIM 3, yellow particles appeared on the membrane's surface on the feed solution side. This could be metallic gold which would account for the lower transport efficiency obatined. The reduction of Au(III) was most likely due to the presence of the vinyl ether units in PEGDVE. It has been reported by Porel et al. that vinyl alcohol can reduce Au(III) [25]. Therefore, only PIM 1 and PIM 2 were selected for further transport studies.

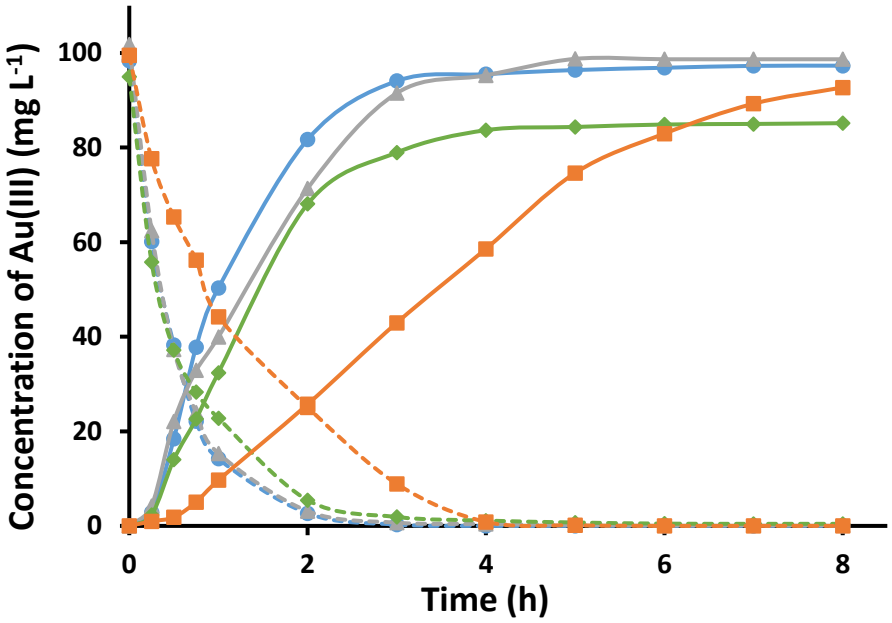

Figure 4. Transient Au(III) concentrations in the feed (dashed lines) and receiving (solid lines) solutions using the PVDF-HFP cross-linked membranes: (●) PIM 1, (▲) PIM 2, (◆) PIM 3 and their respective (■) non-cross-linked PIM. Initial feed solution composition, 100 mg L^{-1} Au(III) and 2.5 M HCl; receiving solution composition, 0.5 M Na_2SO_3. The data points are the average of duplicate experiments. PIMs thickness: PIM 1, 20.1 ± 1.0 µm; PIM 2, 20.1 ± 4.0 µm; PIM 3, 21.5 ± 1.2 µm; non-cross-linked PIM, 18.5 ± 1.8 µm.

3.5. Cross-linked PVDF-HFP-based PIMs stability

One of the most important properties of PIMs requiring evaluation is their stability since their liquid phase can potentially leach into the adjacent aqueous solutions. PIMs capable of multiple use is thus a desirable feature, although single use PIMs are still useful in some applications. The stability of PIM 1 and PIM 2 (Table 1) was evaluated by conducting five consecutive transport experiments using the same PIM. After each experiment, both the feed and receiving solutions were replaced with fresh solutions. The results of the transport experiments are shown in Figures 5a and 5b as well as Table S1. It is clear from Figure 5 that there is a minimal difference in the performance of both PIMs over the five transport experiments. This indicates that the cross-linked Cyphos® IL 104-based PIMs are highly stable under the experimental conditions, and they can be used multiple times without significant loss of performance. There are two possible reasons for this excellent stability. Firstly, the carrier is an ionic liquid with a low solubility (9.1 mg L^{-1}) [26, 27] in the aqueous phase and, secondly, the feed and receiving phases are of high ionic strength. It has been reported that leaching of the PIM's liquid phase to the adjacent aqueous phases is greatly reduced when employing aqueous phases with a high ionic strength [14, 28].

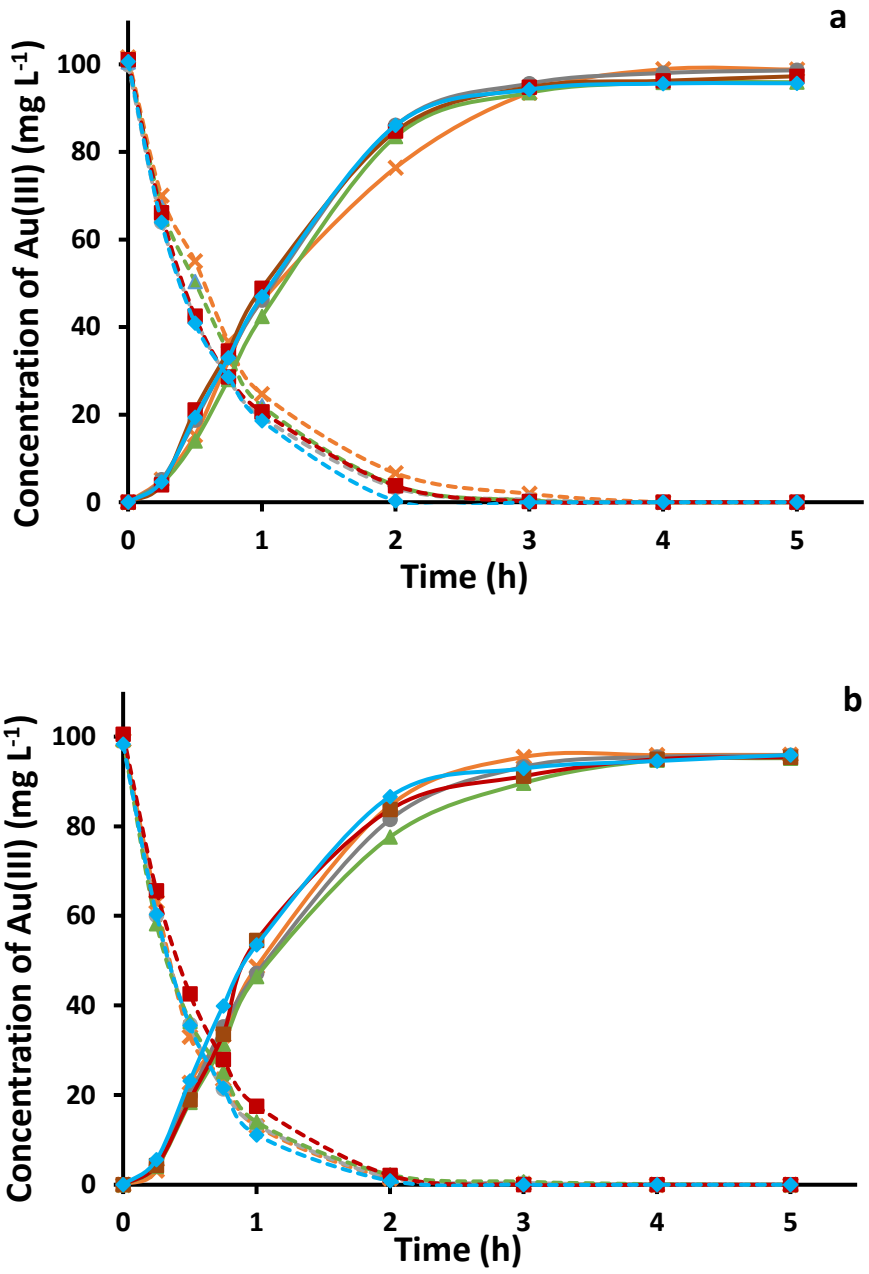

Figure 5. Five consecutive transport experiments using (a) PIM 1 and (b) PIM 2 (Table 1): 1st (×), 2nd (●), 3rd (▲), 4th (■) and 5th (◆) experiment. The transient Au(III) concentration in the feed and receiving solutions is represented by the dashed and solid line, respectively. Initial feed solution composition, 100 mg L^{-1} Au(III) and 2.5 M HCl; receiving solution composition, 0.5 M Na_2SO_3. The data points are the average of duplicate experiments.

3.6. Recovery of Au(III) from digested aqua regia

It has been demonstrated that the rate of Au(III) transport from a 2.5 M HCl solution across a Cyphos® IL 104-based PIM can be significantly increased by cross-linking the PIM polymeric structure with PEGDMA using either DMPA or TASHFP as photo-initiators. Complete transport can be achieved in less than 4 h, rather than over 8 h when using a conventional non-cross-linked PIM. Since the ultimate aim of the present study was the separation of Au(III) from electronic waste digested in aqua regia, it was necessary to test the performance of PIM 1 and PIM 2 with a feed solution consisting of a digested aqua regia solution (total acidity of 6 mol L^{-1}). The results of this transport experiment are shown in Figure 6.

Figure 6a shows that 92% of the Au(III) was transported to the receiving solution in less than 4 h for PIM 2 (Table 1). However, in the case of PIM 1 (Table 1), only about 72% of Au(III) was transported in 4 h when the transport system reached equilibrium (Figure 6b). In addition, it was observed that PIM 1 appeared yellow after transporting gold for 4 h. This unusual behaviour could be associated with the much higher acidity (6 mol L^{-1} compared to 2.5 mol L^{-1}) of the digested aqua regia which, together with the presence of some decomposition products produced during the UV-irradiation of DMPA [29], could have led to the formation of Au(III) complexes in the PIM or its reduction to metallic gold on the receiving solution side of the PIM. However, it is clear from this study that PIM 2 is the most suitable PIM among those studied for recovering Au(III) from digested aqua regia, and it was thus selected for transport experiments involving the recovery of Au(III) from electronic waste digest.

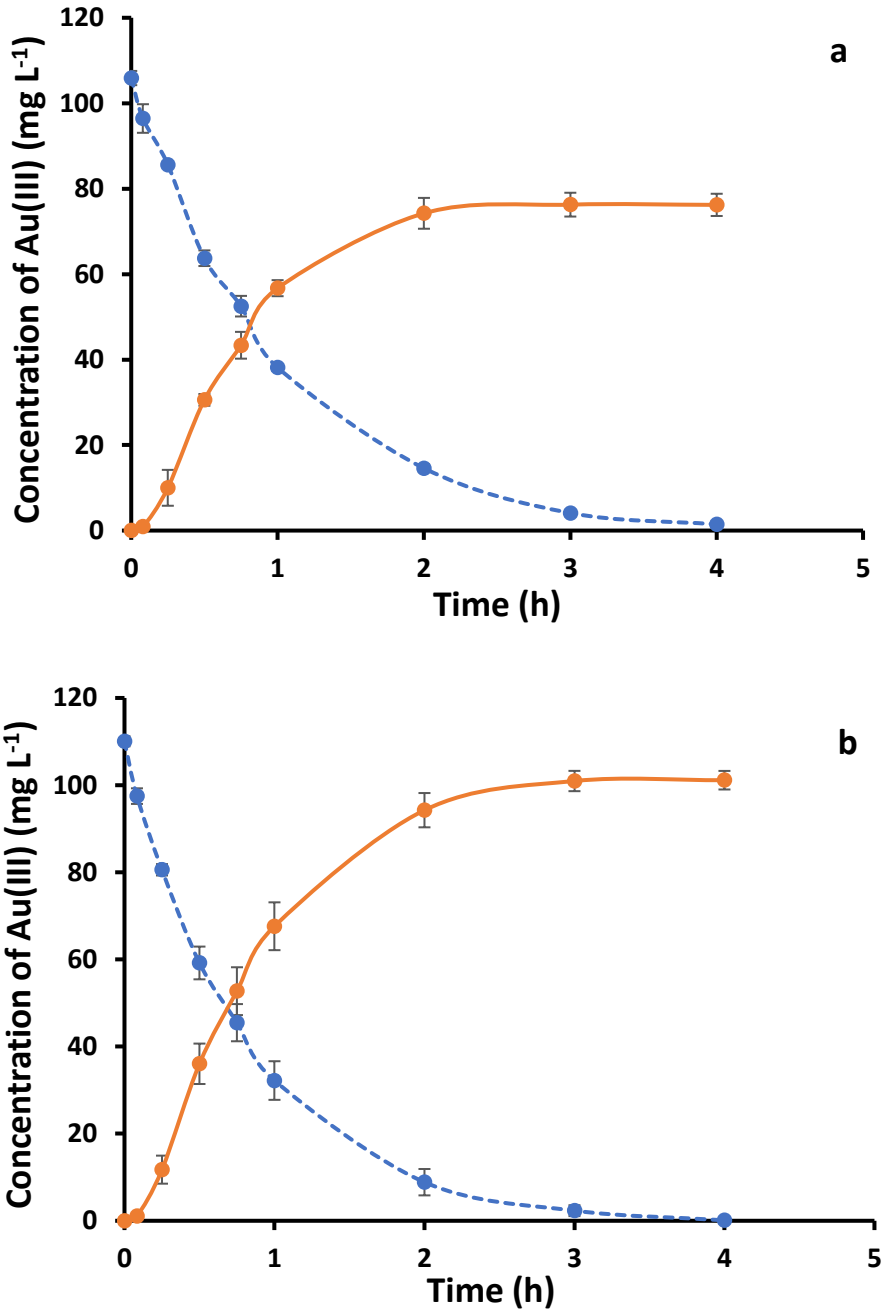

Figure 6. Transient Au(III) concentrations in the feed (dashed line) and receiving (solid line) solutions in transport experiments using (a) PIM 1 and (b) PIM 2 (Table 1). Initial feed solution,110 mg L^{-1} Au(III) in digested aqua regia solution; receiving solution composition, 0.5 M Na_2SO_3. The error bars = ±standard deviation (n=3).

3.7. Recovery of Au(III) from electronic waste digest

The gold coated electronic parts from discarded mobile phones were digested in aqua regia as described in Section 2.6. After digestion, the solution was filtered, and the concentrations of

the metal ions were determined by ICP-OES (Table 3). As expected, the digest contained Al, Cr, Cu, Fe, Ni, and Zn at concentrations much higher than that of Au, i.e., between 12 and 825-fold in terms of mole ratio.

Table 3. Concentrations of the metals present in the electronic waste digest determined by ICP-OES.

Metals	**Concentration (mg L^{-1})**	**Mole ratio of metal : Au**
Al	253	12.3
Au	150	-
Co	31.8	0.709
Cr	1326	33.5
Cu	39930	825
Fe	5541	130
Ni	2919	65.3
Zn	1063	21.3

Transport experiments were carried out as described by Bonggotgetsakul et al. [19] using the digested solution from the electronic waste as the feed solution, and 0.5 M Na_2SO_3 as the receiving solution. The results are shown in Figure 7, where it can be observed that only Au(III) was transported to the receiving solution (insignificant recoveries of 0.1% and 0.01% were obtained for Zn and Cu, respectively), and that 94% of Au(III) transport occurred in less than 24 h.

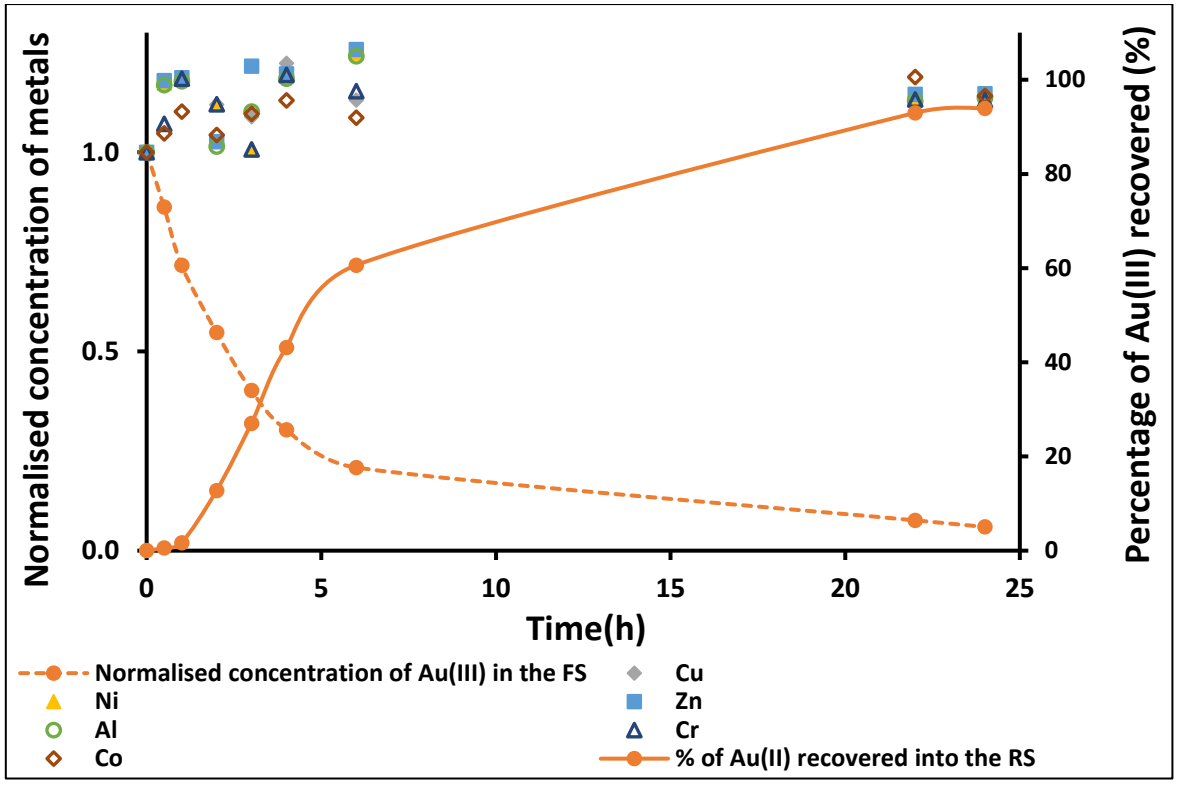

Figure 7. Transient normalized concentration of Au(III) (●) in the feed (dashed line) and receiving solutions (solid line), respectively, and of the major metal ions (i.e., Ni(II), Al(III), Co(II), Cu(II), Zn(II) and Cr(III)) present in the feed solution. The transient percentage of Au(III) recovered is also presented. Feed solution, electronic waste digest; receiving solution, 0.5 M Na_2SO_3. Cross-linked PIM composition, 30 wt% Cyphos® IL 104, PVDF-HFP, PEGDMA (PVDF-HFP to PEGDMA ratio 6:4) and 2 wt% TASHFP. PIMs thickness: 20.1 ± 4.0 µm.

In comparison with the previous transport experiments where the same membrane was used (i.e., PIM 2, Table 1) with digested aqua regia as feed solution (Figure 6b) instead of electronic waste digest, the Au(III) transport took a longer time to be completed in the latter case (4 vs. 24 h), most likely due to the presence of very high concentrations of the other metal ions (Table 2). The majority of transition metal ions present in the digest (i.e., Cu(II), Zn(II), Fe(II/III), Ni(II) and Co(II)) can form anionic chlorocomplexes [30-32] which will compete with the extraction of $[AuCl_4]^-$ (Eq. (1)). However, these metal ions cannot be stripped into the receiving solution because they cannot be reduced by 0.5 M Na_2SO_3 like Au(III) and will thus reduce the PIM permeability to Au(III). It should be highlighted that the proposed cross-linked membrane recovered Au(III) from electronic waste digest faster than previously reported non-cross-linked

PIMs containing either N-[N,N-di(2-ethylhexyl)aminocarbonylmethyl]glycine [6] or Cyphos® IL 104 [19] as the extractant (complete recovery was achieved in 50 h or 28 h, respectively, versus 22 h with the present cross-linked PIM).

Another similar transport experiment was conducted using different electronic digest of the following composition (Table 4) to compare the performance of cross-linked and non-cross-linked PIMs in terms of gold recovery. Feed solution composition is more complex here with very low amount of Au(III) and higher amount of other metals. Results of the gold recovery experiment are shown in figure 8 which indicate that cross-linked PIM was able to recover 50% of the gold while no such recovery was noticed for no-cross-linked PIM. This result establish the superiority and wide applicability of cross-linked PIM in gold recovery.

Table 4. Concentrations of the metals present in the newly prepared electronic waste digest determined by ICP-OES.

Metals	**Concentration (mg L^{-1})**	**Mole ratio of metal : Au**
Al	473	690.6
Au	5	-
Co	47	31.8
Cr	2441	1849.1
Cu	57168	35434
Ni	3668	2461.8
Zn	1351	813

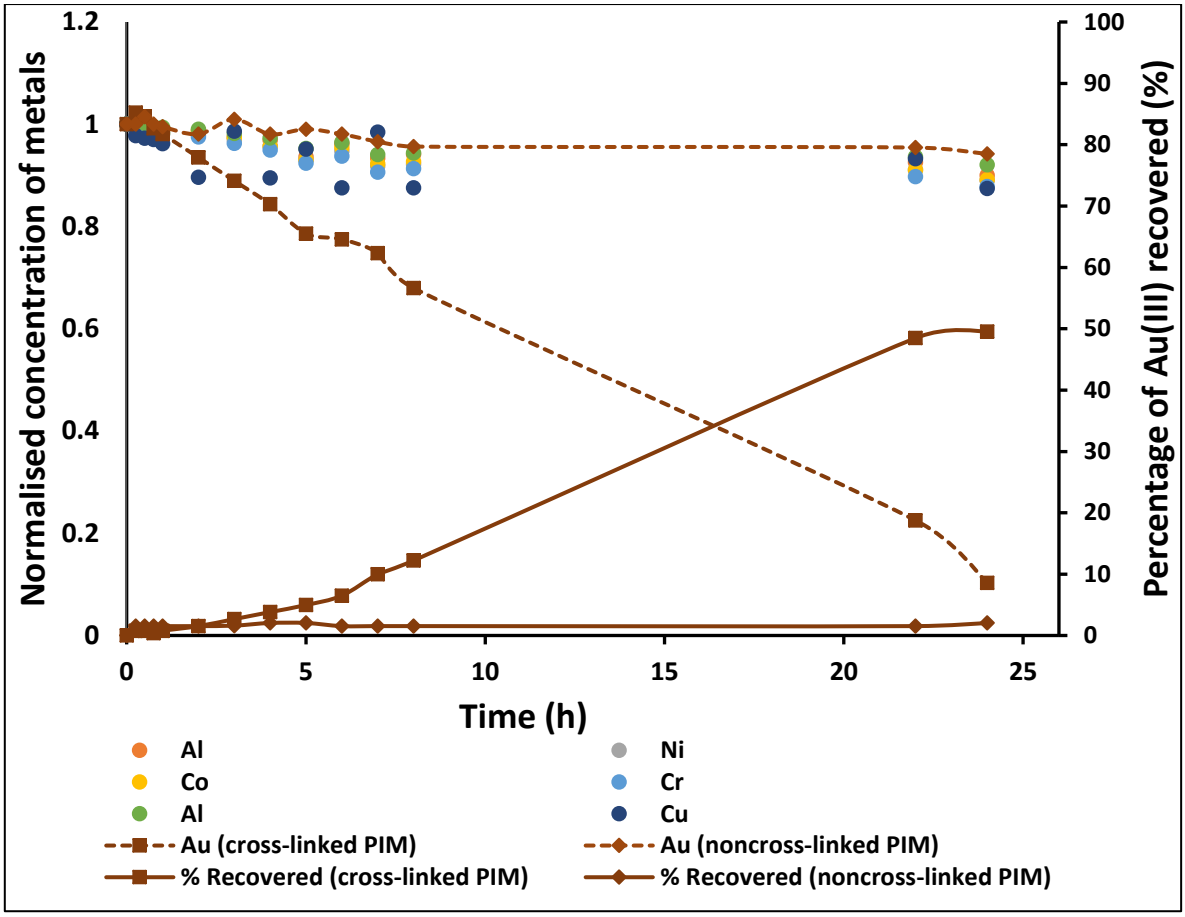

Figure 8. Transient normalized concentration of Au(III) in the feed (dashed line) and receiving solutions (solid line) for cross-linked PIM (■) and non-cross-linked PIM (◆) , respectively, and of the major metal ions (i.e., Ni(II), Al(III), Co(II), Cu(II), Zn(II) and Cr(III)) present in the feed solution. The transient percentage of Au(III) recovered is also presented. Feed solution, electronic waste digest; receiving solution, 0.5 M Na_2SO_3. Cross-linked PIM composition, 30 wt% Cyphos® IL 104, PVDF-HFP, PEGDMA (PVDF-HFP to PEGDMA ratio 6:4) and 2 wt% TASHFP and non-cross-linked PIM containing 30 wt% Cyphos® IL 104, PVDF-HFP.

4. Conclusions

This research has shown that the ionic liquid Cyphos® IL 104 is compatible with the acrylate (PEGDMA) and vinyl ether (PEGDVE) class of cross-linking agents to form homogeneous cross-linked PIMs with PVDF-HFP as the base polymer, and with the vinyl ether (PEGDVE) cross-linking agent when using CTA and NPOE as the base polymer and plasticizer, respectively. DMPA or TASHFP could be used as the photo-initiators to cross-link PEGDMA

and form a homogenous PIM. The same result was achieved with TASHFP and the cross-linking polymer PEGDVE.

All successful cross-linked PVDF-HFP-based PIMs showed superior performances in terms of rate and amount of Au(III) extracted in comparison to their non-cross-linked PIM counterpart, while with the CTA-based PIMs cross-linking did not improve membrane performance. These results are consistent with the surface morphology studies of these membranes which showed that while cross-linking the CTA-based PIM did not change its surface morphology, cross-linking the PVDF-HFP-based PIMs significantly increased their surface area, thus speeding up Au(III) extraction.

The transport performance of the two PVDF-HFP-PEGDMA cross-linked PIMs was similar, with complete Au(III) recovery being achieved in less than 4 h (two times faster than their non-cross-linked counterpart). This performance did not deteriorate in five consecutive transport experiments, thus showing high PIM stability. However, the recovery with the PVDF-HFP-PEGDVE cross-linked PIM was lower due to the likely reduction of some Au(III) on the PIM surface by the vinyl ether units of PEGDVE. When digested aqua regia (6 mol L^{-1} acidity) was used as the feed solution, the PIM with PEGDMA as the cross-linking agent and DMPA as the photo-initiator became yellow and only 72% of Au(III) was transported due to retention of Au within the PIM as a likely result of complexation or reduction to metallic Au by the decomposition products of the photo-initiator. On the other hand, the PIM with PEGDMA as the cross-linking agent and TASHFP as the photo-initiator achieved complete transport of Au(III) from digested aqua regia. The same PIM transported 94% transport of Au(III) from an electronic waste digest in less than 24 h, which is faster than what was achieved with previously reported non-cross-linked PIMs. Cross-linked PIM also appeared to be effective in gold recovery when trace amount of gold is present in the digest but non-cross-linked PIM failed to perform.

References

[1] R. Akram, Natasha, S. Fahad, M.Z. Hashmi, A. Wahid, M. Adnan, M. Mubeen, N. Khan, M.I.A. Rehmani, M. Awais, M. Abbas, K. Shahzad, S. Ahmad, H.M. Hammad, W. Nasim, Trends of electronic waste pollution and its impact on the global environment and ecosystem, Environ. Sci. Pollut. Res., 26 (2019) 16923-16938.

[2] K. Huang, J. Guo, Z. Xu, Recycling of waste printed circuit boards: A review of current technologies and treatment status in China, J. Hazard. Mater., 164 (2009) 399-408.

[3] L. Rocchetti, A. Amato, F. Beolchini, Printed circuit board recycling: A patent review, J. Clean. Prod., 178 (2018) 814-832.

[4] S. Syed, Recovery of gold from secondary sources—A review, Hydrometallurgy, 115 (2012) 30-51.

[5] E.D. Doidge, I. Carson, P.A. Tasker, R.J. Ellis, C.A. Morrison, J.B. Love, A simple primary amide for the selective recovery of gold from secondary resources, Angew. Chem.-Int. Edit., 55 (2016) 12436-12439.

[6] F. Kubota, R. Kono, W. Yoshida, M. Sharaf, S.D. Kolev, M. Goto, Recovery of gold ions from discarded mobile phone leachate by solvent extraction and polymer inclusion membrane (PIM) based separation using an amic acid extractant, Sep. Purif. Technol., 214 (2019) 156-161.

[7] S.M. Abdelbasir, S.S.M. Hassan, A.H. Kamel, R.S. El-Nasr, Status of electronic waste recycling techniques: a review, Environ. Sci. Pollut. Res., 25 (2018) 16533-16547.

[8] Y.J. Park, D.J. Fray, Recovery of high purity precious metals from printed circuit boards, J. Hazard. Mater., 164 (2009) 1152-1158.

[9] M. Gurung, B.B. Adhikari, H. Kawakita, K. Ohto, K. Inoue, S. Alam, Selective recovery of precious metals from acidic leach liquor of circuit boards of spent mobile phones using chemically modified persimmon tannin gel, Ind. Eng. Chem. Res., 51 (2012) 11901-11913.

[10] C. Agarwal, R.W. Cattrall, S.D. Kolev, Donnan dialysis based separation of gold (III) from electronic waste solutions using an anion exchange pore-filled membrane, J. Membr. Sci., 514 (2016) 210-216.

[11] M.I.G.S. Almeida, R.W. Cattrall, S.D. Kolev, Recent trends in extraction and transport of metal ions using polymer inclusion membranes (PIMs), J. Membr. Sci., 415-416 (2012) 9-23.

[12] L. Nghiem, P. Mornane, I. Potter, J. Perera, R.W. Cattrall, S.D. Kolev, Extraction and transport of metal ions and small organic compounds using polymer inclusion membranes (PIMs), J. Membr. Sci., 281 (2006) 7-41.

[13] M.I.G.S. Almeida, R.W. Cattrall, S.D. Kolev, Polymer inclusion membranes (PIMs) in chemical analysis - A review, Anal. Chim. Acta, 987 (2017) 1-14.

[14] S.D. Kolev, M.I.G.S. Almeida, R.W. Cattrall, Polymer inclusion membranes, in: A.K. Pabby, S.S.H. Rizvi, A.M. Sastre (Eds.) Handbook of Membrane Separations: Chemical, Pharmaceutical, Food, and Biotechnological Applications, CRC Press, Boca Raton, 2015, pp. 721-737.

[15] E. Rodríguez de San Miguel, A.V. Garduño-García, J.C. Aguilar, J. de Gyves, Gold (III) transport through polymer inclusion membranes: Efficiency factors and pertraction mechanism using Kelex 100 as carrier, Ind. Eng. Chem. Res., 46 (2007) 2861-2869.

[16] M.E. Núñez, E. Rodríguez de San Miguel, F. Mercader-Trejo, J. Aguilar, J. de Gyves, Selective ω-thiocaprolactam-based recovery of Au (III) from chloride media in solvent extraction and polymer inclusion membrane systems, Sep. Purif. Technol., 51 (2006) 57-63.

[17] M.E. Núñez, E. Rodríguez de San Miguel, J. de Gyves, Polymer inclusion membranes composed of long alkyl chain alcohols for clean gold (III) recovery, J. Chem. Technol. Biotechnol., 89 (2014) 825-834.

[18] Y.Y.N. Bonggotgetsakul, R.W. Cattrall, S.D. Kolev, Extraction of gold (III) from hydrochloric acid solutions with a PVC-based polymer inclusion membrane (PIM) containing Cyphos® IL 104, Membranes, 5 (2015) 903-914.

[19] Y.Y.N. Bonggotgetsakul, R.W. Cattrall, S.D. Kolev, Recovery of gold from aqua regia digested electronic scrap using a poly (vinylidene fluoride-co-hexafluoropropene) (PVDF-HFP) based polymer inclusion membrane (PIM) containing Cyphos (R) IL 104, J. Membr. Sci., 514 (2016) 274-281.

[20] Y. O'Bryan, Y.B. Truong, R.W. Cattrall, I.L. Kyratzis, S.D. Kolev, A new generation of highly stable and permeable polymer inclusion membranes (PIMs) with their carrier immobilized in a crosslinked semi-interpenetrating polymer network. Application to the transport of thiocyanate, J. Membr. Sci., 529 (2017) 55-62.

[21] B. Hoque, M.I.G.S. Almeida, R.W. Cattrall, T.G. Gopakumar, S.D. Kolev, Effect of cross-linking on the performance of polymer inclusion membranes (PIMs) for the extraction, transport and separation of Zn (II), J. Membr. Sci., 589 (2019) 117256.

[22] I. Horcas, R. Fernández, J. Gomez-Rodriguez, J. Colchero, J. Gómez-Herrero, A. Baro, WSXM: a software for scanning probe microscopy and a tool for nanotechnology, Review of scientific instruments, 78 (2007) 013705.

[23] B. Hoque, M.I.G.S. Almeida, R.W. Cattrall, T.G. Gopakumar, S.D. Kolev, Improving the performance of polymer inclusion membranes by cross-linking their polymeric backbone, J. Membr. Sci., (2019) (submitted).

[24] D.G. Smyth, A. Nagamatsu, J.S. Fruton, Some reactions of N-ethylmaleimide, J. Am. Chem. Soc, 82 (1960) 4600-4604.

[25] S. Porel, N. Venkatram, D. Narayana Rao, T. Radhakrishnan, In situ synthesis of metal nanoparticles in polymer matrix and their optical limiting applications, J. Nanosci. Nanotechnol., 7 (2007) 1887-1892.

[26] J. Marták, S. Schlosser, Density, viscosity, and structure of equilibrium solvent phases in butyric acid extraction by phosphonium ionic liquid, J. Chem. Eng. Data., 62 (2017) 3025-3035.

[27] J. Marták, Š. Schlosser, Extraction of lactic acid by phosphonium ionic liquids, Sep. Purif. Technol., 57 (2007) 483-494.

[28] L.J.L. Zhang, R.W. Cattrall, M. Ashokkumar, S.D. Kolev, On-line extractive separation in flow injection analysis based on polymer inclusion membranes: A study on membrane stability and approaches for improving membrane permeability, Talanta, 97 (2012) 382-387.

[29] H. Fischer, R. Baer, R. Hany, I. Verhoolen, M. Walbiner, 2, 2-Dimethoxy-2-phenylacetophenone: photochemistry and free radical photofragmentation, J. Chem. Soc.-Perkin Trans. 2, (1990) 787-798.

[30] W. Libuś, R. Pastewski, Thermodynamic and structural features of chloro-complex formation of bivalent transition metals in dimethylsulfoxide, J. solution chem., 17 (1988) 59-65.

[31] C. Heinrich, T. Seward, A spectrophotometric study of aqueous iron (II) chloride complexing from 25 to 200 C, Geochim. Cosmochim. Acta., 54 (1990) 2207-2221.

[32] D. Parmentier, T. Vander Hoogerstraete, S.J. Metz, K. Binnemans, M.C. Kroon, Selective extraction of metals from chloride solutions with the tetraoctylphosphonium oleate ionic liquid, Ind. Eng. Chem. Res., 54 (2015) 5149-5158.

5. Supplementary materials

Table S1. Concentration of Au(III) (mg L^{-1}) transported in five consecutive transport experiments across PIM 1 and PIM 2 (Table 1). Initial feed solution composition, 100 mg L^{-1} Au(III) and 2.5 M HCl; receiving solution composition, 0.5 M Na_2SO_3.

PIM ID	**Transport cycle**				
	1st	**2nd**	**3rd**	**4th**	**5th**
PIM 1	98.6	98.6	95.9	96.2	95.7
PIM 2	95.9	95.8	95.4	95.2	95.8

Chapter 5
Conclusions and future research

This thesis reports on the use of three cross-linking agents (i.e., poly(ethylene glycol) dimethylacrylate (PEGDMA), poly(ethylene glycol) divinyl ether (PEGDVE) and N-ethylmaleimide (NEM)) and three photo-initiators (i.e., 2,2-dimethoxy-2-phenyl acetophenone (DMPA), triarylsulfonium hexafluorophosphate (TASHFP) and triphenylphosphine oxide (TPO)) in the preparation of cross-linked PIMs using the base polymers poly(vinylidene fluoride-co-hexafluoropropylene) (PVDF-HFP) , poly(vinyl chloride) (PVC) and cellulose triacetate (CTA) , and the extractants di-(2-ethylhexyl)phosphoric acid (D2EHPA), Aliquat 336 and Cyphos® IL 104 for the extraction and separation of the metallic species Zn(II) and Au(III) and the non-metallic species thiocyanate. The performance of these cross-linked PIMs was compared with the corresponding non-cross-linked PIMs in terms of the amount extracted, extraction and transport rates, and stability, and the majority of the results indicated that the cross-linked PIMs exhibited superior performance over the corresponding non-cross-linked ones.

Chapter 2 reports the development of a D2EHPA-based cross-linked PIM for the faster extraction, transport and separation of Zn(II). Among the three base polymers tested (i.e., PVDF-HFP, PVC and CTA), using PEGDMA as the cross-linking agent, both PVDF-HFP- and CTA-based membranes were found to be homogeneous, however the PVC-based cross-linked PIM had oily surfaces, suggesting some incompatibility of the membrane components. The Zn(II) extraction experiments results with PVDF-HFP- and CTA-based cross-linked PIMs revealed that only the CTA-based cross-linked PIM extracted more Zn(II) and at a faster rate than its non-cross-linked counterpart. Its optimal composition consisted of 40 wt% D2EHPA, 10 wt% NPOE, CTA:PEGDMA ratio of 6:4, and 0.6 wt% of the photo-initiator DMPA. This membrane showed excellent selectivity towards Zn(II) in the presence of other frequently encountered heavy metal ions. Morphology analysis of the cross-linked and non-cross-linked PIMs revealed that cross-linking the membrane polymeric backbone increased its effective surface area which was the most likely reason for the faster transport of Zn(II) across the cross-linked PIM.

Chapter 3 describes a study on the applicability of the three cross-linking agents and the three photo-initiators, mentioned above, in the preparation of cross-linked PIMs with the above

mentioned three base polymers and two of the most commonly used extractants, namely D2EHPA and Aliquat 336. Screening of all three cross-linking agents separately with the three photo-initiators, using a PVC-based membrane, lead to the selection of photo-initiator(s) suitable for each cross-linking agent. The results of this screening study showed that DMPA and TASHFP were suitable to cross-link PEGDMA, only TASHFP was appropriate for PEGDVE, and only DMPA was applicable to NEM. After optimising the cross-linking conditions (i.e., concentration of photo-initiator required and UV-treatment time) for each base polymer-cross-linking agent combination, the compatibility of the above mentioned two extractants with these polymeric combinations was assessed. The results indicated that only thirteen homogeneous cross-linked PIMs could be produced out of twenty six possible combinations. The successful cross-linked PIMs were then used for the extraction of either Zn(II) (using D2EHPA-based PIMs) or SCN^- (using Aliquat 336-based PIMs). Twelve of the thirteen cross-linked PIMs exhibited superior extraction performance in terms of the amount extracted and the rate of extraction compared to the corresponding non-cross-linked PIMs.

Chapter 4 describes the development of Cyphos® IL 104-based PIMs for the extraction of Au(III) by screening combinations of the above mentioned base polymers, cross-linking agents and photo-initiators. PVC was not compatible with Cyphos® IL 104 in the presence of any of the cross-linking agents studied. Four homogeneous cross-linked PIMs were produced, out of which three contained PVDF-HFP and one contained CTA as the base polymer. PVDF-HFP-based cross-linked PIMs extracted larger amounts of Au(III) when compared to the CTA-based PIMs or their non-cross-linked counterparts. Therefore, the PVDF-HFP-based PIMs (cross-linked and non-cross-linked) were further studied for their ability to extract and transport Au(III), and the results showed that the cross-linked PIMs containing PEGDMA as the cross-linking polymer transported Au(III) faster than the corresponding non-cross-linked PIMs and more effectively than the cross-linked PIM containing PEGDVE as the cross-linking agent. Both PEGDMA cross-linked PIMs with DMPA and TASHFP used as photo-initiators were very stable over five consecutive uses when the feed solution acidity was 2.5 mol L^{-1}. However, when aqua regia digest was used as the feed solution with an acidity of 6 mol L^{-1}, only the PEGDMA-based cross-linked PIM with TASHFP as the photo-initiator could effectively transport Au(III). Therefore, this membrane was tested for the Au(III) recovery form digested electronic waste with aqua regia, and it was found that Au(III) could be efficiently and selectively recovered in less than 24 h in the presence of other metal ions at much higher concentrations. Morphology analysis indicated that the presence of higher number of

indentations in the cross-linked PIMs increased the membrane surface area, resulting in faster extraction and transport.

The results outlined in the thesis clearly indicate that cross-linking PIMs increases in the great majority of the cases their surface area thus improving their performance in terms of rate of extraction and transport.

Future studies

It should be noted that the cross-linked PIMs were also able to extract more Zn(II), SCN^- or Au(III) than the corresponding non-cross-linked counterparts. Even though the amount of extractant that is available in both membranes is the same, in the case of cross-linked membranes more extractant seems to be readily accessible possibly due to the presence of more complexation sites resulting from the increased surface area. Detailed studies of the structure of cross-linked PIMs using synchrotron-based techniques (e.g., small- and wide-angle X-ray scattering (SAXS/WAXS)) should be conducted to investigate this surface area modification phenomena and understand the role of each PIM component and its effect on the surface morphology. Moreover, it would be an exciting direction of research to test other extractants with the cross-linking agents and conditions established in this thesis in order to expand the applications of cross-linked PIMs.